National Library of Canada
Bibliothèque nationale du Canada

Canadian Theses Service
Service des thèses canadiennes

Ottawa, Canada
K1A 0N4

NOTICE

The quality of this microform is heavily dependent upon the quality of the original thesis submitted for microfilming. Every effort has been made to ensure the highest quality of reproduction possible.

If pages are missing, contact the university which granted the degree.

Some pages may have indistinct print especially if the original pages were typed with a poor typewriter ribbon or if the university sent us an inferior photocopy.

Previously copyrighted materials (journal articles, published tests, etc.) are not filmed.

Reproduction in full or in part of this microform is governed by the Canadian Copyright Act, R.S.C. 1970, c. C-30.

AVIS

La qualité de cette microforme dépend grandement de la qualité de la thèse soumise au microfilmage. Nous avons tout fait pour assurer une qualité supérieure de reproduction.

S'il manque des pages, veuillez communiquer avec l'université qui a conféré le grade.

La qualité d'impression de certaines pages peut laisser à désirer, surtout si les pages originales ont été dactylographiées à l'aide d'un ruban usé ou si l'université nous a fait parvenir une photocopie de qualité inférieure.

Les documents qui font déjà l'objet d'un droit d'auteur (articles de revue, tests publiés, etc.) ne sont pas microfilmés.

La reproduction, même partielle, de cette microforme est soumise à la Loi canadienne sur le droit d'auteur, SRC 1970, c. C-30.

NL-339 (r. 88/04)

Canada

THE UNIVERSITY OF ALBERTA

DEGLACIAL-MARINE SEDIMENTS FROM CLEMENTS MARKHAM INLET, ELLESMERE ISLAND, N.W.T., CANADA

BY

© THOMAS GEORGE STEWART

A THESIS

SUBMITTED TO THE FACULTY OF GRADUATE STUDIES AND RESEARCH

IN PARTIAL FULFILMENT OF THE REQUIREMENTS FOR THE DEGREE

OF DOCTOR OF PHILOSOPHY

DEPARTMENT OF GEOGRAPHY

EDMONTON, ALBERTA

SPRING 1988

Permission has been granted to the National Library of Canada to microfilm this thesis and to lend or sell copies of the film.

The author (copyright owner) has reserved other publication rights, and neither the thesis nor extensive extracts from it may be printed or otherwise reproduced without his/her written permission.

L'autorisation a été accordée à la Bibliothèque nationale du Canada de microfilmer cette thèse et de prêter ou de vendre des exemplaires du film.

L'auteur (titulaire du droit d'auteur) se réserve les autres droits de publication; ni la thèse ni de longs extraits de celle-ci ne doivent être imprimés ou autrement reproduits sans son autorisation écrite.

ISBN 0-315-42842-2

THE UNIVERSITY OF ALBERTA
RELEASE FORM

NAME OF AUTHOR: Thomas George Stewart

TITLE OF THESIS: Deglacial-Marine Sediments from Clements Markham Inlet, Ellesmere Island, N.W.T., Canada

DEGREE: Doctor of Philosophy

YEAR THIS DEGREE GRANTED: Spring 1988

Permission is hereby granted to THE UNIVERSITY of ALBERTA LIBRARY to reproduce single copies of this thesis and to lend of sell such copies for private, scholarly or scientific research purposes only.

The author reserves other publication rights, and neither the thesis nor extensive extracts from it may be printed or otherwise reproduced without the author's permission.

Thomas G. Stewart
(Student's signature)

P.O. Box 1125
(Student's permanent address)

El Cerrito, CA 94530

Date: February 4, 1988

THE UNIVERSITY OF ALBERTA

FACULTY OF GRADUATE STUDIES AND RESEARCH

The undersigned certify that they have read, and recommend to the Faculty of Graduate Studies and Research for acceptance, a thesis entitled DEGLACIAL-MARINE SEDIMENTS IN CLEMENTS MARKHAM INLET, ELLESMERE ISLAND, N.W.T., CANADA submitted by THOMAS GEORGE STEWART in partial fulfilment of the requirements for the degree of DOCTOR OF PHILOSOPHY.

.....
(Supervisor)

.....

.....

.....

.....

Date: February 4, 1988

ABSTRACT

Quaternary sediments at the inner south shore of Clements Markham Inlet, N Ellesmere Island, N.W.T., Canada are related to three stratigraphic intervals. Unit 1 formed as a subaerial, proglacial sandur in front of the advancing ice of the last glaciation. It is the first material of this age recognized in this inlet and indicates that sea level was similar to present during that time. Unit 2, which contains the dominant sediment volume in the inlet, is composed of glaciomarine sediments deposited by retreating tidewater glaciers between ca. 11,000 and 7900 BP. Unit 3 is composed of deposits of prograding subaerial deltas and was deposited during a period of rapid emergence after 7900 BP. Unit 2 sediments are assigned to five lithofacies associations (LA) which occur in a fining-upwards sequence related to ice retreat. LA I is interbedded diamictons, sands and silts deposited by debris flows, turbidity currents and turbid plumes. LA II is gravels and sands deposited by high density mass flows in subaquatic outwash fan channels. LA III is amalgamated and graded sand deposited by high density turbidity currents in subaquatic outwash channels. LA IV is graded, laminated and current-bedded sand deposited on levees by overspill from turbidity current channels. It consists of Bouma sequences, climbing ripples, starved ripples and draped lamination. LA V is interbedded and interlaminated sand and silt and is divided into cyclopsams, cyclopels and non-laminated silt. Cyclopsams are repetitively interbedded and interlaminated graded sands. Cyclopels are silts with interlaminated sand laminae that are as

thin as one grain. These lithofacies are deposited by suspension from progressively decaying, turbulent overflow plumes. Observations by others in southern Alaska show this sand can be transported up to 3.2 km from the ice front, thus, even though it is the most distal lithofacies, LA V is still indicative of an ice-proximal environment. The dominance of subaquatic outwash, cyclopsams and cyclopels indicates that meltwater was able to entrain sediment from the basal, debris-rich ice, a condition that does not occur under present climatic conditions. This suggests that deglaciation was accompanied by a pronounced climatic amelioration.

Acknowledgments

This thesis has been a particularly interminable labor. John England, my supervisor, has maintained a level of encouragement throughout this process that deserves high praise. Thank you, John. Thanks also to my examining committee for ensuring that the thesis is somewhat understandable.

Major support for this research was provided by the Polar Continental Shelf Project, Department of Energy, Mines and Resources, Ottawa. Without their aircraft and logistical support this research, as is true for essentially all scientific research in the Canadian high arctic, would not have been done. Financial support was provided by NSERC (through J. England), the Boreal Institute for Northern Studies, the Department of Geography, and the Arctic Institute of North America. I enjoyed the able field assistance and fine companionship of Darryl Oakley, Brian Fleming, and Dave Jordan.

Discussions with Ross Powell and Ellen Cowan, Department of Geology, Northern Illinois University, DeKalb, greatly aided my interpretation of the fine-grained sediments in Clements Markham Inlet. Their work in Glacier Bay National Park, Alaska is fundamental to our current understanding of turbid plume suspension deposits in the ice-proximal environment.

Last, but certainly not least, I would like to acknowledge Jan Bednarski. His doctoral research forms the platform which I build upon. Our initial explorations in the wind-swept desert (the infamous summer of 1979) finally draw to a close.

TABLE OF CONTENTS

CHAPTER	PAGE
I. INTRODUCTION	1
Bibliography	5
II. DEPOSITIONAL HISTORY OF TWO HIGH ARCTIC GLACIOMARINE DELTAS	9
Introduction	9
Study Area	10
Previous Studies	11
Stratigraphy	13
Arrowhead Delta Complex	15
Surficial Geology	15
Section Descriptions and Interpretations	16
Arrowhead Delta Discussion	31
Piper Pass Kame Delta	35
Surficial Geology	35
Section Descriptions and Interpretations	36
Piper Pass Discussion	51
Ice-shelf versus Tidewater Glacier Sedimentation	55
Conclusions	60
Bibliography	105
III. SUBPOLAR GLACIOMARINE SEDIMENTS FROM CLEMENTS MARKHAM INLET, N.W.T., CANADA	113
Introduction	113
Study Area	114
Deposits-Lithofacies and Lithofacies Associations	115

CHAPTER PAGE

Lithofacies Association I 115

Lithofacies Association II 121

Lithofacies Association III 123

Lithofacies Association IV 126

Lithofacies Association V 132

Collapse of Previously Deposited Sediments 137

Grain Size of Lithofacies 139

Depositional Model 143

Diamictons and Interbedded Sand and Silt 147

Channelized to Overbank Deposition 149

Turbid Plume 155

Summary 156

Glaciomarine Sedimentation, Glacial Limits, and Paleoclimatic Change 156

Bibliography 209

IV. GENERAL DISCUSSION 222

Bibliography 225

APPENDIX I 226

LIST OF TABLES

Table	Description	Page
II-1	Lithofacies Codes for Sediments Observed	63
II-2	Lithofacies Associations and Interpretations	64
II-3	Stratigraphic Differentiation of Lithofacies and Lithofacies Associations	65
II-4	Stratification Types and Thicknesses	66
II-5	Diamicton Fabric Characteristics	67
III-1	Lithofacies Codes for Sediments Observed	160
III-2	Lithofacies Associations and Interpretations	161
III-3	Stratigraphic Differentiation of Lithofacies and Lithofacies Associations	162
III-4	Stratification Types and Thicknesses	163
III-5	Diamicton Fabric Characteristics	164
III-6	Grain Size Characteristics Summary Statistics	165
III-7	Classification of Sorting Values	166
III-8	Characteristics of Channel Forms	167

LIST OF FIGURES

Figure		Page
I-1	Study area	4
II-1.	Study area	68
II-2.	Surficial geology	69
II-3.	Last ice limit in Clements Markham Inlet	70
II-4.	Emergence curve	71
II-5.	The 118 m shoreline	72
II-6.	High oblique view to NE into Lush Acres	72
II-7.	Section locations	73
II-8.	Fence diagrams of Arrowhead delta	74
II-9.	Generalized stratigraphic columns, Arrowhead Delta	76
II-10.	Photographs of section 2	79
II-11.	Cyclopels and Cyclopsams	82
II-12.	Disrupted, fluidized-liquefied bed	82
II-13.	Paleocurrent measurements, sections 1 and 2	84
II-14.	Trace fossils	85
II-15.	Cyclopels and Cyclopsams	86
II-16.	LA VII, cross-bedded gravelly sand (GSt)	86
II-17.	Steepening, coarsening-upward delta foresets	88
II-18.	Gravel-filled chute	89
II-19.	Topset beds of 103 m delta surface	90
II-20.	Fence diagram for Piper Pass sections	91
II-21.	Generalized stratigraphic columns Piper Pass	93
II-22.	Sketch from photograph of section 18A	96
II-23.	Photographs of section 18B	97
II-24.	Paleocurrent measurements from section 18A/B	99

Figure		Page
II-25.	Paleocurrent measurements, sections 19 and 20	100
II-26.	Sketch of section 21	101
II-27.	Photographs from section 21	102
II-28.	Sketch of ice retreat pattern in Piper Pass	103
III-1.	Study area	168
III-2.	Surficial geology	169
III-3.	Diamicton photographs	170
III-4.	Bivariate plots of S1 vs. S3	171
III-5.	Contoured Schmidt nets of pebble fabric	172
III-6.	Photographs of graded, amalgamated sand	175
III-7.	Graded sand, draped lamination, starved ripples	177
III-8.	Type B climbing ripples	178
III-9.	Starved ripples and draped lamination	178
III-10.	Photograph of fining-upward sequence	180
III-11.	Deformed mass flow and cyclopsams	182
III-12.	Examples of cyclopels	183
III-13.	Ungraded silt overlain by cyclopsams	185
III-14.	Large-scale slump fold	186
III-15.	Contorted bedding	187
III-16.	Sketch of section 21	189
III-17.	Sketch of submarine slope failure	190
III-18.	Ternary plots of grain-size samples	191
III-19.	Grain-size curves	192
a.	Diamicton matrix	193
b.	Silts within diamictons and cyclopels	194
c.	Amalgamated sand and Bouma sequences	196

Figure		Page
III-19.		
d.	Starved ripples	198
III-20.	Bivariate plots, all grain-size samples	199
III-21.	Flow-sediment transformations	200
III-22.	Channels observed in Clements Markham Inlet	201
III-23.	Sketch of subaquatic outwash fan	206
III-24.	Sketch of turbid plumes	207

I. INTRODUCTION

Recent studies of contemporary glaciomarine environments and ancient glacigenic sequences have increased our understanding of depositional processes and the range of stratigraphic sequences resulting from glaciers bordering marine environments (Powell 1980, 1981, 1982, 1983, 1984; Gravenor et al. 1984; Mackiewicz et al. 1984; Eyles et al. 1985). These stratigraphic sequences are generally summarized in facies models. However, while the major purpose of such facies models is to facilitate observations and explanations of the geologic record, they must be continually refined by well-documented examples so that increasingly sophisticated models become available (Walker 1984). Despite this need for representative examples, the best-documented facies models pertaining to the late Quaternary glacial record are predominantly limited to the mid-latitudes (e.g. Cheel and Rust 1982; Thompson 1982; Domack 1983, 1984; McCabe 1986; McCabe et al. 1984). In contrast, stratigraphic-sedimentologic studies on the terrestrially exposed sequences of arctic Canada are rare (e.g. Nelson 1981; Mode et al. 1983; Andrews 1985; Retelle 1986b; Bednarski, in press), and for Greenland are non-existent, despite the dominance of glacier-land-sea interactions on the Quaternary record in this region (Prest 1970; Weidick 1975; Dyke 1979; Boulton et al. 1982; England 1983, 1985; Hodgson 1985; Retelle 1986a). In addition, cold-based glaciers in high latitudes may deposit distinctive sedimentary sequences (Shaw 1977, 1982, 1986; Eyles et al. 1983, 1986) and therefore we cannot assume that mid-latitude observations can be accurately applied to this region.

Furthermore, a large and critical gap in the high arctic's Quaternary database lies in the offshore marine basins which will inevitably gain increasing attention. A logical place to begin is the immediate foreshore or nearshore if glaciomarine processes are to be well-documented. Therefore, this investigation was undertaken to examine the geomorphic, stratigraphic and sedimentologic relationships of two emergent, glaciomarine-subaerial deltas from Clements Markham Inlet, northern Ellesmere Island, N.W.T. (Fig. I-1). These observations are aided by a well-established glacial and sea level history based on numerous radiometric dates (Stewart and England 1983, 1986; Bednarski 1984, 1986). This permits the stratigraphy and sedimentology to be related both to paleowater depths and adjacent landforms.

This study is presented in two main parts. The second chapter utilizes lithofacies associations to describe the stratigraphy of two glaciomarine-subaerial delta complexes. Based on this stratigraphy I interpret both the depositional history and the pattern of glacial retreat at these sites. The third chapter describes and interprets the individual lithofacies that are grouped into the lithofacies associations utilized in chapter 2. This third chapter utilizes a more detailed discussion of the sedimentology which allows the development of a depositional model for these lithofacies associations.

Lithofacies observed in Clements Markham Inlet are strikingly similar to those documented by contemporary process studies in temperate regions such as Glacier Bay in southeast Alaska (Powell 1980, 1981, 1983; Mackiewicz et al. 1984; Powell and Cowan 1986).

As well, the vertical lithofacies association successions in Clements Markham Inlet are similar to those predicted by several facies models (Eyles et al. 1983, 1986; Powell 1985) demonstrating greater similarity between mid- and high latitude glaciomarine environments than was initially expected. Despite the present polar desert climatic regime, conditions during deglaciation at this high arctic site were much warmer implying that differentiation of the major glacioclimatic environments in the geologic record will be more difficult than previously expected.

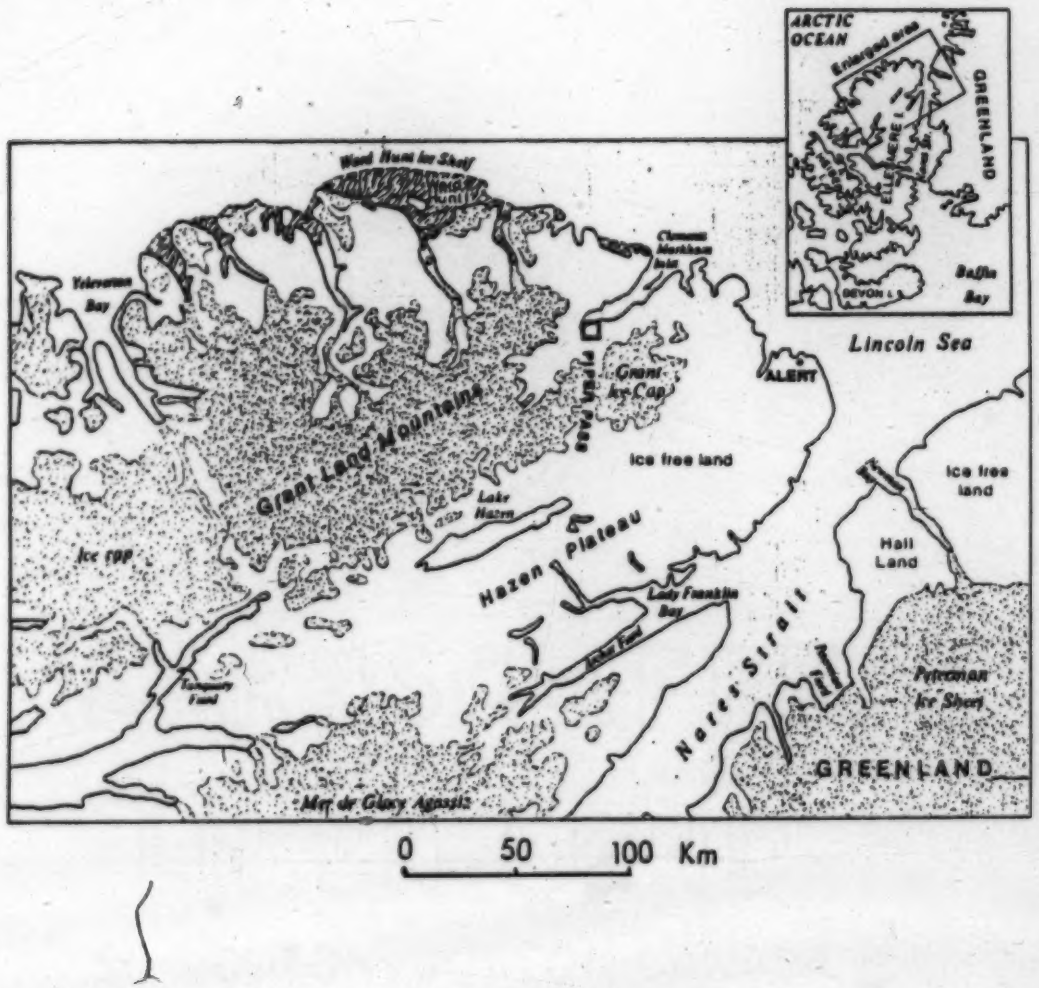

Figure I.1. Northern Ellesmere Island. Study area is located at the north end of Piper Pass where it joins Clements Markham Inlet. Note the extent of permanent icefields and outlet glaciers (stippled) which cover most of the Grant Land Mountains. Inset shows the relationship of Ellesmere Island to NW Greenland.

BIBLIOGRAPHY

Andrews, J.T. 1985. Grain-size characteristics of Quaternary sediments, Baffin Island region. in J.T. Andrews, ed., Quaternary environments-eastern Canadian arctic, Baffin Bay, and western Greenland, 124-153.

Bednarski, J. 1984. Glacier fluctuations and sea level history of Clements Markham Inlet, northern Ellesmere Island. Unpub. Ph.D. thesis, University of Alberta, 232p.

Bednarski, J. 1986. Late Quaternary glacial and sea level events, Clements Markham Inlet, northern Ellesmere Island, Arctic Canada. Canadian Journal of Earth Sciences 23, 1343-1355.

Bednarski, J. in press. The geomorphology of glaciomarine sediments in a high arctic fiord. Geographie physique et Quaternaire.

Boulton, G.S. et al. 1982. A glacio-isostatic facies model and amino acid stratigraphy for late Quaternary events in Spitsbergen and the Arctic. Nature 298, 437-441.

Cheel, R.J. and Rust, B.R. 1982. Coarse grained facies of glaciomarine deposits near Ottawa, Canada. in R. Davidson-Arnott, W. Nickling and B.D. Fahey, eds. Research in glacial, glacio-fluvial, and glacio-lacustrine systems, 279-295.

Domack, E.W. 1983. Facies of late Pleistocene glacial-marine sediments on Whidbey Island, Washington: an isostatic glacial marine sequence. in B.F. Molnia, ed. Glacial-marine sedimentation, 535-570.

Domack, E.W. 1984. Rythmically bedded glaciomarine sediments on Whidbey Island, Washington. Journal of Sedimentary Petrology, 54, 589-602.

England, J. 1983. Isostatic adjustments in a full glacial sea. Canadian Journal of Earth Sciences, 20, 895-917.

England, J. 1985. The late Quaternary history of Hall Land, N.W. Greenland. Canadian Journal of Earth Sciences 22, 1394-1408.

Eyles, C.H., Eyles, N. and Miall, A.D. 1985. Models of glaciomarine sedimentation and their application to the interpretation of ancient glacial sequences. Palaeogeography, Palaeoclimatology, Palaeoecology, 51, 15-84.

Eyles, N., Eyles, C.H. Miall, A.D. 1983. Lithofacies types and veritical profile models; an alternative approach to the description and environmental interpretation of glacial diamict and diamictite sequences. Sedimentology, 30, 393-410.

Eyles, N., Eyles, C.H. and Miall, A.D. 1986. Reply to Shaw's comments. Sedimentology 33, 151-155.

Gravenor, C.P., Von Brunn, V. and Dreimanis, A. 1984. Nature and classification of waterlain glacigenic sediments, exemplified by Pleistocene, late Paleozoic and Precambrian deposits. Earth-Science Reviews 20, 105-166.

Hodgson, D.A. 1985. The last glaciation of west-central Ellesmere Island, Arctic Archipelago, Canada. Canadian Journal of Earth Sciences, 22, 347-368.

Mackiewicz, N.E., Powell, R.D., Carlson, P.R., and Molnia, B.F. 1984. Interlaminated ice-proximal glacimarine sediments in Muir Inlet, Alaska. Marine Geology, 57, 113-147.

McCabe, A.M. 1986. Glaciomarine facies deposited by retreating tidewater glaciers: an example from the late Pleistocene of Northern Ireland. Journal of Sedimentary Petrology 56, 880-894.

McCabe, A.M., Dardis, G.F. and Hanvey, P.M. 1984. Sedimentology of a late Pleistocene submarine-moraine complex, County Down, Northern Ireland. Journal of Sedimentary Petrology 54, 716-730.

Mode, W.N., Nelson, A.R. and Brigham, J.R. 1983. A facies model of Quaternary glacial-marine cyclic sedimentation along eastern Baffin Island, Canada. in, B.F. Molnia, ed., Glacial-marine sedimentation, 495-533.

Nelson, A.R. 1982. Quaternary glacial and marine stratigraphy of the Qivitu Peninsula, northern Cumberland Peninsula, Baffin Island. Geological Society of America Bulletin 92, Part I, 512-518, Part II, 1143-1281.

Powell, R.D. 1980. Holocene glacimarine sediment deposition by tidewater glaciers in Glacier Bay, Alaska. Unpub. Ph.D. thesis, Ohio State University, 420p.

Powell, R.D. 1981. A model for sedimentation by tidewater glaciers. Annals of Glaciology, 2, 129-134.

Powell, R.D. 1983. Glacial-marine sedimentation processes and lithofacies of temperate tidewater glaciers, Glacier Bay, Alaska. in B.F. Molnia, ed. Glacial-marine sedimentation, 185-232.

Powell, R.D. 1984. Glacimarine processes and inductive lithofacies modelling of ice shelf and tidewater glacier sediments based on Quaternary examples. Marine Geology, 57, 1-52.

Powell, R.D. and Cowan, E.A. 1986. Depositional processes at McBride Inlet and Riggs Glacier. In, P.J. Anderson, R.P. Goldthwait, G.D. Mackenzie, eds., Observed Processes of glacial deposition in Glacier Bay, Alaska. Ohio State University, Institute of Polar Studies Miscellaneous Publication No. 236, 101-112.

Prest, V.K. 1970. Quaternary geology of Canada. In, Geology and economic minerals of Canada. Geological Survey of Canada, Economic Geology Report No. 1, 675-764.

Retelle, M.J. 1986a. Glacial geology and Quaternary marine stratigraphy of the Robeson Channel area, northeastern Ellesmere Island, Northwest Territories. Canadian Journal of Earth Sciences 23, 1001-1012.

Retelle, M.J. 1986b. Stratigraphy and sedimentology of coastal lacustrine basins, northeastern Ellesmere Island, N.W.T. Geographie physique et Quaternaire 40, 117-128.

Shaw, J. 1977. Tills deposited in arid polar environments. Canadian Journal of Earth Sciences 14, 1239-1245.

Shaw, J. 1982. Melt-out till in the Edmonton area, Alberta, Canada. Canadian Journal of Earth Sciences, 19, 1548-1569.

Shaw, J. 1986. Discussion: Lithofacies types and vertical profile models; an alternative approach to description and environmental interpreation of glacial diamict and diamictic sequences. Sedimentology 33, 149-150.

Stewart, T.G. and England, J. 1983. Holocene sea-ice variations and paleoenvironmental change, northernmost Ellesmere Island, N.W.T., Canada. Arctic and Alpine Research, 15, 1-17.

Stewart, T.G. and England, J. 1986. An early Holocene caribou antler from northern Ellesmere Island, Canadian Arctic Archipelago. Boreas, 15, 25-31.

Thompson, W.G. 1982. Recession of the late Wisconsin ice sheet in coastal Maine. in, G.J. Larson and B.D. Stone, eds., Late Wisconsin glaciation of New England, Kendall/Hunt Publishing Company, 211-228.

Walker, R.G. 1984. General introduction: facies, facies sequences and facies models. in R.G. Walker, ed. Facies models, 2nd ed., Geoscience Canada reprint series 1, 1-9.

Weidick, A. 1975. A review of Quaternary investigations in Greenland. Ohio State University, Institute of Polar Studies Report No. 55, 161p.

II. DEPOSITIONAL HISTORY OF TWO HIGH ARCTIC GLACIOMARINE DELTAS

Introduction

Throughout Arctic Canada and Greenland, the ages and elevations of raised marine shorelines provide the cornerstone for deciphering past glacial activity. Nonetheless, only a few sedimentologic investigations of their related marine sediments have been conducted (e.g. Nelson 1981; Andrews 1983; Mode et al. 1983; Retelle 1986a; Bednarski, in press) despite the fact that they comprise the principle surficial deposits over vast areas (e.g. Andrews 1970; Prest 1970; Weideck 1975; Dyke 1979; England 1985; Hodgson 1985). This gap is particularly noticeable given our increased understanding of glaciomarine sedimentation in recent years and the considerable paleoenvironmental record they contain (Powell 1981, 1982, 1983, 1984; Eyles et al. 1983, 1985; Gravenor et al. 1984).

This and a companion paper discuss the geomorphic, stratigraphic and sedimentologic relationships of two emergent, glaciomarine-subaerial deltas from Clements Markham Inlet, northern Ellesmere Island, N.W.T. (Fig. II-1). These observations are aided by a well documented glacial and sea level history based on > 100 radiocarbon dates (England 1983; Stewart and England 1983; Bednarski 1984, 1986). This permits the stratigraphy and sedimentology to be related to both paleowater depths and adjacent landforms. These observations document vertical lithofacies successions that are similar to those

predicted by several facies models developed in midlatitudes and indicate greater similarity between mid- and high latitude glaciomarine environments than might be expected. This has important implications for the paleoenvironmental conditions prevailing during the deglaciation of the high arctic and adds new constraints to our ability to differentiate major glacioclimatic environments in the geologic record. The chronologic, geomorphic and stratigraphic information presented in this chapter provides the basis for the more detailed sedimentologic analysis of the lithofacies and their depositional mechanisms in the second chapter.

Study Area

Clements Markham Inlet is 50 km long, 8 km wide, and trends NE-SW, extending from the Arctic Ocean-Lincoln Sea into the Grantland Mountains (Figs. II.1 and II.2). The inlet parallels the structural trends of the late Proterozoic to late Tertiary sedimentary strata (Christie 1964; Trettin 1972; Bednarski 1984, 1986). Summits rise to 2000 m above sea level (asl) at the inlet head and decline to 600 m asl along the outermost coast. Despite this high relief, the adjoining valleys such as the Clements Markham and Piper Pass rivers occur at low elevations and have low gradients for many kilometers before reaching the inlet. The lower parts of these valleys are now dominated by active sandurs emanating from the numerous outlet glaciers that occur ca. 8 to 30 km inland. High postglacial seas (> 100 m asl) previously transgressed these valleys and strongly influenced the nature of

sedimentation and the rate of glacial retreat. All the rivers and smaller gullies incise extensive postglacial sediments that emerged after the deglaciation of the inlet head (Figs. II.2, II.3)

Mean annual temperatures range from -18 °C at the coastal station of Alert to -23 °C in the continental interior surrounding Lake Hazen (Fig. II.1). The region has a polar desert climate with a water balance close to zero (Bovis and Barry 1974). Despite this aridity and short ablation seasons (ca. 50 to 80 days, Bradley and England 1978) large volumes of meltwater are produced as indicated by the large, active floodplains of the major valleys. Today, the outlet glaciers surrounding the inlet are subpolar (Fig. II.1). This is shown by their low englacial temperatures (-24 °C at 1805 m a.s.l., Hattersley-Smith 1960); minor penetration of meltwater during the ablation season (Muller and Aiken 1973; Muller 1976; Aiken 1977); and thick, sediment-rich basal ice (Stewart and Bednarski 1986).

Previous Studies

Marine Silts

Previous investigators reported that marine silts were the most widespread Quaternary deposit surrounding the raised deltas of Clements Markham Inlet (Christie 1967; Stewart 1981; Bednarski 1986). These silts are saline and they exhibit a strong brine smell upon excavation and abundant salt effloresences upon desiccation. At their base they contain a very sparse marine fauna dominated by Portlandia arctica and Thyasira dunbari

prompting their description as barren silts (Stewart 1981). The upper part of these barren silts ends where the fauna increase in frequency and diversity. Commonly Hiatella arctica and Mya truncata dominate this transition and these samples are often used for radiocarbon dating the marine limit (Bednarski 1986).

The paleoenvironmental explanation for the faunal transition assumes that there was a reduction in the turbid freshwater influx as tidewater glaciers retreated onto land (Stewart 1981). Therefore the bulk of the barren silts predating the faunal transition are glaciomarine rather than prodeltaic. These fine-grained sediments and faunal sequence are similar to those reported elsewhere on Ellesmere Island and from more distant localities (Bloom 1963; Wagner 1970; England 1978; Hodgson 1985). The distribution and stratigraphic relationships of these glaciomarine silts to the adjoining lithofacies provide an important link to deciphering the depositional record of ice retreat at this high arctic site.

Last Ice Limit and Sea Level History

Bednarski's (1986) reconstruction of the last ice limit shows that both the main Clements Markham trunk glacier and adjacent cirque glaciers did not infill the inlet but rather terminated in a full glacial sea at 11,000 BP (Fig. II.3). In Clements Markham Inlet the limit of the full glacial sea ranges from 92 m asl at the outermost coast to 124 m asl at the inlet head (Fig. II.3; Bednarski 1986). This gradient on the limit of the full glacial sea is due to the decreasing amount of glacioisostatic loading and unloading that occurs with increasing

distance beyond an ice load (Walcott 1970, 1972). Inside the last ice limit, the marine limit declines because some emergence occurred beneath the thinning ice prior to its retreat (restrained rebound, Andrews 1970). Therefore, the degree to which the marine limit declines in this zone is controlled by the local date of deglaciation and the preceding rate of unloading (Andrews 1970; Dyke 1979; England 1983; Bednarski 1986). This chapter is concerned with an area just inside the last ice limit where glaciers in this sea retreated into two interconnected valleys: 1)Arrowhead-Lush Acres; and 2)Piper Pass (Figs. II.2, II.3). The local marine limits at these two sites are 118 m and 114 m asl, respectively, and based on local radiocarbon dates and the emergence curve, this indicates that deglaciation occurred around 8000 to 8500 BP.

Stratigraphy

Generalized Sections and Fence Diagrams

The stratigraphy of the two deltas is discussed in relationship to both composite sections and fence diagrams (Figs. II.8, II.9; see also Piper Pass section). The sections present information at a lithofacies level utilizing a shorthand code (Table II-1). Lithofacies differentiation is based on field criteria such as: grain size; sorting; sedimentary structures; and bed thickness. The lithofacies are grouped together into lithofacies associations (LA I to VI, Table II-2). All of these criteria contributed to the field descriptions and stratigraphic differentiation (Table II-3). The fence diagrams represent the

three-dimensional relationships of the recorded sections. They are generalized from these sections utilizing the lithofacies associations (Table II-3). The lithofacies associations are similarly based on groupings documented in the field.

The lithofacies associations (LA, Table II-2) predominantly relate to the retreat of glaciers that were in contact with the sea. Rapid retreat resulted in the deposition of interbedded diamicton, sand and silt of LA I (cf. Powell 1981). Stabilization at valley confluences allowed production of subaquatic outwash fans with deposition of channel gravels (LA II); sands (LA III); and related levee-overbank (LA IV) deposits. The largest volume of sediments in Clements Markham Inlet are silts (and related sands) derived by suspension settling from turbid plumes (LA V). When the glaciers retreated onto land, sandurs and fan (Gilbert) deltas of LA VI prograded over the previously deposited glaciomarine deposits.

The sediments from these two deltaic complexes can be subdivided into three stratigraphic intervals (Table II-3). These include: 1)deposition related to glacial advance; 2)glaciomarine sedimentation during the subsequent retreat of a tidewater glacier; and 3)the establishment and progradation of terrestrial sandurs and related deltas and deltaic foreset beds as glaciers retreated inland. Deposits of unit 3 can be further subdivided into deltas and beaches related to the initial interval of slow emergence (rsl >100 m asl, 10,000 to 7800 BP, Fig. II.4) and to the interval of rapid emergence after 7800 B.P. (rsl <100 m asl). Only the deposits related to the earlier interval (10,000 to 7800

BP) are discussed here. Units 1 and 3 comprise a relatively minor part of the total sediment volume in Clements Markham Inlet. Therefore their related deposits are described and interpreted in this chapter only, within the context of the deltas' history. Those deposits related to the actual glaciomarine phase are presently discussed only in sufficient detail to justify depositional interpretations within a stratigraphic context. Although the lithofacies associated with this glaciomarine sedimentation are utilized here (Tables II-1 to II-3), their differentiation and interpretation, together with a depositional model, are elaborated in chapter 3.

Arrowhead Delta Complex

Surficial Geology

The marine limit is located immediately east of the Arrowhead delta where a horizontal bench abuts a bedrock slope at 118 m asl at the eastern end of Lush Acres (Figs. II.2, II.5, II.6, II.7). This horizontal bench is ca. 15 m wide and 75 m long with a pea gravel surface. The next lowest shoreline observed is the prominent sandur developed within Lush Acres that grades to a delta lip marking a 103 m relative sea level 1 km to the NW. The sandur surface has well developed paleochannels and several large kettle lakes (Fig. II.6).

The 118 m bench is 6 m lower than the limit of the full glacial sea directly across the inlet (Fig. II.3; Bednarski 1986). Presumably, when relative sea level was at 124 m asl, the sea was excluded from Lush Acres by distributary ice from Piper Pass which coalesced with ice flowing down the Arrowhead valley

from the Grant Ice Cap to the inlet (Fig. II.3, 11,000 BP). By the time local sea level had fallen to 118 m asl, the Arrowhead glacier had retreated along its eastern margin allowing the entry of the sea. The oldest samples of driftwood and marine shells collected directly in front of the Arrowhead delta dated 8915±115 BP (S-2211, Stewart and England 1983) and 7965±65 BP (SI-4316, Bednarski 1986), respectively. Because shorelines at 118 m asl were not observed elsewhere in Lush Acres it is concluded that the ice, though stagnating, still occupied most of this area until sea level had fallen to ca. 103 m. Based on the history of postglacial emergence between 118 and 103 m asl (Bednarski 1986; Figs. II.6, II.7) it is apparent that this ice stagnation must range from ca. 10,000 to 7900 BP. Finally, the sandur prograded over this stagnant ice as indicated by the prominent kettle lakes on the surface of the 103 m delta (see Bednarski 1986; Fig. II.6). Paleochannels on the 103 m sandur also rise towards Piper Pass indicating that ice from that source contributed meltwater through Lush Acres to the 103 m shoreline at the Arrowhead Delta (Fig. II.6). This means that ice from Piper Pass remained in contact with the westernmost margin of Lush Acres until ca. 7900 BP.

Section Descriptions and Interpretations

The sections within the Arrowhead delta are presented in a sequence from most distal, to most proximal, and then to slightly more distal parts of the complex. This sequence utilizes the marine silt distribution as a stratigraphic marker horizon which

permits differentiation of the stratigraphic sequence of units 1 to 3. Sections 11 and 12 (Fig. II.7) were discussed in Stewart (1981) and Stewart and England (1983) and relate to the interval of rapid emergence. They are not discussed here.

Sections 1 to 4, and the area distal to the 103 m delta lip

Description

Sections 1 to 4 occur along the lower, east side of the Arrowhead River near the valley wall (Figs. II.2, II.7, II.8, II.9). Here extensive glaciomarine silts have been dissected by large asymmetric gullies up to 0.5 km long and > 20 m deep generally revealing coarser sediments at depth. The 103 m delta did not prograde over these sections. Depending on the individual stratigraphic sequence in these secions, fining upwards is shown by LA II (gravels) overlain by LA III (amalgamated, graded sand) overlain by IV (graded, laminated and current bedded sand) overlain by LA V (interbedded and interlaminated sand and silt). In these sections the sand lithofacies (III and IV) display the following sedimentary structures: graded and amalgamated beds, convolute lamination, water escape structures, dish structures and type B pillars, climbing ripples and starved ripples (Fig. II.10). Thin-bedded or thinly-laminated mud drapes are interspersed throughout.

Wherever it occurs LA III sand diminishes upwards. This is particularly well shown in section 2, with its progressive upward fining and decrease in bed thickness. Concomitantly there is an increase in the number and thickness of silt beds until these become dominant (Figs. II.10a, b, c, d).

Section 4 is the only location where a prominent channel was observed adjacent to the Arrowhead river (Figs. II.8, II.9). This channel trends NE and is ca. 40 m wide and 5 m deep. The section consists of a fining upward sequence of LA II (gravel), LA III (sand), LA Va (Scps, cyclopsams) and LA Vb1 (Fcpl, cyclopels). The gravels are only exposed at the channel's north side and dip gently to the south, i.e. toward the channel. LA III sands conformably overlie LA II gravel and have the same dip. LA V overlies these two lithofacies as in the other sections but here it drapes and accentuates the underlying channel.

The LA II gravels are poorly exposed but the few excavated beds were medium- to thickly-bedded with the largest clasts being ca. 5 to 7 cm (b-axis). Beds are both reverse and normally graded and the gravels are both matrix- and clast-supported. Gravelly sand, sand and mud drapes occur. As noted, the LA III sand beds conformably overly the LA II gravels and have the same dip but, whereas the gravels disappear beneath the upper units when traced to the south, the LA III sand beds terminate <u>against</u> overlying LA V sand and silt. At this position packets of LA III sand, 0.5 to 1.0 m thick, have slumped towards the channel (south). These, in turn, are overlain by undeformed LA V. On the south side of the channel these sands also form slumped packets towards the channel (i.e. to the north).

LA Va sand and Vb silt comprises the central and upper part of section 4 but are mostly inaccessible. Along the channel's south margin, however, certain characteristics of LA Va are evident. Individual laminae that do not vary in thickness are

horizontal where they overly the horizontally-bedded LA III. However, these same beds conformably drape the channel margin and become horizontal again within the channel. These beds are graded and composed of alternating laminae of fine sand, silt and mud drapes (Fig. II.11). Isolated cobbles and small pebble clusters also occur. Furthermore, an unusual and distinctive wedge-shaped bed of disrupted LA Vb1 silt with silt clasts is found here (Fig. II.12).

A separate and prominent area composed of LA Vb1 occurs immediately distal to section 7 and the 103 m delta lip (Figs. II.2, II.8). Here a silt ridge rises to ca. 101 m asl, just two meters lower than the delta lip. The area is extensively gullied exposing individual sections up to 40 m high. Traverses through this area failed to reveal any diamictons, gravel or sand lithofacies within the LA Vb1 silts. Individual sand beds and laminae do occur but these are interspersed within the silts.

Interpretation

The sedimentary structures of LA II and III reflect deposition by relatively proximal, turbidity current and mass flow processes of both high and low density (Table II-2; Lowe 1982; Hein 1982; Walker 1985; Chapter 3). In a glacial environment these characteristics cumulatively suggest deposition on a subaquatic outwash fan (Rust 1977; Cheel and Rust 1982; Thomas 1984a, b). However, features of LA IV, such as graded beds, climbing ripples, and even starved ripples, have been reported from deposits attributed to environments that range from proximal bottomset beds of a marine fan (Gilbert) delta (Shearer

1974; Wightman 1977) to subaerial outwash (Gustavson et al. 1975; Allen 1982; Thomas et al. 1985). The well exposed fining-upward stratigraphic sequence at section 2, therefore, is particularly useful in differentiating between these interpretations.

The barren silts in Clements Markham Inlet are marine based on the documented sea level history and its associated fauna. Therefore in section 2, the gradational down-section change from the marine silts of LA Vb1 to the sands of LA IV and III (Figs. II.8, II.9, II.10) also necessitates their deposition in a marine environment. Furthermore, the glacioisostatic history from Clements Markham Inlet precludes a slow transgression after deglaciation. Rather, these conditions show an overstep condition whereby the sea immediately replaced the retreating ice up to an elevation of ca. 103 to 124 m asl (Bednarski, in press). Therefore these underlying gravels and sands cannot reflect subaerial deposits following ice retreat because they were deposited from 36 to 60 m below the deglacial marine limit. Because these sands are not associated with a corresponding subaerial fan-delta they cannot be proximal bottomset beds. The only alternative process for deposition of these sands then is subaquatic outwash. The presence of subaquatic outwash has important paleoclimatic implictions that will be discussed later.

The LA II gravels in section 3 and 4 particularly demonstrate proximity to a sediment source. In section 4 the gravel and sand beds are interpreted as outwash within a subaquatic fan channel close to the ice front. The change from LA III to LA Va and Vb deposition in this channel records a transition from traction to

suspension sedimentation which likely coincides with ice retreat. Nonetheless, some traction currents continued to occur as indicated by the undercutting and slumping of sands together with the erosional and contorted bedding within the silt beds.

The base of sections 1, 2, 3, and 4 represent deposition within a single turbidity current channel on a subaqueous outwash fan. This is indicated by their similar stratigraphic sequence; their location along the same valley wall; and the consistent paleocurrents of their overbank/levee sediments (LA IV). The paleocurrents recorded in sections 1 and 2 are oriented towards the NNW (Fig. II.13). Orientations were not observed in the opposite direction possibly because the channel was so close to the valley wall limiting exposures. Gilbert (1983) reports the presence of such valley-wall channels from contemporary fiords on Baffin Island.

LA Va and Vb are suspension deposits as indicated by their conformable draping of underlying beds (e.g. section 4) and their lack of sedimentary structures indicating bedload transport in the sand laminae. Additionally, the thick, poorly-sorted silts of LA Vb indicate deposition by flocculation. These deposits resemble those reported from the contemporary glaciomarine environment where turbid overflow plumes of buoyant glacial meltwater override the saline, and therefore denser, fiord water generating suspension settling (Elverhoi et al. 1980; Powell 1980, 1983; Mackiewicz et al. 1984). Initial turbulence in these plumes is sufficient to transport large amounts of sand in suspension. Although most of this sand quickly drops from these

plumes diminishing quantities can be transported up to 3.2 km (Powell 1980; Mackiewicz et al. 1984). At such distal locations this produces fine sand laminae and partings as thin as one grain within the dominant flocculated silts and clays. These repetitive deposits of sand and silt are termed cyclopels (Mackiewicz et al. 1984). In more proximal locations suspension settling of sand dominates and produces thinly-bedded and laminated sands which are termed cyclopsams (Mackiewicz et al. 1984; Cowan et al. 1986). The interpretation of LA Va and Vb1 as cyclopsams and cyclopels is particularly relevant to the stratigraphy of Clements Markham Inlet. First, it shows that when glacial meltwater streams shift position, or the ice face retreats, proximal subaquatic outwash will be replaced by turbid plume sedimentation. Second, this style of sedimentation is consistent with the deglacial biostratigraphic evidence whereby a marked faunal transition occurs within the barren silts as the glaciers retreated onto land. Third, even though turbid plume deposition may predominate, larger-scale turbidity currents and underflows still reach more distal sites (cf. Mackiewicz et al. 1984) accounting for the undercutting and slumping of the sand facies in section 4.

Sections 8, 9, 10

Description

Section 8 is located along the lower west side of the Arrowhead River where it erodes into sediments 1 km seaward of the 103 m delta (Figs. II.7, II.8, II.9). The section begins at

21 m asl and consists of ca. 12 m of medium- to thin-bedded LA Vb1. Here, the bedding planes of the lower part of the section contain abundant, well preserved trace fossils (Fig. II.14). These beds are unconformably overlain by horizontally-bedded gravels. Further along the exposure at sections 9 and 10 (Fig. II.8) the upper level consists of horizontally-bedded sands and silts with common plants and marine shells. Plants collected from these bedded sands were dated at 7070±115 BP (S-2504).

Interpretation

The upper portions of sections 9 and 10 are prodeltaic bottomset beds. The date of 7070 BP indicates they were deposited in ca. 70 m of water during the period of rapid emergence following deglaciation (ca. 7800 BP). The beds at section 8 underlie these and are the same as the cyclopel beds described above. These likely relate to the earlier period of slow emergence (ca. 10,000 to 7800 BP) when the glaciers were in contact with the sea.

The trace fossils are a fish trail and unidentified trackways. The abundance of trace fossils here indicates considerable biological activity during deglaciation despite the high influx of fresh, turbid water (see Marine Silts). Trace fossils may be much more abundant in Clements Markham Inlet as exposures where the bedding planes can easily be separated are not common. Thus trace fossils are likely common in other areas of glaciomarine sediments on Ellesmere Island and Greenland and provide an added component for paleoenvironmental interpretation (Dale et al. 1987). Additionally, the intricate structure preserved along

these bedding planes underscores the fine detail that can be preserved in these monotonous barren silts.

Sections 8, 9 and 10 provide an important extension of the sedimention recorded at sections 1 to 4 to the east. Collectively, this area of the Arrowhead delta demonstrates the diversity of submarine environments during and immediately following deglaciation. These sections are just a small sample of the hundreds of exposures in proximal prodelta sediments in the lower inlet and would be important sites for documenting Gilbert-delta sedimentary environments as well as Holocene paleoenvironments (Stewart 1981; Stewart and England 1983).

Section 6

Description

Section 6 is located beneath the kettled sandur along the creek which drains a large kettle lake in the center of Lush Acres (Figs. II.2, II.6, II.8, II.9). The section is composed of ca. 44 m of LA Vb1 directly overlain by ca. 1 to 2 m of gravels from the 103 m delta surface. Only the lower 6 m of the section is easily accessible but it is well exposed almost to the delta surface. Across the width of the exposure the beds are horizontal (30 m). The lower part of the section consists of individual fining-upward sequences ca. 0.3 to 1.5 m thick. These sequences consist of the following. 1)Thin- (a few medium-) bedded sands often with load casts, ball and pillow, and water escape and flame structures (Fig. II.15). Erosive contacts are rare. 2)Very thinly-laminated to very thinly-bedded sands interbedded with

very thinly- to thinly-bedded silty clays. The sands form distinct partings a few grains to 1 to 2 cm thick within the silty clays (Fig. II.15). At some sites these sands exhibit micro-flame, micro-loading, and micro-water escape structures on a scale of 1 mm; 3)Thin-to-medium bedded silty clays some of which are 0.6 m thick. Sand partings in these silty clays are rare but color variations may indicate textural variations.

Above the accessible lower 6 m the same repetition of beds as the lower part is readily apparent. At ca. 68 and 72 m there are slumped, loaded and convoluted horizons, each ca. 1 m thick with fold amplitudes of ca. 0.5 to 1 m (Fig. II.9). Faults with a ca. 5 cm displacement occur at individual fold noses.

Along the main face described above the fine-grained sediments are directly overlain by the 103 m topset gravels. However, intervening sediments were observed ca. 75 m upstream within a small tributary to the main creek. At this site gravelly sands form trough cross beds ca. 0.5 m thick (Fig. II.16). This unit is ca. 5 m thick and is overlain by the gravel topsets of the 103 m delta.

Interpretation

The very thinly-bedded sands are interpreted as cyclopsams derived from the coarser fraction of turbid overflow plumes. The adjacent silt beds are interpreted as cyclopels and are the flocculated counterparts of the same turbid overflows. The sandy partings and silt (Fig. II.15) display a striking correspondence to the turbid plume cyclopels described by Mackiewicz et al. (1984) and to photographs in Powell and Cowan (1986; also E.

Cowan, pers. comm., 1986). Erosive contacts that smear out some of the mm-thick sand partings indicate some transport by traction currents. The micro-flame and loading structures in these sand partings indicate settling due to density gradients and varying water contents between the different laminae. The small scale of these features again underscores the level of detail present in the seemingly homogeneous barren silts.

The sediments of section 6 were deposited as the ice front retreated into Lush Acres. LA V is present up to ca. 100 m asl indicating that parts of this marine basin were virtually filled by the fine-grained sediments. However, the topography infilled by the prograding 103 m delta was irregular as shown by the cross-bedded gravelly sands that underlie the delta topset beds just upstream from this section. These beds are interpreted as distributary mouth bars of a prograding delta front platform. In other areas along the upper part of this creek, the basin was infilled with LA Va and Vb1 such that a true delta front platform or other prodelta deposits were not formed until the vicinity of section 7 (see below).

Section 5

Description

Section 5 (Figs. II.2, II.7, II.8, II.9) is located ca. 200 m downstream from section 6. The bottom 10 m begins with bedded sand with minor gravel and coarsens upwards to a gravel horizon that terminates beneath a 1.0 to 1.5 m thick diamicton. The diamicton is overlain by ca. 39 m of LA Vb1 and these silts are

finally overlain by gravels of the 103 m delta.

The lowermost sand has a crude horizontal bedding and dispersed granules and gravels. A 1.5 m wide channel is incised into the gravelly sand (Fig. II.9). The channel fill begins with cross-bedded sands and coarsens to gravel over a height of 1.4 m. The average size of the largest clasts is 11.6 cm (b-axis, n=7). Above this are sand and mud with gravel lenses displaced by a prominent, low-angle reverse fault with a throw < 0.5 m towards the inlet. Above the fault are cross-bedded, alternating cobbles and pebbles to sands some of which are terminated by silt drapes. The gravel sets are obscured by colluvium near their base but the crossbeds are at least 1.5 m thick. They have apparent dips of ca. 15° towards the north (inlet). The coarser fraction is both normal and reverse graded. Pebbles are well rounded and clast orientation is parallel to the cross bedding. Most gravel beds are clast-supported with sand filling the interstices but one prominent layer is clast-supported without sand.

The contact between the gravel and the overlying diamicton is sharp; however, there are individual rounded cobbles in the overlying diamicton that project into the gravel bed. These appear to have been partially lifted out of the underlying bed. Furthermore, the diamicton's coarse fraction is dominated by rounded cobbles similar to those of the underlying cross-bedded gravels and angular, fragmented phyllite clasts are subdominant. Textural variations include normal- to reverse-graded diamictons as well as sand and silt interbeds. Three fabrics were measured in the diamicton (fabrics 5.1, 5.2, 5.3, Table II-5). These have

S1 eigenvalues of .38, .55 and .51, respectively. The overlying silts (39 m thick) are desiccated and the surface was fragmented so sedimentologic observations were not recorded. The sandur gravels form a capping of ca. 1 to 2 m but are poorly exposed here.

Interpretation

The origin of the sand and gravel in the base of this section is problematic. These sediments exhibit features common to both gravelly braided streams (Miall 1977; Steel and Thompson 1983) and proximal subaquatic outwash (Cheel and Rust 1982) which is analogous to proximal mass flow deposits of deep sea fans or submarine canyons (Winn and Dott 1976; Walker 1977; Hein 1982). This difficulty in distinguishing between subaerial and subaquatic deposits is a problem encountered in several marine limit-related glaciomarine sequences (Armstrong 1981; Clague 1984). A means of demonstrating marine origin for such gravels is their presence below marine limit (Rust and Romanelli 1975) or their association with deep water turbidite facies which precludes a subaerial interpretation (Winn and Dott 1976; also sections 3 and 4 above). Finally, subaquatic mass flows may also produce cobble orientations with an a-axis parallel to flow (Walker 1977; Hein 1982). The large-scale planar cross beds in section 5, however, are inappropriate for this analysis. Therefore the classification of these deposits as marine versus terrestrial rests upon their stratigraphic relationships which are discussed below.

The sharp contact between the diamicton and the gravel appears erosive suggesting a disconformable relationship between the two units. In glacial sequences such erosive contacts are often overlain by meltout or lodgement tills (Eyles et al. 1983). However, in this section no structures indicative of these facies was seen. Rather the reverse grading; the interbedding of the diamictons with sands and silts; and the low eigenvalues of the diamicton fabrics suggest that they originated as debris flows (Table II-5; see chapter 3 for detailed discussion of the diamictons). The erosive contact would then represent glacier overriding which incorporated the well-rounded cobbles from the underlying deposit. Subsequent glacier retreat resulted in debris flows from the debris-rich basal ice. This interpretation infers that the cross-bedded unit was not a subaquatic outwash fan deposited during ice retreat and therefore it is not approximately coeval with the diamictons but, rather, that it is an older deposit.

Further support for this is the presence of rounded cobbles in the diamicton, but a lack of <u>angular</u> phyllite from the diamicton incorporated in the cross-bedded gravels. The phyllite is locally derived from outcrops along the sides of Lush Acres and the angularity reflects its glacial origin. If the sub-diamicton gravels were derived directly from the glacier and deposited as subaquatic outwash then some angular phyllite would be in the cross beds. If the gravels were transported across a subaerial sandur then the phyllites would be rounded; thus this is the preferred interpretation. Therefore the basal unit of

sand-to-gravel represents a coarsening-upward, subaerial, proglacial outwash produced during the glacial advance which ultimately deposited the overlying diamicton. If this is correct this lower unit is the first deposit yet recognized in Clements Markham Inlet that is older than the diamicton units and thus older than the last deglaciation (i.e. ca. 10,000 to 11,000 BP).

The silts overlying the diamicton are turbid plume deposits related to ice retreat into Lush Acres. The overlying gravels relate to the subsequent deposition of the uppermost Arrowhead delta at 103 m. At this site, the silts infilled this trough so that little relief exisited during sandur progradation which precluded the deposition of any delta-front platform or delta foreset sediments.

Section 7

Description

Section 7 is located ca. 200 m downstream along the same creek from section 5 (Figs. II.2, II.7, II.8, II.9). The section occurs beneath the outermost edge of the 103 m delta and is about 45 m high (Fig. II.17). It forms a coarsening-upward sequence from horizontally-bedded sands and silts of LA Va and Vb, through sandy and then gravelly beds with increasing dips. These are capped by the surface gravels of the 103 m delta. Eight meters from the top, a channel 1 m deep and 3.75 m wide is infilled with gravelly sands (Fig. II.18). The gravel is clast-supported at the base and becomes matrix-supported at the top. The 103 m surface gravels are well sorted and have both pebble imbrication and an interlocking fabric (Fig. II.19).

Interpretation

Section 7 represents glaciomarine sedimentation during ice retreat and the subsequent progradation of the 103 m delta. The LA ,Va and Vb beds at the base of this section are similar to section 6 and represent turbid plume suspension and minor turbidity current deposition related to ice retreat into Lush Acres. The subsequent deltaic progradation is indicated by the upward coarsening and increasing dip of the primary bedding which are interpreted as foreset beds of a Gilbert delta (Fig. II.17). The channel (Fig. II.18) is interpreted as a chute produced, and infilled by, debris slumping down the foreset beds (cf. Prior et al. 1982). The topset gravels capping the delta were transported to the site as glacial outwash derived from Lush Acres. The interlocking structure of these gravels resembles beach facies shown by Nemec and Steel (1984) and may indicate subsequent wave reworking.

Arrowhead Delta Discussion

The landforms and sediments of the Arrowhead Delta record: 1)deposition related to glacial advance; 2)glaciomarine sedimentation during the subsequent retreat of a tidewater glacier; and 3)the establishment and progradation of terrestrial sandurs and related deltas as glaciers retreated inland. Deglacial sediments (Unit 2) constitute the largest volume of surficial sediments in the inlet. These are glaciomarine sediments deposited beyond the glaciers as subaquatic outwash and turbid plume sediments. The spatial and temporal distributions of

these glaciomarine sediments provides important information on the configuration and nature of ice retreat.

The basal sands and gravels of section 5 (Unit 1) represent the only surficial deposits in Clements Markham Inlet that may predate the arrival of ice during the last glaciation. These deposits range from an elevation of ca. 52 to 62 m asl. Relative sea level at that time is still unknown, though a terrestrial interpretation of these sediments requires that it was somewhere below 52-62 m asl. There are two alternatives to this interpretation. One, that they are <u>not</u> terrestrial sandur but rather subaquatic outwash produced by progradation beyond the advancing glaciers of the last glaciation. In this case relative sea level was in fact higher than 52 to 62 m asl. Two, the unit is a much older and isolated erosional remnant and hence unrelated to the last ice advance.

The question concerning a < 52 to 62 m sea level during the last glacial advance is relevant because, to date, no one has documented a transgression to the marine limit. Because of this lack of documentation, and because earlier intervals of high sea levels along Nares Strait descend from 285 to 175 m asl during the past million years, England (1983, 1987) has suggested that sea level may have in fact dropped to what was the Holocene marine limit (ca. 120 m). This could be due to a long term diminishment of the Quaternary ice load and/or the long term effects of regional tectonic uplift. Therefore, resolution of these interpretations would provide an important datum for sea level position immediately preceding the last glaciation.

In sections 1 through 4, subaquatic outwash followed by deposition from turbid plume suspension characterized the glaciomarine environment during deglaciation. This area is well removed (distal) from the 103 m delta and therefore the upper parts of these sections naturally do not exhibit interaction with that younger feature. Surprisingly, even the area immediately distal to 103 m delta lip (i.e., area marked morainal bank, Fig. II.8) does not display any influence from that delta. Additionally, unlike sections 1 to 4, it does not contain coarser sediments from subglacial streams. Furthermore, the deltaic sediments of section 7 are inset behind this area and with an approximately vertical contact between them (Fig. II.8). This contact represents the former presence of a glacier with a vertical front. This glacier naturally precluded deposition of sediments until its removal when infilling of this area by the deltaic sediments of section 7 occurred. The lack of subaquatic outwash in the area immediately distal to this glacier front is therefore not expected.

The absence of subaquatic outwash demonstrates considerable spatial differences in the glacial depositional processes along the ice front. While the glacier occupied the mouth of the Arrowhead-Lush Acres valley an englacial stream exited near section 4 accounting for the gravel deposition and formation of the prominent channel. Distally this graded to the channel and interchannel deposits of LA III and IV of sections 1 to 3. While these subaquatic outwash deposits were forming the related turbid overflow plumes deposited the thick sequence of LA Vb1

immediately in front of the glacier. The ice then retreated into Lush Acres producing a deep basin at section 7 which was subsequently infilled by the foresets of the 103 m delta related to stratigraphic unit 3.

This reconstruction is similar to the conditions which presently border the retreating tidewater margin of McBride Glacier in Glacier Bay, Alaska (Powell and Cowan 1986). There, retreat between 1975 and 1986 created an 80 m deep basin near the ice front. At its 1975 margin, however, there is a prominent ridge of sediment which rises to form a shoal at low tide. Distal to this shoal the submarine contours decline gradually whereas towards the ice the contours decline quickly. This depositional feature is called a morainal bank (Powell 1981) and is composed of coarse-grained deposits as suggested by their ice-contact nature and prominent reflectors in seismic profiles (Seramur and Powell 1987). In Clements Markham Inlet, the dominance of coarse-grained subaquatic outwash at sections 1 to 4 and the pronounced stratigraphic break between section 7 and the area distal to the 103 m delta lip, indicates that this valley mouth marks a prolonged terminal position of the Arrowhead glacier. Therefore the large area of fine-grained glaciomarine deposits distal to the 103 m delta is geomorphically interpreted as a morainal bank.

This interpretation suggests that morainal banks may be constructed by fine-grained turbid plume sediments derived from immediately proximal ice. (Certainly other glaciers in the vicinity contributed fine-grained sediment to this bank). It also

indicates that the areal distribution of glaciomarine silts and adjacent lithofacies can provide important information on former ice limits. The extended presence of the subglacial stream along the valley side at sections 1 to 4 contributed to the localized ice retreat by undercutting that ice and initiating a small calving bay. This allowed invasion of the sea and formation of the 118 m shoreline at the northern edge of the Arrowhead delta (Figs. II.5, II.6) while the sea was still excluded from the rest of the area.

As the ice retreated further into Lush Acres it continued to contact the sea as shown by the occurrence of the turbid plume deposits of LA V both at sections 5 and 6. In places, these plumes infilled the basin to within meters of the contemporary sea level whereas at other sites in the same basin many meters of local relief existed on the sea floor.

Piper Pass Kame Delta

Surficial Geology

The Piper Pass kame delta is the upvalley counterpart to Lush Acres (Fig. II.7). The highest shoreline formed here occurs at 114.5 m a.s.l., only 10 m lower than the maximum marine limit observed in the inlet (Bednarski 1986). This shoreline occurs only on a small bedrock knob which protrudes above local terraces at 103 m and 96 m asl (Figs. II.2, II.7). These terraces do not have discernible gradients that descend to a delta lip and, combined with their large kettle lakes, they are interpreted as ice-contact kame deltas. Surface paleochannels on these emanate from a small valley incised into the bedrock spur to the east of

the kame deltas. This valley leads into the west end of Lush Acres where it merges with the upper level of the sandur indicating that the kames formed contemporaneously with the deposition of the Lush Acres/Arrowhead outwash (Figs. II.2, II.7). Runoff through these paleochannels subsequently formed stream terraces inset below the 96m surface.

During the interval when relative sea level fell from 124 to 114 m asl it is apparent that glaciers excluded the sea from the Piper Pass valley. An estimate on the time of local deglaciation is provided by a caribou antler found in marine sediments at 25 m a.s.l., ca. 12 m above a diamicton-dominated horizon which is the lowest stratigraphic unit found in this area (sections 13, 14). This antler dates 8415±135 BP (S-2501) and provides a minimum date on deglaciation as well as an indication of biological refugia during the last glaciation (Stewart and England 1986). The next oldest radiocarbon date from this area is 7860±330 BP (UQ-262, Bednarski 1986) obtained on marine shells collected at 67 m asl at the westernmost end of Lush Acres. These two dates correspond with those shown on the emergence curve for the 114 m and 103 m shorelines respectively (8400 and 7860 BP). Collectively, the geomorphic and chronologic data indicates that the depositional environment at Piper Pass was dominated by a dynamic, ice-contact environment between 8400 and 7800 BP. Following this interval deglaciation and unloading were rapid (Bednarski 1986).

Section Descriptions and Interpretations

The fence diagram and generalized sections for Piper Pass

(Figs. II.20, II.21, respectively) utilize the lithofacies codes (Table II-1) and lithofacies associations (Table II-2) in the same manner as the Arrowhead delta. The sections are presented in an order which generally reflects the stratigraphic sequence. This begins with the diamicton-dominated section that represents the basal stratigraphic unit in the area.

Sections 13 and 14

Description

Sections 13 and 14 are facing exposures on the east and west shores of the Piper River, respectively (Figs. II.7, II.20, II.21). Section 14 is set against the bedrock slope which rises immediately to the west. Section 13 is unconstrained to the east and leads directly upslope to the kame delta ca. 0.5 km distant (Figs. II.2, II.7). Sections 13 and 14 are ca. 50 m apart and they were examined laterally for ca. 75 and 40 m, respectively. The lower parts of both sections consist of thick- to thin-bedded diamictons with interbedded sands, silts and muds that are very thinly- to medium-bedded (LA I). Clasts within the diamictons are commonly striated. Many clasts deform the underlying fine-grained sediments and are draped by them. At most locations, however, a diamicton bed deforms the underlying fines without individual clast penetration. The diamicton beds also contain silt intraclasts. At several sites excavation into apparently single diamicton beds exposed intact, horizontal silt interbeds. The clasts within some diamicton beds exhibit normal or reverse grading although in most cases grading is apparent. Eight fabrics

were measured in these two sections (Table II-5).

In section 14, LA I is overlain by thinly-bedded to thinly-laminated LA Vb1, although minor amounts of sand laminae with ripples are also present. Above the diamicton, the slope has retreated back from the river exposing medium-bedded LA Vb1. The diamictons in section 13 are also overlain by LA Vb1 and slope retreat has exposed a further ca. 5 to 7 m of LA Vb (Stewart and England 1986, Fig. II.3). At 25 m asl a caribou antler was collected from these sediments (LA Vb) and it was radiocarbon dated at 8415±135 BP (S-2501, Stewart and England 1986). Burrows are also present at ca. 28 m asl. The uppermost surface of both sections 13 and 14 has been removed by subaerial erosion during postglacial emergence. The stratigraphic sequence of LA I to LA V that occurs in sections 13 and 14 is also present along the Piper River to the northeast. However, sections 13 and 14 record the southernmost extent of this sequence.

Interpretation

The clasts that deform underlying sediments and which have subsequent sediment drapes are interpreted as dropstones from icebergs and/or sea ice. The majority of diamictons, however, are interpreted as proximal, subaquatic debris flow deposits derived from sediment-rich basal ice. This is based on their: 1)horizontal bedding; 2)erosive contacts with silt beds and the presence of silt intraclasts; 3)erosive or amalgamated lower contacts within diamicton beds; and 4)weak fabric strength (low eigenvalues, Table II-5, see chapter 2). Many of the diamictons are evenly-bedded for distances > 10 m, however, debris flow

noses were not observed (cf. Hicock et al. 1981; Domack 1983; Eyles 1987).

The interbedded sands, silts and clays are interpreted as deposits from turbid plumes and, less frequently, from turbidity currents. The interbedding of the diamictons and finer-grained sediments indicate repetitive debris flows, suspension settling, and turbidity currents proximal to the ice. This alternation of diamictons and silts is similar to that reported by Bednarski (1984, 1986, in press) from the main Clements Markham River valley that is interpreted as uniform retreat of glaciers in contact with the sea. At sections 13 and 14 the stratigraphic sequence therefore indicates that the calving bay that occupied inner Clements Markham Inlet continued into Piper Pass. However, the presence of the adjacent kame delta which is confluent with the Lush Acres sandur, together with the sections described below, indicate that the ice halted in this vicinity before continuing further into Piper Pass.

Section 16

Description

Section 16 is 1 km east of section 15 and occurs along the actively eroding east bank of the Piper River (Figs. II.7, II.20, II.21). The slope was inaccessible due to instability from continuous melting of interstitial ice and therefore it was observed only from the opposite shore of the river. The section consists predominantly of medium- to thin-bedded sands overlain by silt. Convolute bedding is visible at the base of one sand layer. The most prominent feature is a channel ca. 2 to 3 m deep

and ca. 15 m wide (chapter 2, Fig. II.22c). The channel has an orientation down the NW flank of the kame delta. During previous work in the area (Stewart 1981) a small part of this section was accessible just north of the channel. The sediments there were characterized by sandy, starved and climbing ripples interbedded within silty clay beds. The ripples had an approximately northerly (down-river) paleocurrent direction.

Interpretation

This section is interpreted as a turbidity current channel which transported materials down the flank of the kame delta and into the central portion of the valley. The dominant material transported to this site was sand and silt. The climbing and starved ripples are interpreted as levee-overbank deposits produced by overspill from the channel.

Section 15

Description

Section 15 is ca. 2 km NW from sections 13 and 14 and it occurs in a local basin confined by bedrock on all but its eastern side (Figs. II.2, II.7, II.20, II.21). The lower part of this section consists of horizontal, medium-bedded, and graded sandy silts of LA Vb2 (Table II-2). The upper part consists of very thinly- to thinly-laminated, graded, sandy silts. Within this upper part the horizontal bedding is disturbed. The beds are compressed into two sets of minor folds with amplitudes of 0.5 m. These pass upward into a more severely distorted layer in which

the beds are both tightly folded and fragmented. The beds overlying the disturbed layer are horizontal.

Interpretation

The lower, medium-bedded part of the section represents deposition from turbid plumes which have either lost, or never contained, coarser sediment. It resembles what Powell and Cowan (1986) call homogeneous mud. Despite this apparent distal position the upper part of the section consists of more proximal cyclopsams or coarse cyclopels. Although individual beds of LA Vb2 occur in other sections this is the only location in Clements Markham Inlet where LA Vb2 was observed in considerable thickness. Observations at sections 16, as well as 18 to 20, indicate that major channels are oriented away from this local basin suggesting it was isolated from the subaquatic outwash which was being deposited at adjacent sites.

The contorted and fragmented bedding in the upper section indicates downslope movement with severe bed disruption. The fragmented materials overlain by horizontal beds initially suggests an erosional contact. This progression from disturbed beds to overlying horizontal beds could represent a genetically-related sequence of slope failure, turbidity current generation, erosion and deposition. However, such an interpretation is problematic because the overlying beds/laminae are interpreted as cyclopsams which are suspension deposits. The alternative is that the disrupted beds represent a shear zone with severe disruption produced by the slumping of the overlying beds. A very similar contact and disruption is illustrated by Coniglio (1986) for

shear-zone contorted sediments. Because of the suspension origin for the sediments overlying the disrupted horizon a slumping origin is the preferred interpretation.

Section 17

Description

Section 17 is located ca. 200 m from the lip of the 103 m kame delta (Figs. II.7, II.20, II.21) and it contains the only sorted gravels that were observed locally. These gravels occur at the lower 4 m of the section, have apparent dips of 6 to 22°, are 5 to 15 cm thick, and are ungraded and matrix- to clast-supported. Average size of the largest clasts is 7.25 cm (b-axis, n=10). The basal gravel of individual beds is overlain by sand laminae or additional gravel beds. The upper 5 m of the section consists of thinly-bedded to thinly-laminated sands and silts of LA Vb1. The overlying LA Vb1 is evenly-bedded and conformable with the gravels. These silts can be traced upslope where they contact the 103 m kame delta lip. Downgully from the dipping gravels a transverse section is exposed in the LA Vb1 revealing two cross-cutting channels (chapter 3, Fig. II.22g).

Interpretation

The grain size and dips of the gravel in the lower part of this section resemble Gilbert foreset beds. However, here they cannot be traced up-section through a coarsening upward sequence related to the progradation of the overlying kame delta into the sea. Indeed, the gravels are overlain by silts indicating a transgressive, rather than progradational, sequence. These

gravels are therefore interpreted as proximal, subaquatic outwash from ice contacting the adjacent bedrock and the gully which leads into Lush Acres. These sediments are similar to the gravelly, steeply dipping section illustrated by Sollid and Reite (1983, Fig. 55) which they interpreted as ice-contact, subaquatic slope deposits. Such sequences are common in Norway and are called Tronder moraines. This high-energy, proximal site likely supplied the fine materials which occur in sections 16 and 18A/B (see below). This subaquatic outwash, with its direct link to the bedrock valley which leads into Lush Acres, forms the core of the kame delta.

The overlying fines of section 17 are cyclopels and minor cyclopsams deposited by suspension on this steep slope. This slope provided the potential energy for the slumping and generation of high-energy turbidity currents down the flank of the kame delta. Their high-energy character is indicated by the presence of cross cutting channels within otherwise fine-grained material. Because the channels are filled with turbid plume suspension deposits and not turbidites the erosive turbidity currents must have outran this particular site and deposited the eroded materials further downslope.

Sections 18A and 18B

Description

Sections 18A and B are ca. 200 m to the southwest of the kame delta on an erosional remnant of the deposits which blanket the Lush Acres-Piper Pass junction (Figs. II.2, II.7, II.20, II.21). These sections exhibit three prominent channels

designated channel 1, 2, and 3 from lowest to highest (Figs. II.21, II.22). These channels incise older deposits which are preserved along the channel margins (Fig. II.23). These uneroded beds extend upwards to a point where they extend towards and into the channel. Therefore, these beds drape the same channel margins which cuts through them (Figs. II.22, II.23b).

The sediments which form the unchannelized lower part of the section are medium- to thinly-bedded, fine sands, silts and clays of LA IV. Sedimentary structures are arranged in sequences of graded sands; draped lamination (Gustavson et al. 1975); type B climbing ripples; starved ripples (Eriksson 1982); and clay drapes. Along the margin of channels 1 and 2 packets of these adjacent sediments have rotationally slumped into the channel. Climbing ripples indicate a southerly paleocurrent direction away from the kame delta and into Piper Pass whereas the bearing of the channel 2 margin is ca. 220° (SSW, Fig. II.24). Thus there is a general divergence between the climbing ripples and the channel.

Sediments within channel 2 (Fig. II.23a, b) are thinly-bedded and graded sands with water escape structures, convolute lamination and flame structures. Individual sand beds are commonly draped by thinly-laminated mud. Several of these infilling beds can be traced over the channel margin to the adjacent interchannel surface. Sediments within channel 3 are predominantly lithofacies Vb1 but thin-bedded sands with convolute bases do occur. Several dropstones are interspersed in these finer grained sediments.

Interpretation

The graded sands within the channels indicate deposition by high and low density turbidity currents and mass flows. Their presence within cross-cutting channels suggests that they are channel fill deposits. The sedimentary structures of the LA IV deposits along the channel margin are similar to features attributed by Mutti (1977), Eriksson (1982), Pickering (1983) and Walker (1985) to be levee or interchannel deposits of submarine fans. This section is similarly interpreted as a subaquatic outwash fan. The paleocurrents in the interchannel climbing ripple sequences, however, indicate sediment transport towards the ice front (i.e. towards Piper Pass) but slightly oblique to coeval channel 2. The interpretation is that section 18 represents deposition on the flank of a submarine fan. The fine sediment was derived from lateral transport (over-spill) from the relatively stable stream exit at section 17. Sediment build-up on this flank caused instability and slumping, generating localized turbidity currents which eroded into the interchannel deposits. While this was occurring there was continued lateral transport (overspill) from the section 17 channel to section 18 where that sediment was deposited. This indicates a syndepositional origin for the two sediment types. Other fan flank deposits are described from deep sea fans by Macpherson (1978) and Pickering (1983). Jorgenson (1982) describes glaciolacustrine sediments similarly deposited against, but perpendicularly to, a glacier front.

The finer-grained nature of channel 3, and its mimicking of channel 2, indicates depositional draping of channel 2 by turbid plume suspension deposits. This may have occurred after ice retreat from the immediate site and during the formation of the 103 m kame delta surface.

Sections 19 and 20

Description

Sections 19 and 20 are SE-facing sections ca. 0.5 km SE of section 18A/B (Figs. II.7, II.20, II.21). They border the kame delta and together with section 21 they form a sequence progressively more proximal to the southward retreating ice margin in Piper Pass. The base of section 19 consists of LA III sands that are medium-bedded, graded to ungraded with both bed amalgamation and convolute bedding. At one site near the upper part of the sands abundant gravels and cobbles are being removed from the section producing a thick colluvium. This covering was pod-shaped but too extensive to excavate. Several gravel horizons could be observed along its margin and these pinched out within the surrounding sands. From the available exposure these gravel lenses appear to thicken towards the center of the gravel pod. The enclosing sands continue for ca. 1.5 m above the gravel where they are conformably overlain by horizontally and thin- to medium-bedded LA IV. Graded beds occur in LA IV but climbing and starved ripples are predominant. When individual beds are traced along section they are seen to be truncated along low gradient erosional surfaces with depths of ca. 0.5 m. Prominent channeling on the scale observed in adjacent section 20 (see below) is not

present. All of the paleocurrents measured in these beds trend NW (Fig. II.25).

Section 20 consists of thin-bedded, graded sands with abundant convolutions and water escape structures. These sands alternate with repetitive sequences of climbing and starved ripples and mud drapes. These are all representative of LA IV. Three cross-cutting channels, 0.5 to 1.5 m deep, are present along the section at this level and contain mud rip-up clasts along their bases. Where climbing ripples occur adjacent to these channels their paleocurrent directions were approximately normal to the channel margins (NW, Fig. II.25). A large fold occurs at the center of the section in the LA IV. Above ca. 27 m LA Vb1 becomes dominant.

Interpretation

The individual bed thickness and the dominance of bed amalgamation in the LA III sands of section 19 indicates deposition by high density turbidity currents and mass flows. Though actual channel margins were not observed these are interpreted as subaquatic outwash channel deposits by analogy with submarine fan models (Walker 1978; Howell and Normark 1982). The presence of gravels near the upper part of the sand may be the result of a high density mass flow from the same (glacial) source as the sands. If so, these gravels would resemble the gravel cell chutes described by McCabe et al. (1984). The overlying LA IV are interpreted as interchannel deposits.

The northwesterly paleocurrents in LA IV (Fig. II.25) diverge from the SW-NE trend of the small channels and indicate

channel overspill or flow spreading beyond the turbidity current channel (see chapter 3 for more detailed discussion). The interbedding of graded sands, climbing and starved ripples and mud drapes indicates repeated overtopping of a channel by turbidity currents (Mutti 1977; Eriksson 1982; Pickering 1983; Walker 1985). The upward trend from channel to interchannel to turbid plume deposits represents the progressive diminishment in the sediment source due to ice retreat.

Section 21

Description

Section 21 is exposed horizontally for ca. 70 m in a gully just south of section 20 (Figs. II.7, II.20, II.21, II.26). The upper part of the section is composed of LA Vb1. However, along the base of the section, from NW to SE, the lithologies vary from graded sand with burrows; to massive and cross-bedded gravel; to diamicton; and finally to disrupted LA Vb1 (Figs. II.20, II.21, II.26).

The basal, medium-bedded sand at the NW part of the section is abruptly overlain by interbedded sands and silts. Some starved ripple structures are present and individual beds are folded with amplitudes of ca. 0.4 m. Three separate burrow structures occur here (Fig. II.26d) that are similar to those of section 13.

Near the center of the section the gravel at the base is sharply overlain by LA Vb1 though at one site there are gravels, granules and sands interlaminated in the lower part of LA Vb1, 0.4 m above the contact (Fig. II.26b, c). Also at this position

is a curious elongated pod structure of thickly-laminated sand and silt (Figs. II.26, II.27a). Further up-gully the base consists of diamicton overlain by LA Vb1. Small faults occur in these silts but cannot be traced into the diamicton. Also within the LA Vb1 silts individual beds drape over similar beds that pinch out against them giving the appearance of a channel margin (Figs. II.26a, II.27b).

Interpretation

The gravels along the base of the section are interpreted as ice-contact subaquatic outwash or subglacial conduit gravels. Pebble imbrication indicates a northward transport direction so the rapid downgully transition to the sand means that the gravels were transported only a short distance (< 10 to 20 m). Extensive gravels do not occur in other sections in this vicinity so it is unlikely that they are part of a large subaquatic outwash fan. Therefore, gravel deposition within or immediately in front of an englacial tunnel is the favored interpretation. This accounts for the rapid proximal to distal facies transition form gravel to sand at the base of the section (Fig. II.26).

The extremely sharp contact between the gravels and overlying LA Vb1 relates to rapid ice retreat from the site with deposition of only minor intermediate deposits of LA IV. The disruption of LA Vb1 adjacent to the diamicton, plus the small faults that terminate at the diamicton, suggests that underlying glacier ice melted causing disruption of the blanketing sediments.

Interpretation of the apparent channel margin and pod

structure are more enigmatic. If the observed draping and pinching out in LA Vb1 (Figs. II.26a, II.27b) is related to erosion and deposition along a channel margin then it would indicate that these must have been eroded by turbidity currents that were undersupplied with sediment because coarser-grained material or differences in sedimentary structures are not evident. An alternative is that this is not a channel-margin but rather the preserved forward edge of a slide mass similar to those described by Gawthorpe and Clemmey (1985). If so, then a coherent mass of LA Vb1 failed down a local gradient that is not evident in the present exposures. This explanation gains added support from the pod-shaped structure which may be a cross-section through a roll structure formed at the base of a slump sheet (arrow in Figs. II.26, II.27a). A similar feature is illustrated by Cooke (1979, Fig. 24; also Cooke et al. 1982, Fig. 31) at the base of a slump sheet of continental slope deposits.

Section 22

Description

Section 22 consists of ca. 6 m of LA Va overlain by LA Vb1. These beds are horizontal over a distance of ca. 40 m. LA Va consists of thinly bedded, graded fine sand to silty fine sand (see chapter 2, Fig. II.11). Some individual sand beds are contorted (amplitude ca. 20 cm). Multiple graded sand layers and mud drapes are common. At ca. mid-section there is a transition from sand-dominated to a silt-dominated lithology of LA Vb1. Numerous Mya truncata and Hiatella arctica shells occur on the surface immediately above this section and these date 7860±330

(UQ-262, Bednarski 1986).

Interpretation

The lower part of the section is interpreted as cyclopsams deposited by proximal turbid plumes. Minor amounts of mass flow were generated in these sediments after their deposition from suspension. These deposits represent a proximal position < 2 km from the ice margin. Continued ice retreat is shown by the gradual restriction of sand and the concomitant increase in cyclopels which dominate the upper part of the section as ice retreated further inland.

Piper Pass Discussion

Unlike the Arrowhead delta, the landforms and sediments at Piper Pass only record sedimentation by a retreating tidewater glacier (unit 2, Table II-3). Powell (1980, 1981) has documented how stratigraphic sequences and sediment thickness associated with tidewater glaciers vary in relation to rates of retreat. Rapid retreat produces a transition from diamictons to deep-water suspension sediments whereas slow retreat allows the buildup of thick ice-contact meltwater sediments. A similar range of sediments occurs in Piper Pass and there is some evidence to suggest that these are related to the style of ice retreat. These sediments are discussed in relation to three phases of ice retreat (Fig. II.28).

The LA I to LA Vb1 transition (diamicton to cyclopel) at sections 13 and 14 is similar to the stratigraphic sequences reported from other valleys of Clements Markham Inlet (Christie

1967; Stewart 1981; Bednarski 1984, 1986, in press). The same sequence is also present along the length of the Piper River to the NE of the kame. This abrupt transition from diamictons to turbid plume suspension deposits suggest rapid up-valley ice retreat to the vicinity of the kame delta at T1 in Figure II.28a (cf. Powell 1981; Bednarski 1984, 1986, in press).

The diamictons at sections 13 and 14 are interpreted as debris flows because of the presence of bed amalgamation, silt rip-up clasts, and low fabric eigenvalues (Fig. II.20). Furthermore, individual fabrics from these diamictons trend southward towards the former ice front. This suggests that several debris flows originated from remobilized materials at higher elevations which flowed into the depression created by the retreating ice. These debris flows were deflected within Piper Pass and reoriented up or down valley although azimuths in all quadrants exist. Such debris flows, derived from valley sides, may be significant contributors to the basal diamictons where rapid ice retreat occurs in steep valleys.

After the initial phase of rapid ice retreat, the geomorphic and radiometric evidence indicate that the glacier subsequently stood at the Piper Pass-Lush Acres junction for ca. 600 years (T1 to T3, Fig. II.28). During this interval, the Piper Pass sections record a thick accumulation ranging from subaquatic outwash fans and turbid plumes to subaerial kame gravels at the stable ice front. A subglacial stream debouched near section 17 depositing the basal gravels (Figs. II.20, II.28a) in a subaquatic channel. Turbidity currents generated within the channel overspilled it

and flowed southward towards the adjacent ice face as recorded by the overbank deposits of section 18 (Fig. II.28a). Continued sediment buildup caused slumping which generated new turbidity currents that eroded new channels on the flanks of this subaquatic outwash fan. Overspill from the main channel at section 17 continued while this slumping and channel formation was occurring. This is shown within the channel and along its margins which are filled and draped by overbank sediments. The fact that erosive channels are overlain by these overspill sediments indicates that some of these turbidity currents outran their position of generation.

Although a subaquatic fan is envisioned to explain sections 17 and 18 there is a lack of equivalent coarser sediments along the projected thalweg to the NE. One explanation may be that the coarser sediments do exist but that these sediments are buried by LA Vb1 turbid plume deposits. Considering the orientation of the major channel at section 16 another possibility is that the coarser sediments were deposited along the axis of the valley and have been removed by the postglacial erosion of the Piper River.

During the retreat of the ice margin from positions T1 to T2 a change in the trajectory of the subquatic drainage occurred (Fig. II.28b). This produced a lateral transition between the flank deposits of the subaquatic fan at section 18 and the channel deposits at sections 19 and 20 (Fig. II.20). Paleocurrents on interchannel deposits indicate that at section 18 flow was to the south (Fig. II.24) while at sections 19 and 20 it was to the north (Fig. II.25). The subaerial channels on the

nearby kame surface emanate from the small valley leading into Lush Acres and this shows that ice must have remained in that position until sea level had fallen to ca. 103 m asl (ca. 7800 BP, Fig. II.28b). The glacier and related subglacial stream were stable for sufficient time to produce a transition from LA III channel sands to LA IV levee/overbank sedimentation at sections 19 and 20 (Fig. II.28b).

At ca. ice margin T2 gravels with northerly paleocurrents were deposited at section 21 (Figs. II.26c, II.28c). Toward the end of ice margin T2 a more rapid, but variable, rate of retreat is indicated by varying sediment thicknesses of coarse basal units. Whereas sections 19 and 20 indicate slow retreat, section 21 indicates more rapid retreat followed by a return to slow retreat at section 22 (T3, Fig. II.28c). The slow ice retreat is indicated at sections 19 and 20 by the buildup of thick channel sands and levee-overbank deposits (Fig. II.20). The ice then retreated more rapidly depositing thin channel gravels and sands at section 21 which are abruptly overlain by fine-grained turbid plume deposits (Fig. II.26). At T3 retreat slowed sufficiently that several meters of turbid plume cyclopsams were built up with a transition to cyclopels at section22 reflecting progressive ice retreat (Fig. II.28c).

These variations in ice retreat from the Lush Acres-Piper Pass juncture were probably controlled by topography. For example, the ice front was probably pinned in the valley constriction located between section 13 and the bedrock knob behind the Piper Pass kame (Fig. II.28a). Subsequent retreat

resulted in the unpinning of this ice front as it encountered the larger opening into Lush Acres (Fig. II.28b). Later, retreat was slowed again when the ice front coincided with the constriction at the entrance to Piper Pass proper (Fig. II.28c). However the distances involved here are short and these sections may alternatively reflect variations in meltwater and sediment influx rather than small-scale variations in ice retreat. Nonetheless, the thick subaquatic outwash which coincides with the documented 600 year stillstand reinforces the argument that retreat rate has controlled the style of sedimentation.

Ice-shelf Versus Tidewater Glacier Sedimentation

The lithofacies and stratigraphic sequences in Clements Markham Inlet clearly indicate retreat of glaciers in contact with the sea. Such glaciers form either grounded, nearly vertical tidewater fronts or continue flowing beyond a grounding line, forming ice shelves (Powell 1981, 1984; Eyles et al. 1985). On Ellesmere Island and Greenland many contemporary glaciers that contact the sea form ice shelves (Hattersley-Smith et al. 1969) and there is morphologic evidence for their existence during past glaciations (England et al. 1978). Although the bedrock glacial record is commonly interpreted in relation to ice shelf models the stratigraphic and sedimentologic differentiation between ice shelves and tidewater glaciers is uncertain and debatable (Eyles et al. 1985, p. 30-33). In the case of Clements Markham Inlet differentiation between tidewater glaciers and ice shelves is also difficult.

The clearest evidence for the existence of former ice shelves is the deposition of horizontal moraines along the fiord side produced by the floating margin (England et al. 1978; Sugden and Clapperton 1982; Hodgson and Vincent 1985). At the glacial maximum within Clements Markham Inlet such morphologic evidence has not been observed (Bednarski 1984, 1985, in press). Nonetheless, during the last glaciation, the main trunk glacier terminated within inner Clements Markham Inlet in contact with the full glacial sea at ca. 124 m asl. The limit of the full glacial sea trims the landscape throughout the remainder of the inlet except where it was excluded by local cirque and valley glaciers. Therefore, if an ice shelf occupied inner Clements Markham Inlet during the last glaciation, it could have been several kms in length.

Although no one has cored beneath an ice shelf, the stratigraphic sequence commonly assumed to originate from one includes massive diamicton overlain by thinner-bedded diamicton with interbedded suspension sediments in turn capped by marine sediments (Gravenor et al. 1984; Eyles et al. 1985). Such interbedded diamictons and marine sediments are similar to the stratigraphic sequence observed in the Clements Markham River and Piper Pass valleys. One reason an ice shelf origin is invoked for these thick diamicton sequences is that thick massive diamicton implys prolonged stability at a single position with sediment delivery at the grounded ice shelf margin. Since an ice shelf loses its debris supply over a belt several kilometers wide it might deposit a thick sequence of diamicton from settling through

the water column. However, a grounded tidewater glacier at a single position would similarly deliver large amounts of sediment to a single point where it could be resedimented by debris flows. Tidewater glaciers also calve and supply ice-rafted debris beyond the grounded margin. Additionally, thick massive diamictons are not unique to marine sequences. For example, Saunders et al. (1987) report diamictons 60 and 40 m thick that they interpret as lodgement till. Because both tidewater glaciers and ice shelves are grounded they could be responsible for some of the reported sequences. Indeed, the grounded interpretation for the thick massive diamicton has been applied by some workers (Powell 1984; Eyles et al. 1985).

It is apparent that existing sedimentological criteria for ice shelves versus tidewater glaciers are weak (Eyles et al. 1985). In the present case, no thick massive diamicton exists and only interbedded diamicton and marine sediments occur. Although some of these interbedded diamictons originate from ice rafting, the majority result from resedimentation by debris flows. Resedimentation of ice-rafted debris certainly occurs in the ice shelf environment. However, the diamictons in Clements Markham Inlet lack the bimodal diamicton matrix indicative of both an ice-rafted and a turbid plume component. This suggests that in Clements Markham Inlet settling beneath an ice shelf was not the prime contributor.

The stratigraphic relationships from Clements Markham Inlet also constrain an ice shelf interpretation. At the Arrowhead delta the section 4 channel indicates that a grounded margin had

to be close to supply the coarse subaquatic outwash (Fig. II.8). The elevation of the LA III to LA Va transition is at 81 m asl (Fig. II.9), therefore the paleodepth at this transition was only 37 m in relation to the marine limit at 118 m asl. A floating ice margin could have overtopped this site and then retreated allowing deposition of the finer lithofacies up to the upper elevation of section 4 at 92 m asl. However, the stratigraphic break between the section 7 foreset beds and the LA Vb1-dominated area distal to the 103 m delta indicates that ice occupied this area as well. Thus a paleogrounding line is indicated across the mouth of the Arrowhead delta. At section 7, LA Va and Vb occur up to an elevation of ca. 63 m asl which, if produced in front of an ice shelf, would indicate that the lower portion of the area in front of the 103 m delta must have been influenced by the ice shelf as well. The meager ice-rafted component in these silts is difficult to explain if it was beneath an ice shelf for any prolonged period. Additionally, the break between this area and the inset 103 m delta foresets is essentially vertical. This geometry is particularly difficult to reconcile with an ice shelf but does conform with that expected of a tidewater glacier. If the glacier retreated to this site as an ice shelf its floating part quickly calved back and converted to a grounded tidewater margin.

Morphologic evidence of the marine limit along the lower Piper River to the north of the kame delta is not preserved (Bednarski 1984). Thus no evidence exists to allow differentiation an ice shelf versus tidewater glacier. Though an

ice shelf could be responsible for the basal diamicton sequence along this valley, the stratigraphy around the delta severely constrains an ice shelf configuration there. The gravel at section 17 indicates that ice was grounded at this juncture (Fig. II.20). Section 18 represents overspill from that channel which requires the grounding line be to the south of section 18 to allow for deposition to occur. The transition to suspension sedimentation in channel 3 at section 18 occurs at ca. 30 m asl (Fig. II.21) indicating ca. 80 m of water depth above that position. This is sufficient depth to allow the ice to be grounded further towards Piper Pass proper and still allow deposition of the lower section 18 sequence. However, the ice contact face of the Lush Acres sandur and the presence of coarse gravels on the kame delta surface requires the presence of grounded ice delivering coarse sediment to those sites when sea level had fallen to 103 m asl. Therefore, if there initially was a floating ice front it must have transformed to a grounded margin in the interval between deposition of the base of sections 17 and 18 and formation of the subaerial gravels.

The basal diamicton sequence from Clements Markham Inlet closely resembles sequences reported from the literature that are interpreted as resulting from ice shelves (e.g. Gravenor 1980) though that interpretation is equivocal (Eyles et al. 1985). Definitive morphologic evidence (i.e. ice shelf moraines) for the existence of ice shelves is lacking despite the generally good preservation of morphologic features in this area. At the ice-proximal sites the stratigraphic evidence provides no definitive

evidence for ice shelves. Indeed it allows for only very short floating margins on the order of 1 km. Considering the lack of criteria for ice shelf identification (Eyles et al. 1985) and the regional abundance of such margins on Ellesmere Island and Greenland additional stratigraphic and sedimentologic studies in the region are warranted.

Conclusions

At ca. 11,000 BP the glaciers of Clements Markham Inlet terminated in a full glacial sea (Bednarski 1986). These glaciers retreated, eventually separating into individual lobes where side valleys joined the inlet. The rapid retreat within the main valleys produced horizontally-bedded diamictons with interbedded sands and silts (LA I) overlain by the thick glaciomarine silts of LA Vb. The diamictons are predominantly of debris flow origin and are interspersed with finer-grained mass flow and turbid plume sediments. In Piper Pass these debris flows were deposited at a depth of ca. 100 m whereas at the Arrowhead delta they were deposited at a depth of ca. 40 m.

The character and distribution of the subaquatic outwash at the Arrowhead and Piper Pass deltas are site specific due to differences in the configuration of the ice and the exit loci of subglacial streams. At the Arrowhead delta, the subaquatic outwash was confined to the NE margin producing well developed channels and levee-overbank fills in the vicinity of the valley wall. This lateral constriction of the subglacial stream allowed turbid plume sediments to be deposited right up to the ice front producing a fine-grained morainal bank behind which the 103 m

delta was inset.

At Piper Pass, subaquatic outwash produced a fan which prograded to the NW while abundant sediments overspilled this channel to the S in the direction of the ice front. Slumping of these materials produced subsidiary channels on the flank of the subaquatic outwash fan in close proximity to the ice. Subsequent retreat created space for deposition of another set of channel and related levee-overbank sediments (sections 19, 20) followed by turbid plume cyclopsams (section 22). These deposits were progressively inset against the previously deposited materials of section 18 and then sections 19 and 20. Turbid plume sediments were deposited in more distal locations and subsequently blanketed more proximal sequences as ice retreat continued into Piper Pass.

The glaciomarine sediments of subaquatic outwash and turbid plumes have the largest volume in the inlet. This dominance suggests that glacial deposition was accompanied by large quantities of meltwater. Although these glaciers were certainly cold-based during full glacial time they did not deposit thick sequences of massive diamictons as have been inferred for such environments (cf. Eyles et al. 1985, 31). The lack of substantial deposition by ice during the last full glacial is likely due to the climatic conditions which were even colder and more arid than today (England and Bradley 1978; England 1983, 1986). Despite this, the predominance of subaquatic outwash, cyclopsams, and cyclopels all bear a striking similarity to both modern temperate tidewater environments (e.g. Glacier Bay, Alaska) and to lower-

latitude, late Pleistocene glaciomarine lithofacies (e.g. Puget Sound). The abundance of these lithofacies indicates that during deglaciation abundant meltwater was produced and that it reached the sediment-rich basal ice (Stewart and Bednarski 1986). The sediment volume indicated by these facies shows that the meltwater style during deglaciation was in sharp contrast to present conditions where meltwater is generally restricted to the surfaces of glaciers. Consequently, deglaciation must have been accompanied by a marked amelioration, and this is also recorded by the initial penetration of driftwood previously excluded from the full glacial sea of Clements Markham Inlet (Stewart and England 1983).

TABLE II - 1

Lithofacies codes for sediments observed in Clements Markham Inlet (modified from Eyles et al. 1983)

Code	Lithofacies Type	Description
Dmm(r)	Diamicton, matrix-supported massive, evidence of resedimentation	Intraformational rip-up clasts, bed amalgamation, bedding planes evident
Dmg	Matrix-supported, graded	Variable vertical grading in matrix or clasts
Gm	Gravel, massive or crudely bedded	Horizontal bedding, graded, imbrication, planar crossbeds
Gp	Gravel, stratified	Planar crossbeds
GSt	Gravelly sand, stratified	Trough crossbeds
GSf	Gravelly sand, bedded	Large-scale deltaic foreset beds
Sm	Sand, massive to graded	Dish structures, $\bar{x}$ = 2 - 4 phi
SB	Sand, graded to laminated	Bouma sequences, Tabc, Tac, Tae
Scr	Sand, rippled	Climbing ripples, type B dominant
Ssr	Sand, rippled	Starved ripples
Sl	Fine sand to coarse silt, laminated	Draped lamination
Scps	Sand, graded, laminated	Cyclopsams
Fcpl	Mud, interlaminated	Cyclopels
Fm	Mud, massive	Clast poor
Fl	Mud, laminated	

TABLE II-2

Facies Association	Interpretation
I. Interbedded Diamicton, Sand, Silt	Subaquatic Debris Flow, Mass Flow, Turbid Plume, Ice Rafting
II. Gravels	Subaquatic Outwash Channel, Englacial Stream
III. Amalgamated/Graded Sand	High Density TCs, Mass Flow, Channelized
IV. Graded Laminated and Current Bedded Sand	Levee-Interchannel Turbidity Current (TC) Deposit
A. Bouma Sequence	Low Density TC
B. Climbing Ripples	Traction-Suspension TC
C. Starved Ripples	Traction w. Low Sediment Concentration
D. Draped Lamination	Suspension Sedimentation from TC
V. Interbedded and Interlaminated Sand	Suspension Sedimentation from Turbid Plume
A. Cyclopsams	Proximal
B1. Cyclopels	Distal
B2. Silts, non-laminated	Distal
VI. Gravels, Large-Scale Crossbeds	Sandur and Related Deltaic Sediments

TABLE II-3

Stratigraphic Differentiation of Lithofacies and Lithofacies Associations

Stratigraphic Event	Lithofacies	Lithofacies Association
3. Glacial Retreat: prograding sub-aerial deltas	Gp, Gm, GSt, GSf	VI
2. Glacial Retreat: glaciomarine sediments	Scps, Fcpl, Fm	V
	Sm, SB, Scr, Ssr	IV
	Sm, SB	III
	Gm, Gp	II
	Dmm(r), Sm, Fl, Fm	I
1. Pre-last Glaciation: prograding subaerial sandur (?)	Gp, Gm, GSt, St	VI

Note that the stratigraphic sequence of event 2 represents a fining-upwards trend related to ice retreat

TABLE II-4

Stratification types and thicknesses (after Ingram 1954)

Very thickly bedded	> 1 m
Thickly bedded	30 - 100 cm
Medium bedded	10 - 30 cm
Thinly bedded	3 - 10 cm
Very thinly bedded	1 - 3 cm
Thickly laminated	3 - 10 mm
Thinly laminated	1 - 3 mm
Very thinly laminated	< 1 mm

TABLE II-5

Diamicton fabric characteristics from Clements Markham Inlet

Section. Sample	Vector Strength R	Eigenvalues S1	S2	S3	Principal Eigenvector Azimuth A	Plunge P
5.1	27.3	0.38	0.26	0.36	348.0	33.2
5.2	16.9	0.55	0.25	0.2	194.8	41.8
5.3	24.3	0.51	0.34	0.15	151.8	16.3
13.4	39.0	0.64	0.22	0.14	23.5	21.0
13.5	29.8	0.43	0.36	0.2	139.5	23.0
14.1	17.8	0.56	0.32	0.12	7.9	22.0
14.2	32.7	0.5	0.31	0.19	0.6	2.4
14.3	31.1	0.48	0.38	0.19	19.5	23.3
14.4	37.7	0.61	0.18	0.21	9.8	28.8
14.5	15.5	0.5	0.23	0.26	137.5	8.2
14.6	34.0	0.55	0.23	0.21	157.0	5.6
1*		0.51	0.44	0.05	218.0	11.4
2*		0.6	0.32	0.08	13.5	5.8
3*		0.58	0.16	0.26	175.0	43.7
4*		0.61	0.28	0.11	333.0	4.0

* unpublished data provided by J. Bednarski

Figure II.1. Northern Ellesmere Island. Study area is located at the north end of Piper Pass where it joins Clements Markham Inlet. Note the extent of permanent icefields and outlet glaciers (stippled) which cover most of the Grant Land Mountains. Inset shows the relationship of Ellesmere Island to NW Greenland. Square at the head of the inlet corresponds to the field area shown in Figure 2.

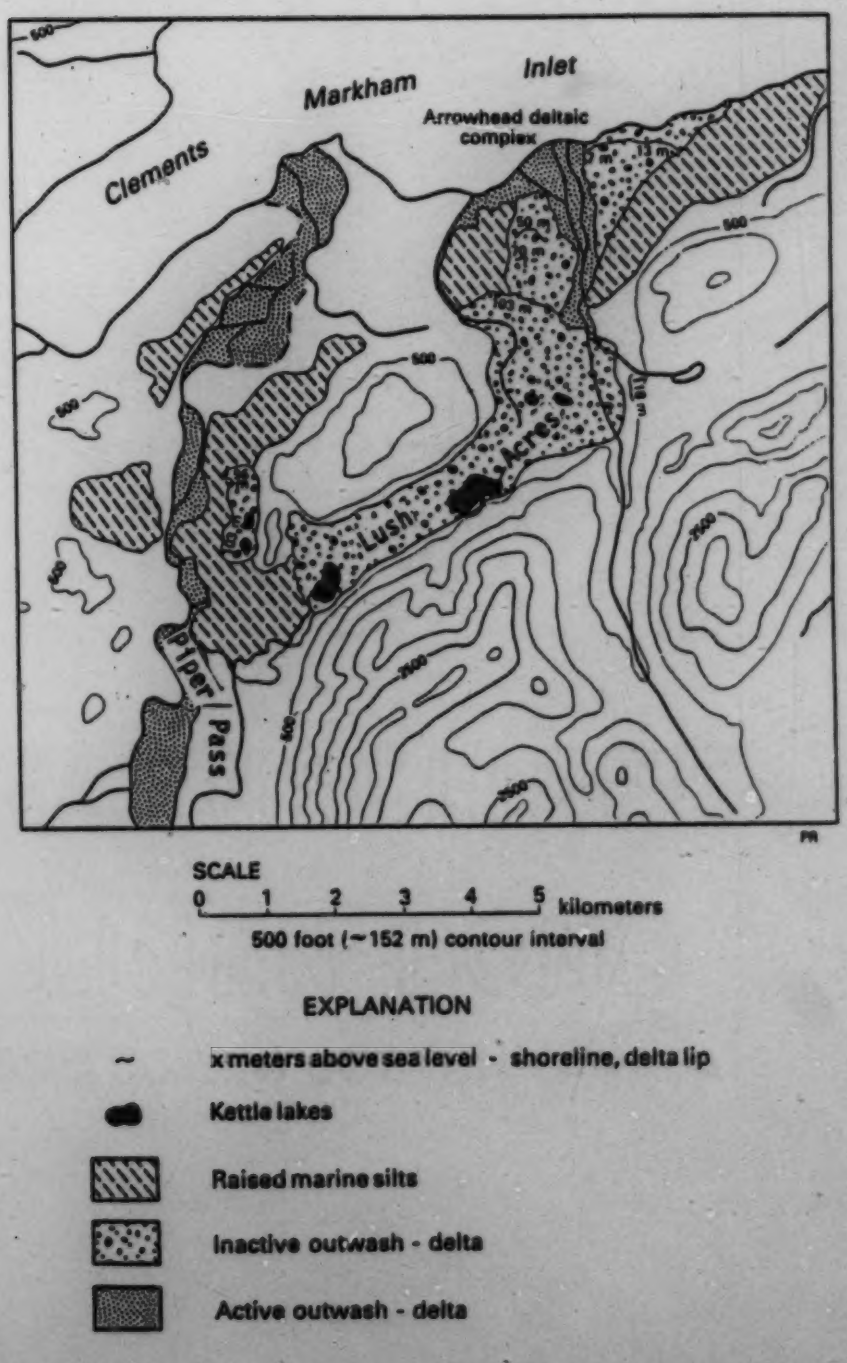

Figure II.2. Surficial geology of the Arrowhead and Piper Pass area.

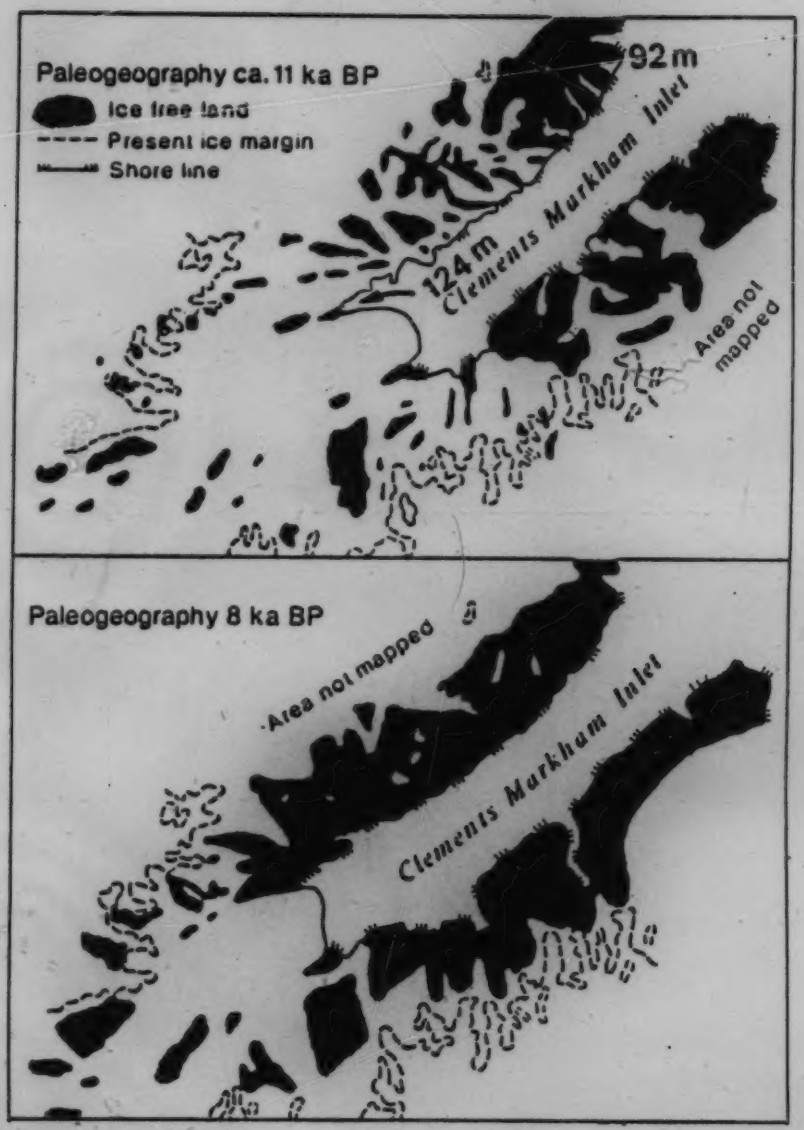

Figure II.3. The last ice limit in Clements Markham Inlet (top) and the subsequent margin, during retreat, at 8000 BP (bottom). Height of the full glacial sea at 11,000 BP is shown in meters above present sea level (modified from Bednarski 1986).

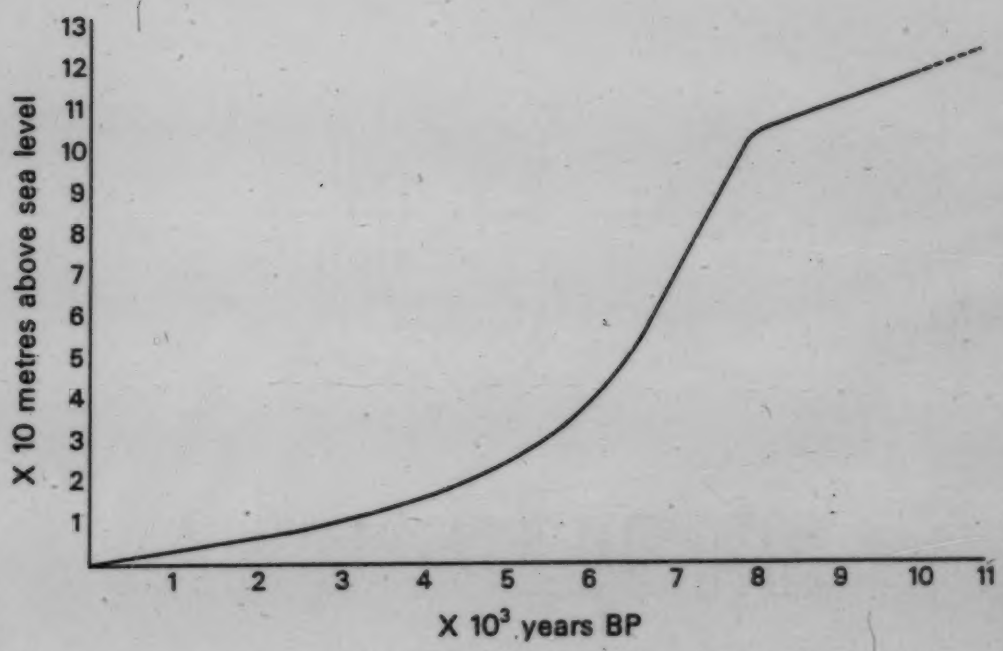

Figure II.4. Emergence curve for inner Clements Markham Inlet (after Bednarski 1986). Note slow rate of emergence, hence slow glacial unloading, between ca. 11,000 to 8000 BP. After 8000 BP the rate of ice retreat and unloading was rapid. Sea level prior to 11,000 BP is unknown.

Figure II.5. The 118 m a.s.l. shoreline at the Arrowhead delta complex. View is to the south up the Arrowhead valley. Lush Acres extends to the east (right) where it intersects Piper Pass.

Figure II.6. High oblique view to NE into Lush Acres. Note paleochannels extending across the sandur. Arrow indicates position of 118 m shoreline (Fig. II.5). Note prominent kettle lakes near the edge of the ice-contact, Arrowhead delta and on the sandur itself.

Figure II.7. Section locations. Note that sections 9-11 relate to postglacial prodeltaic depositional environments and are not discussed here (see Stewart 1981; Stewart and England 1983). The Xs denote the location of the marine limit shorelines at the two deltas. The Os delimit the outer lip of the highest delta or kame surface.

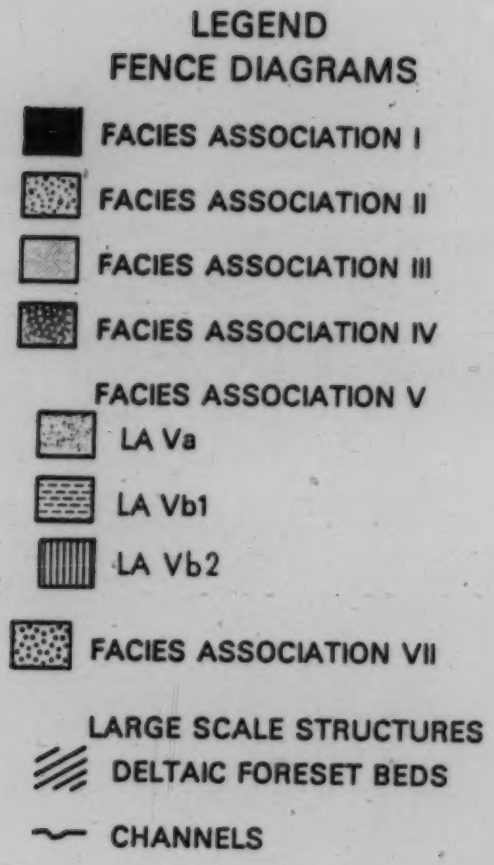

Figure II.8. Fence diagram of Arrowhead delta complex sections.

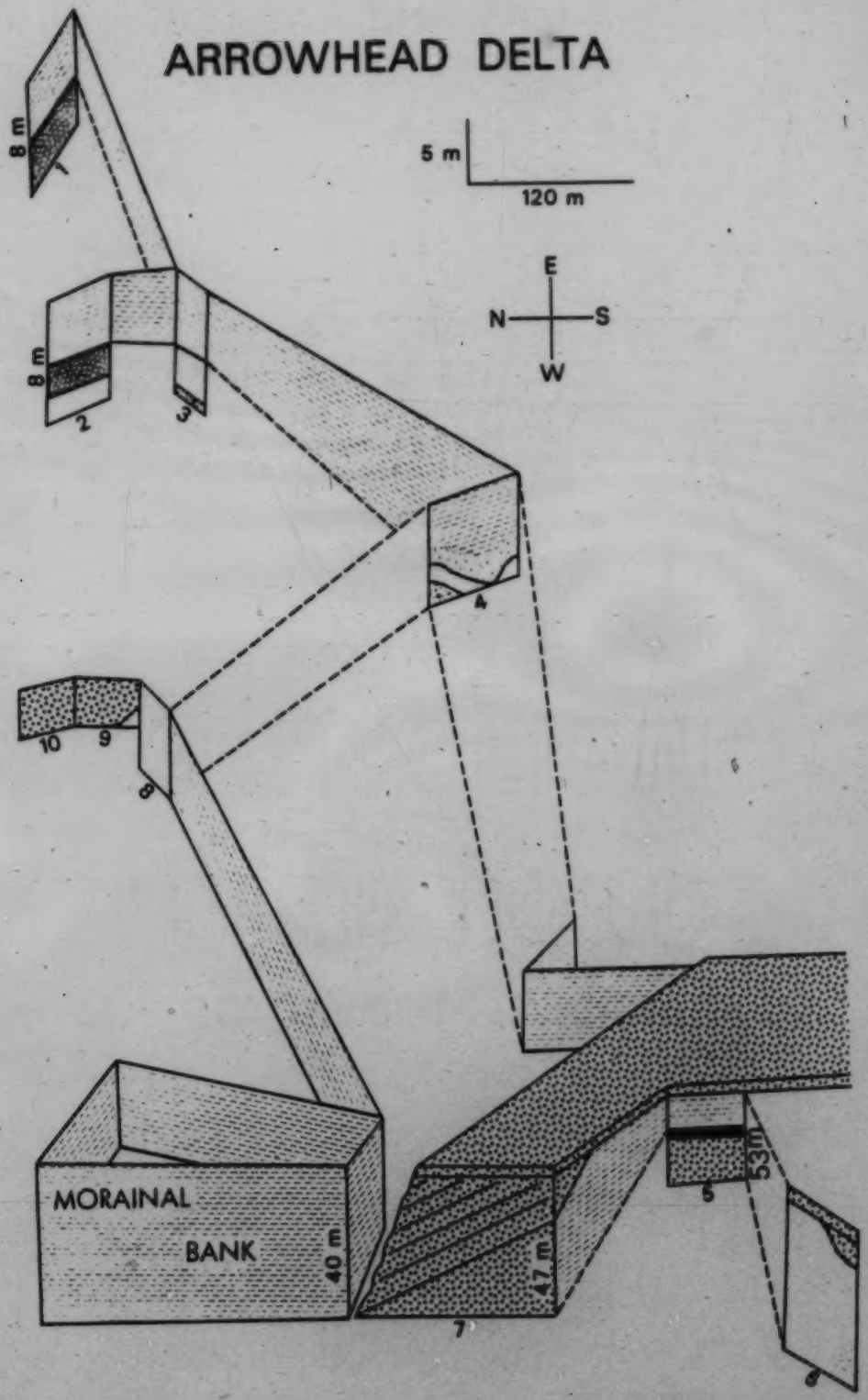
ARROWHEAD DELTA
5 m
120 m
E
N
S
W
8 m
1
8 m
2
3
4
10
9
8
MORAINAL
BANK
40 m
7
47 m
53m
5
6

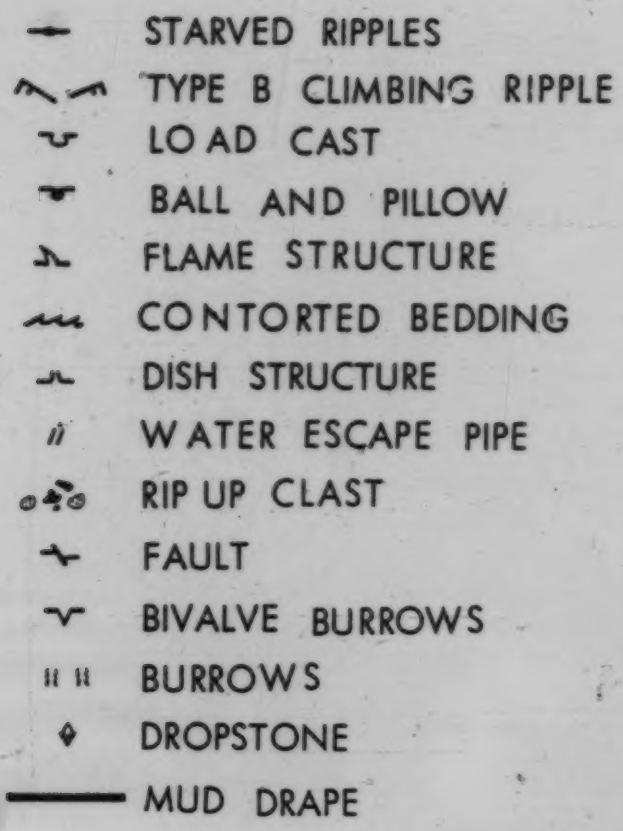

Figure II.9. Generalized stratigraphic columns for Arrowhead delta sections. Left part of columns identifies the lithofacies association. Grain size at bottom of column: Si, silt; SiS, silty sand; S, sand; GS, gravelly sand; G, gravel; D, diamicton.

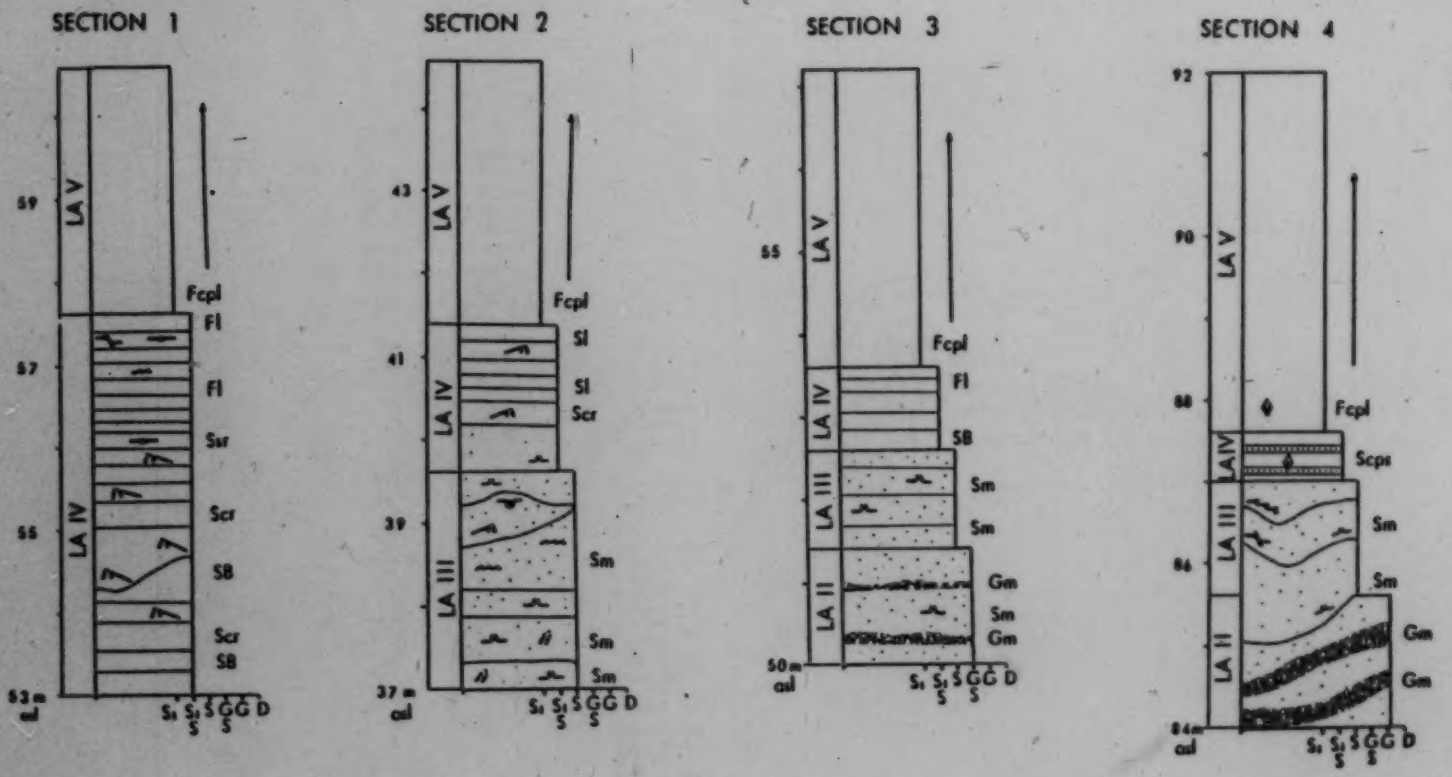
SECTION 1
SECTION 2
SECTION 3
SECTION 4
LA V
LA IV
LA III
LA II
Fcpl
Fl
Sr
Scr
SB
Sl
Sm
Gm
Scps
59
57
55
53 m asl
43
41
39
37 m asl
55
50 m asl
92
90
88
86
84 m asl
S₁ S₂ S G G D

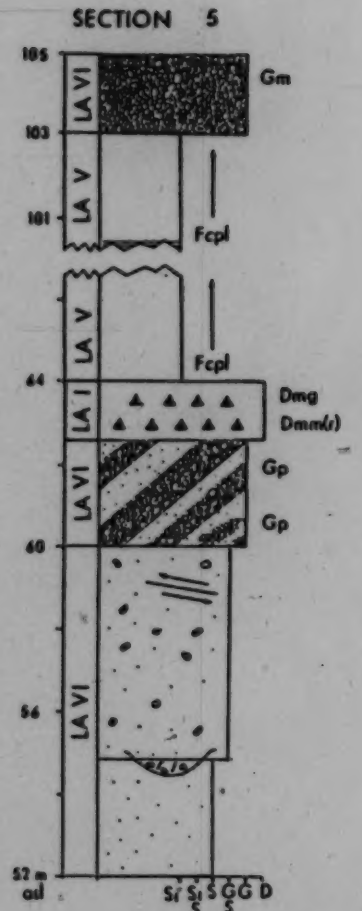
SECTION 5
105
103
101
44
40
36
52 m asl
LA VI
LA V
LA I
LA VI
LA V
LA VI
Gm
Fcpl
Fcpl
Dmg
Dmm(r)
Gp
Gp
Si Si S G G D
S S

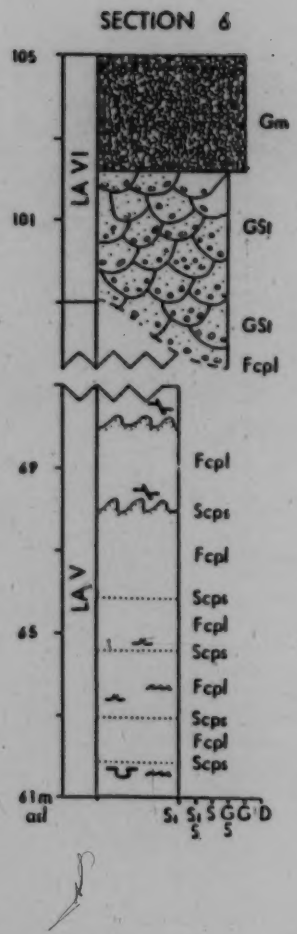
SECTION 6
105
101
69
65
61m asl
LA VI
LA V
Gm
GSt
GSt
Fcpl
Fcpl
Scps
Fcpl
Scps
Fcpl
Scps
Fcpl
Scps
Si Si S G G D
S S

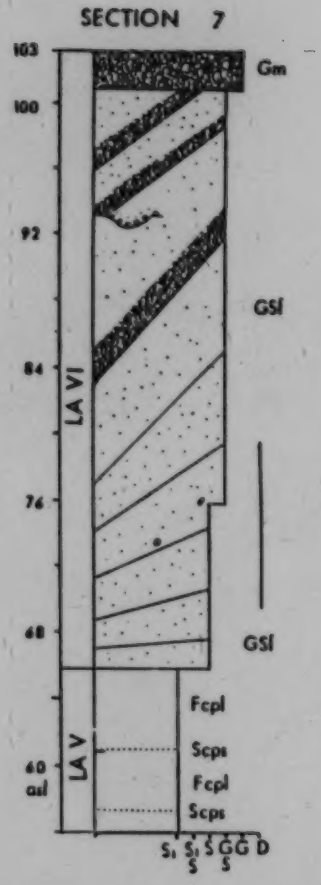
SECTION 7
103
100
92
84
76
68
60 asl
LA VI
LA V
Gm
GSt
GSt
Fcpl
Scps
Fcpl
Scps
Si Si S G G D
S S

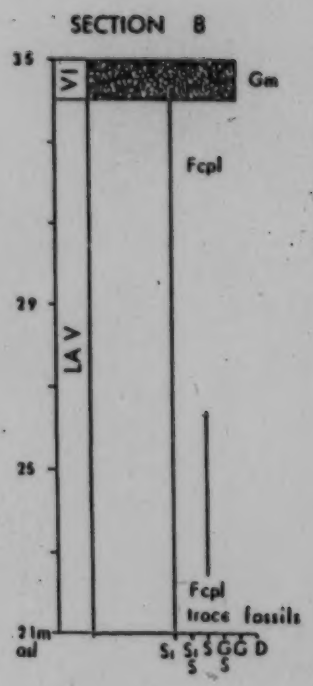
SECTION 8
35
29
25
21m asl
VI
LA V
Gm
Fcpl
Fcpl
trace fossils
Si Si S G G D
S S

Figure II.10 a, b, c, d. Photographs of section 2 illustrating features of specific lithofacies and the fining-upward trend of the section. Photographs are placed stratigraphically from the bottom to the top of the page.

a)Lowest portion of section illustrating medium-bedded sand of LA III (channelized turbidity current and mass flow deposits). Lighter colored sediments are predominantly sand size. The thin, dark laminae are silty sand. These finer sediments outline ripple forms and water escape pillars. Note how the bed 1/3 up the shovel (1 m) thins to the left indicating erosion (amalgamation) of this bed by the current which deposited the overlying bed. Other beds display similar amalgamation but are more difficult to see in this photograph. Paleocurrent direction of ripples is from left to right (north). The lowest beds are ca. 30 cm thick.

b)LA III (channelized turbidity current and mass flow deposits). Sediment is predominantly sandy but ripple forms are defined by silty sand. This indicates that the depositing current had sufficient velocity to transport sand but repeatedly slowed to allow deposition of the silts which outline the climbing ripple forms. Individual ripples have their crests pierced by water escape pipes. Small-scale reverse faults define graben structures formed by collapse resulting from water loss. Paleocurrent direction is to the right (north). Upper part has well developed ball and pillow which also shows as the darker horizon at the top of 10a. Ruler is 15 cm long.

c)LA IV (levee). Thin-bedded, massive to graded sand. Note how the top of many of these sand beds are formed into ripples that are draped by silts and clays. There is also an upward decrease in sand thickness and concomitant increase in number of silt laminae (the thinly-laminated, horizontal part at the top is LA Vba, cyclopels). This is evident both in this photograph and in comparison to the previous (underlying) examples.

d)Transition from LA IV (levee) to LA Vb1 (cyclopels). This photograph also illustrates an upward-fining and thinning. Note ca. 1 cm thick laminae in cleared area to right of shovel; ca. 0.5 cm sand partings above left of shovel; and desiccated "flaggy" appearance of silts in upper right. Flagginess is produced by the very thinly-laminated to one grain thick sand partings.

a)

b)

c)

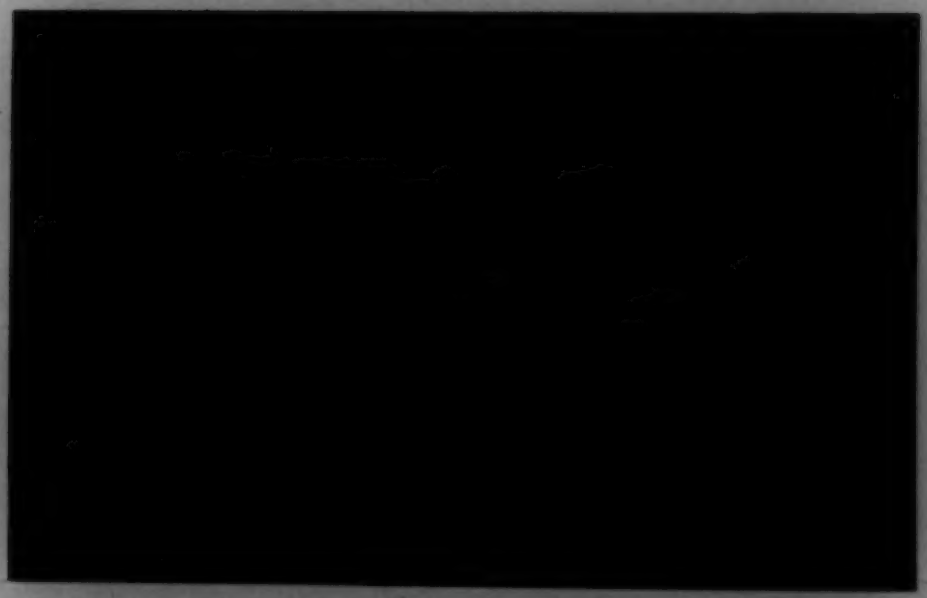

d)

Figure II.11. Lower and upper part show thinly laminated to very thinly bedded LA Va (cyclopsams) in section 4. Note that some coarse laminae produce load structures in the underlying fine-grained laminae (e.g., laminae along base of ruler and at right center). The finer-grained beds in the center of the photograph are LA Vb1 (cyclopels).

Figure II.12. Disrupted, fluidized-liquefied LA Vb1 (cyclopel) of Section 4 (cf. Pickering 1982). Beds below and above this unit are also LA Vb1 (cyclopels).

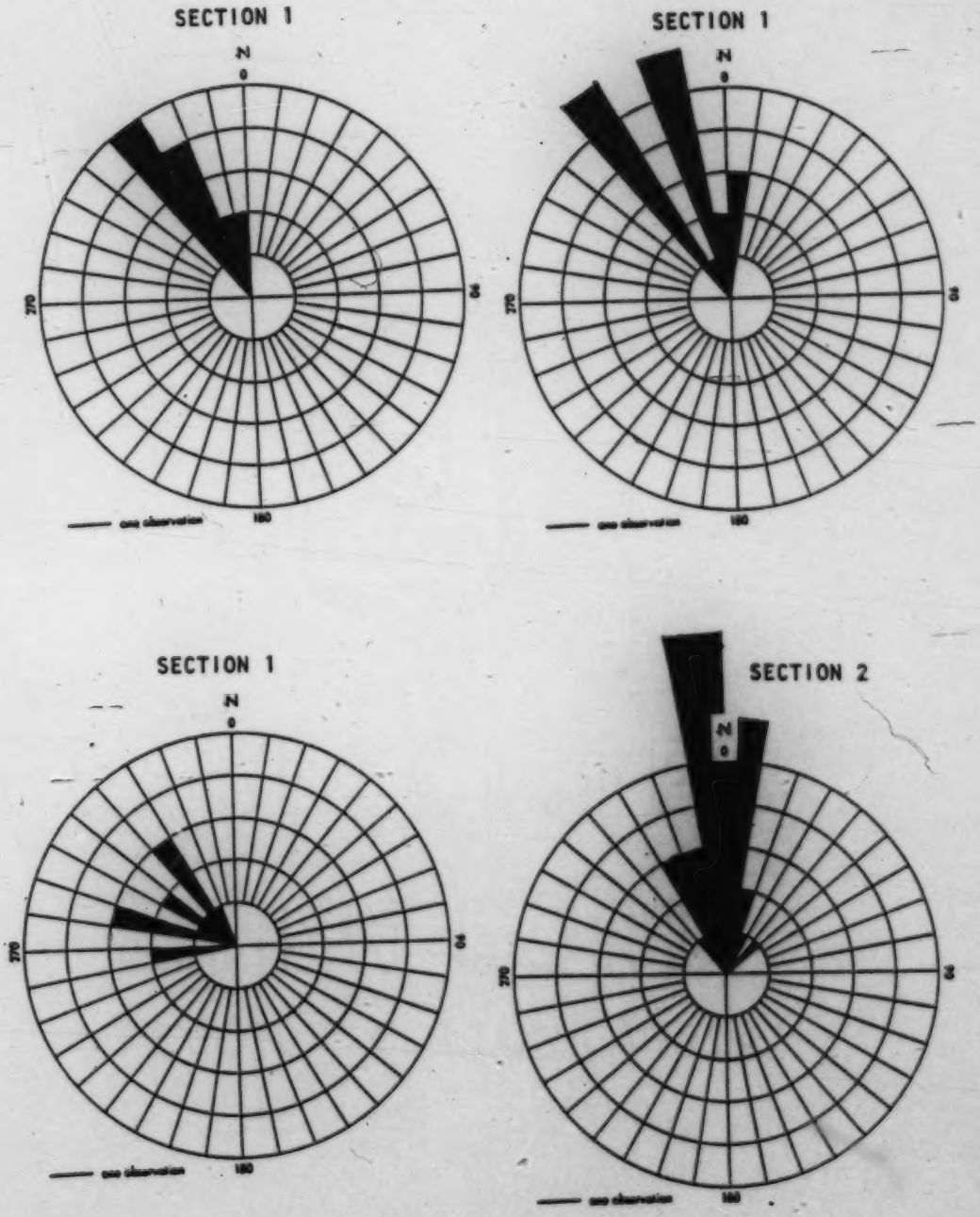

Figure II.13. Paleocurrent measurements from LA IV in sections 1 and 2.

a)

b)

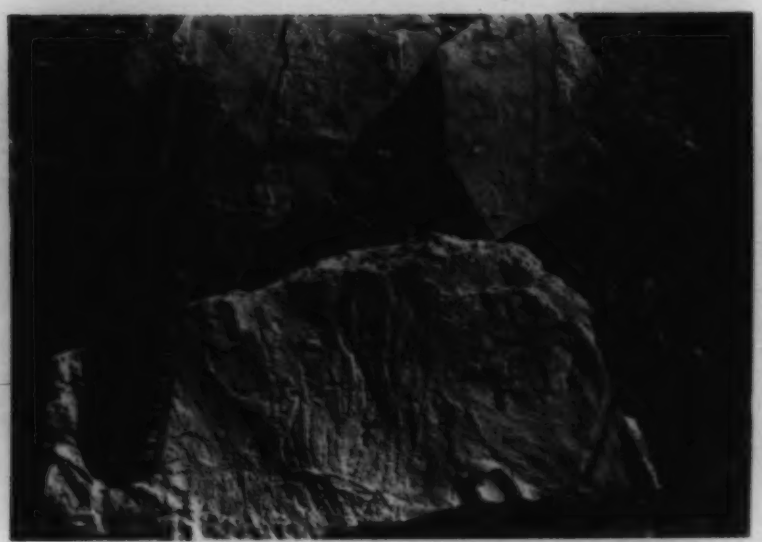

Figure II.14. Trace fossils preserved on bedding planes of LA Vb1 at section 8. a)Fish trail on sediment slab that is opened booklike. Left slab is imprint, right slab is cast. Center imprint of trail results from back-and-forth movement of tail. Outside imprints result from pushing with fins. Trail is crossed by unidentified, segmented impression. b)Unidentified trackways.

Figure II.15. Section 6. Central part of photograph consists of very thinly laminated sand within silty clay. Highly contorted, thickly-laminated to very thinly-bedded sands occur at the base and near the upper right. The central part is LA Vb1 (cyclopels) whereas the thicker sands are LA Va (cyclopsams).

Figure II.16. Section 6. LA VII, crossbedded gravelly sand (GSt) deposited on a delta front platform of the 103 m delta. Gravelly delta topsets of that surface are visible in top of photograph.

Figure II.17. Steepening- and coarsening-upward delta foreset beds of the prograded 103 m Gilbert delta. Cleared portion left of upper center (arrow) marks the chute in Figure II.17. Area to upper right of that is location of topsets shown in Figure II.18. Horizontally-bedded part at lower right is LA Vb1 similar to section 6.

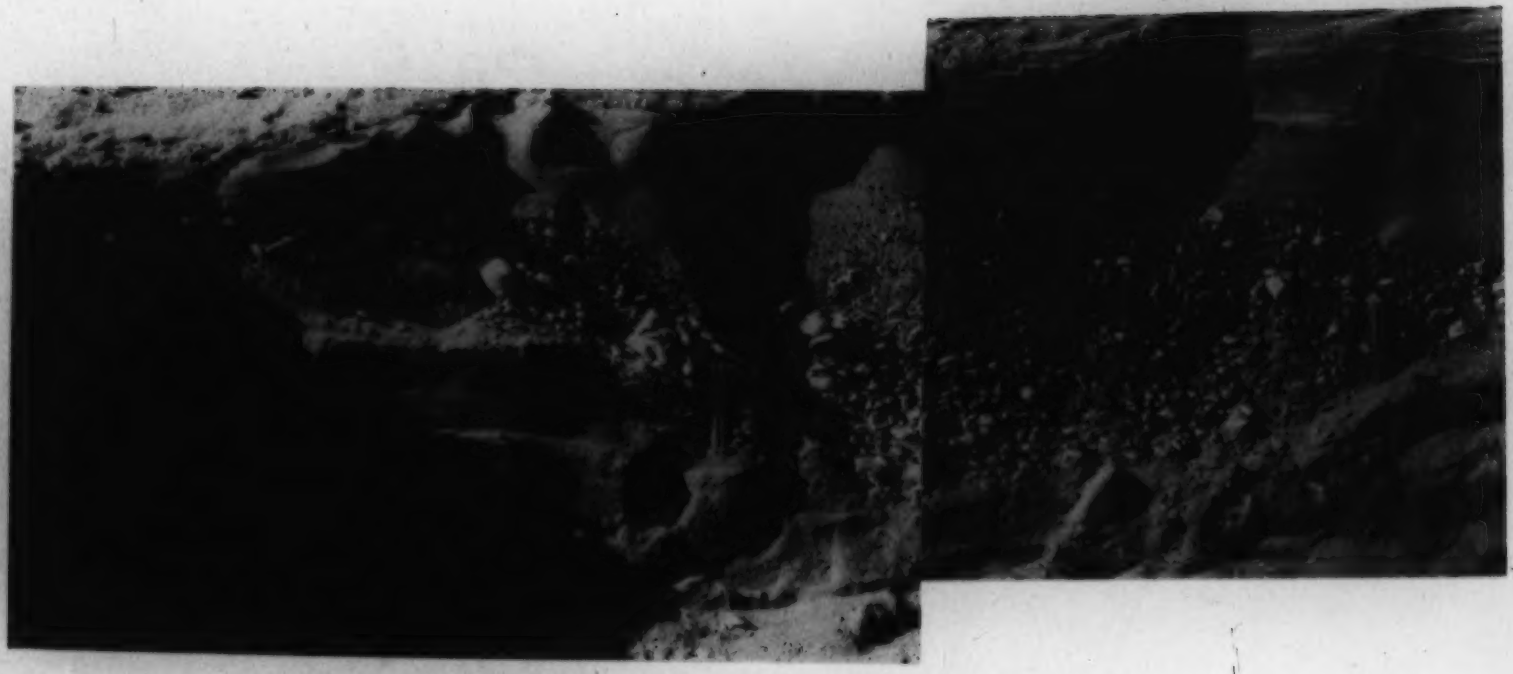

Figure II.18. Photo composite of gravel-filled chute cut into upper foreset beds, 8 m below the surface of the 103 m delta. Base of the chute was eroded by gravels cascading down the foreset bed. Infilling occured by frictional freezing producing a fining-upward fill. Note how the gravels "overspill" the margin to the left. Chute is ca. 0.5 m deep and 3.75 m wide. 15 cm ruler is at right center for scale.

Figure II.19. Topset beds of the 103 m delta surface. Imbrication to the left (downstream) is common but an interlocking structure (indicative of wave reworking?) is also apparent.

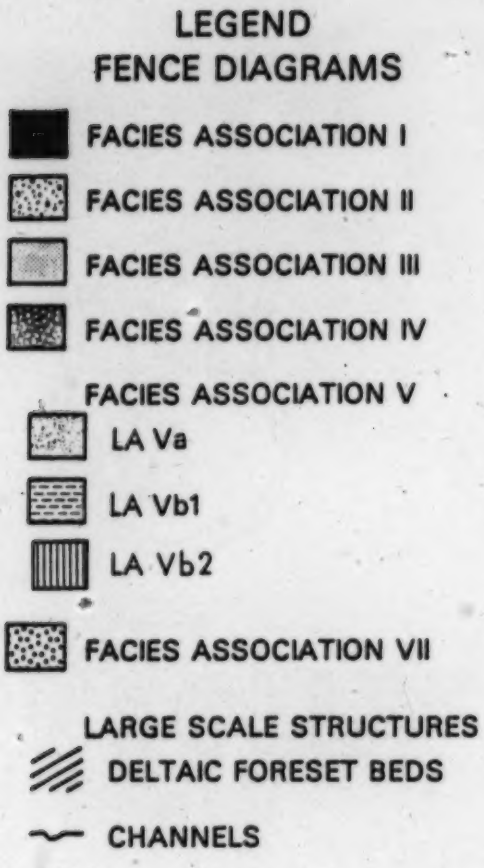

Figure II.20. Fence diagram for Piper Pass sections.

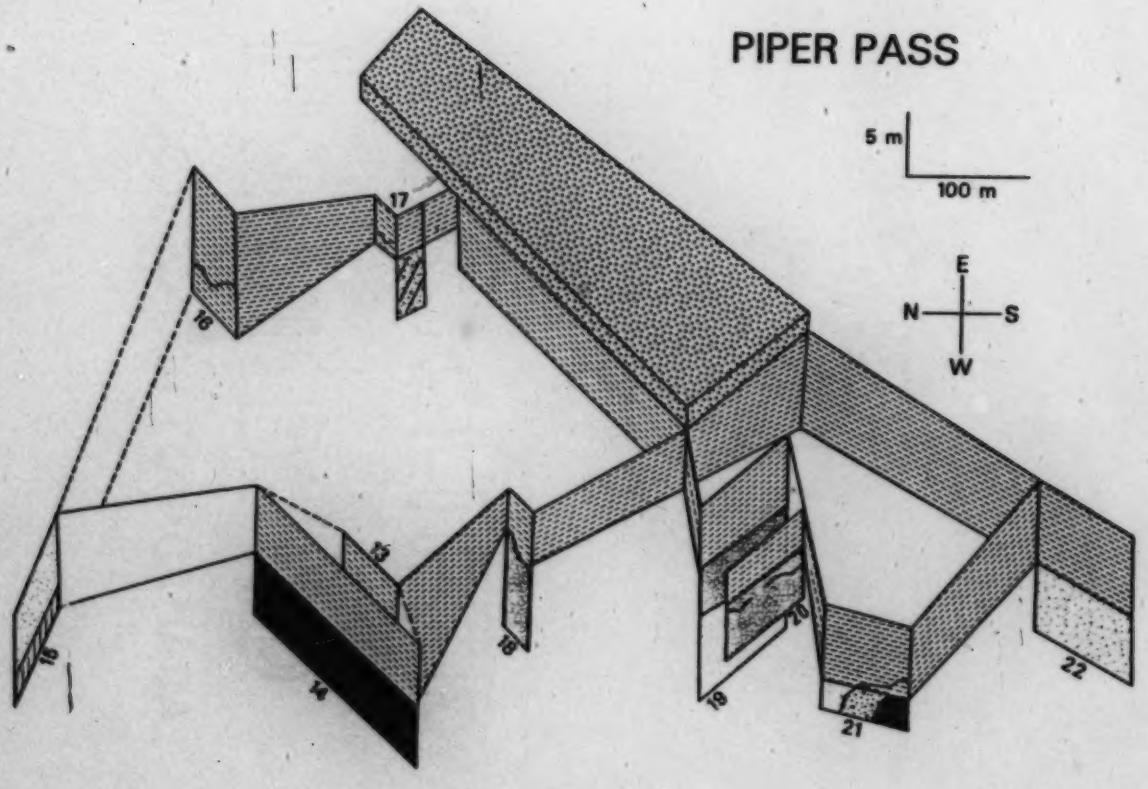
PIPER PASS
5 m
100 m
E
N
S
W
16
17
13
14
18
19
20
21
22

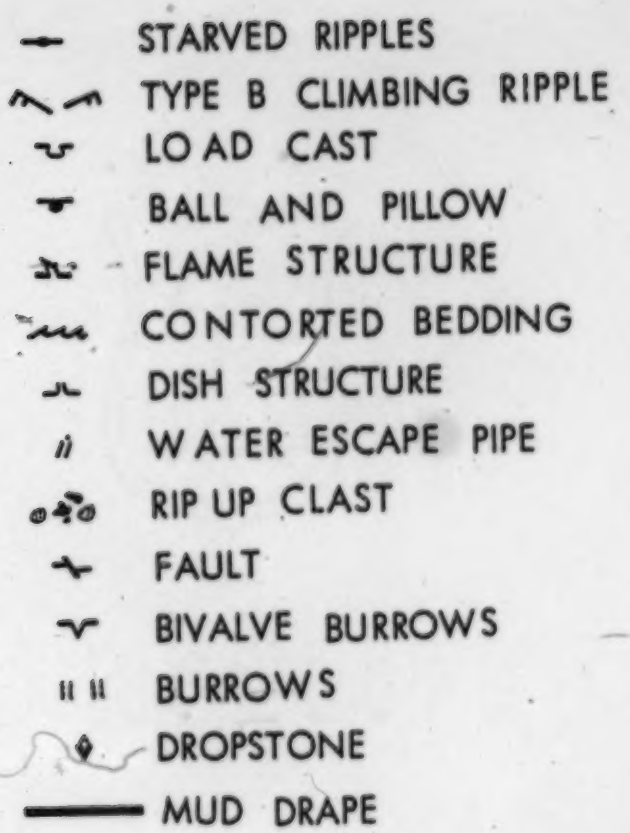

Figure II.21. Generalized stratigraphic columns for Piper Pass sections. Left part of columns identifies the lithofacies association. Grain size indicated at bottom of column: Si, silt; SiS, silty sand; S, sand; GS, gravelly sand; G, gravel; D, diamicton.

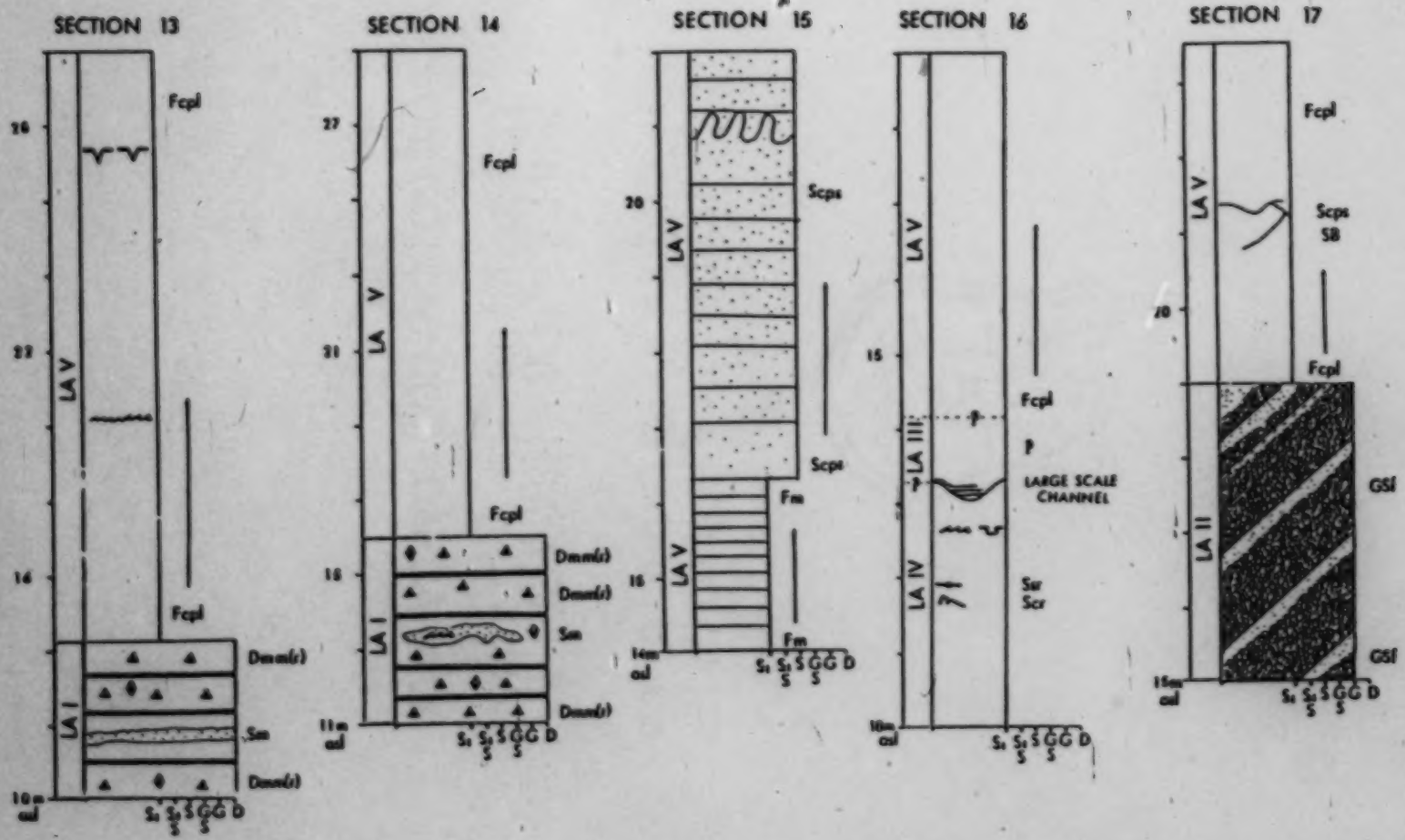
SECTION 13
SECTION 14
SECTION 15
SECTION 16
SECTION 17
Fcpl
Scps
Fm
Dmm(s)
Sm
LA V
LA I
LA II
LA III
LA IV
LARGE SCALE CHANNEL
Sw
Scr
GSI
SB
D
G
S

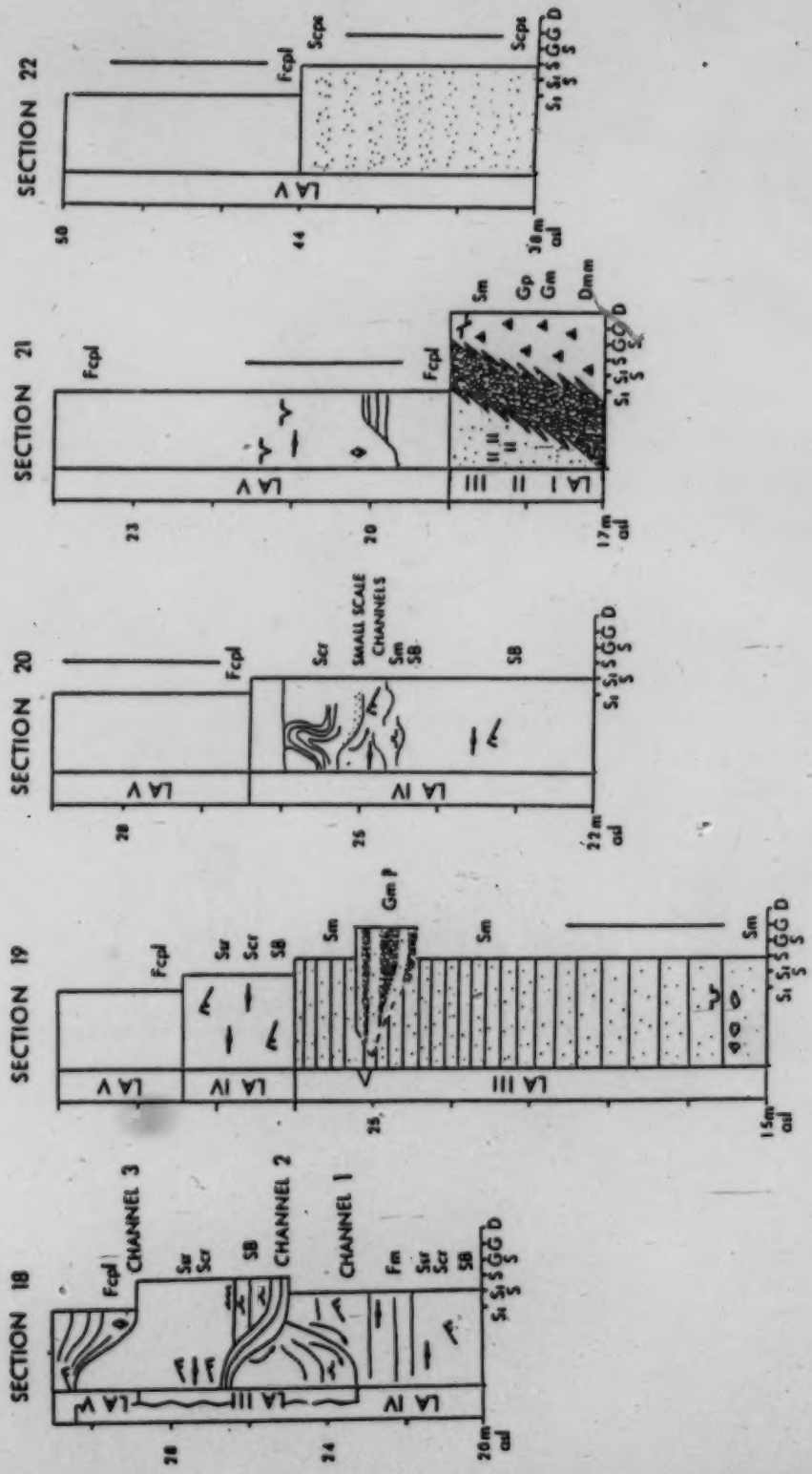
SECTION 22
Fcpl
Scps
Scps
LA V
50
44
30m asl
SECTION 21
Fcpl
Fcpl
Sm
Gp
Gm
Dmm
LA V
LA II
LA I
23
20
17m asl
SECTION 20
Fcpl
Scr
SMALL SCALE CHANNELS
Sm
SB
SB
LA V
LA IV
28
25
22m asl
SECTION 19
Fcpl
Scr
Scr
SB
Sm
Gm P
Sm
Sm
LA V
LA IV
LA III
28
15m asl
SECTION 18
Fcpl
CHANNEL 3
Scr
Scr
SB
CHANNEL 2
CHANNEL 1
Fm
Scr
Scr
SB
LA V
LA III
LA IV
28
24
20m asl

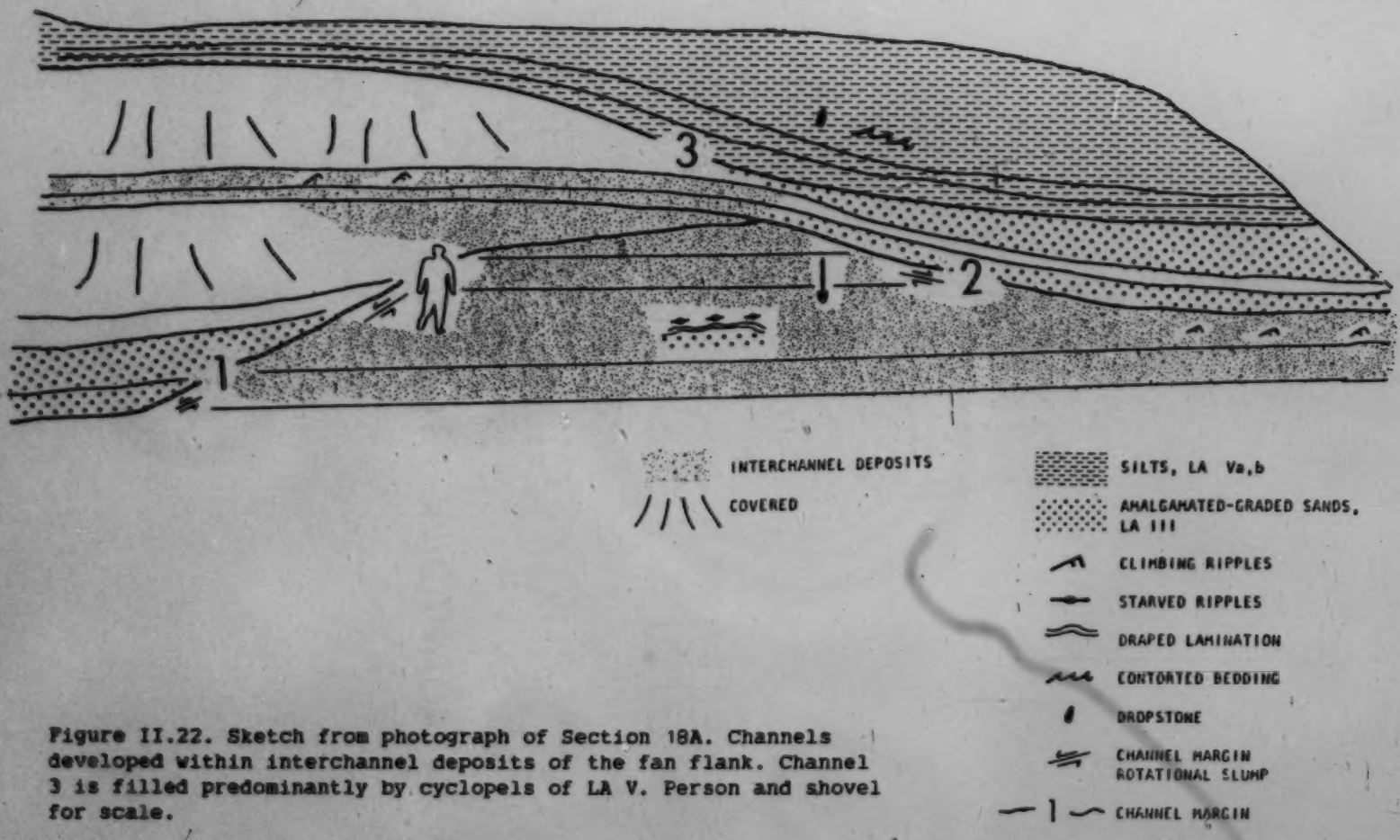

Figure II.22. Sketch from photograph of Section 18A. Channels developed within interchannel deposits of the fan flank. Channel 3 is filled predominantly by cyclopels of LA V. Person and shovel for scale.

Figure II.23a, b.

a)Looking west to section 18B. Dave Jordan is standing on interchannel deposits of lithofacies association IV. Note that the beds he is standing on are truncated by channel 2 whereas those at hip-to-shoulder level behind him can be traced to the left down into channel 2. Arrow points to location of Figure 10b.

b) Channel 2 margin: contact between margin drape suspension deposits and interchannel deposits with starved ripples and graded beds. Note rotational slumping of the interchannel deposits to left of one foot ruler.

a)

b)

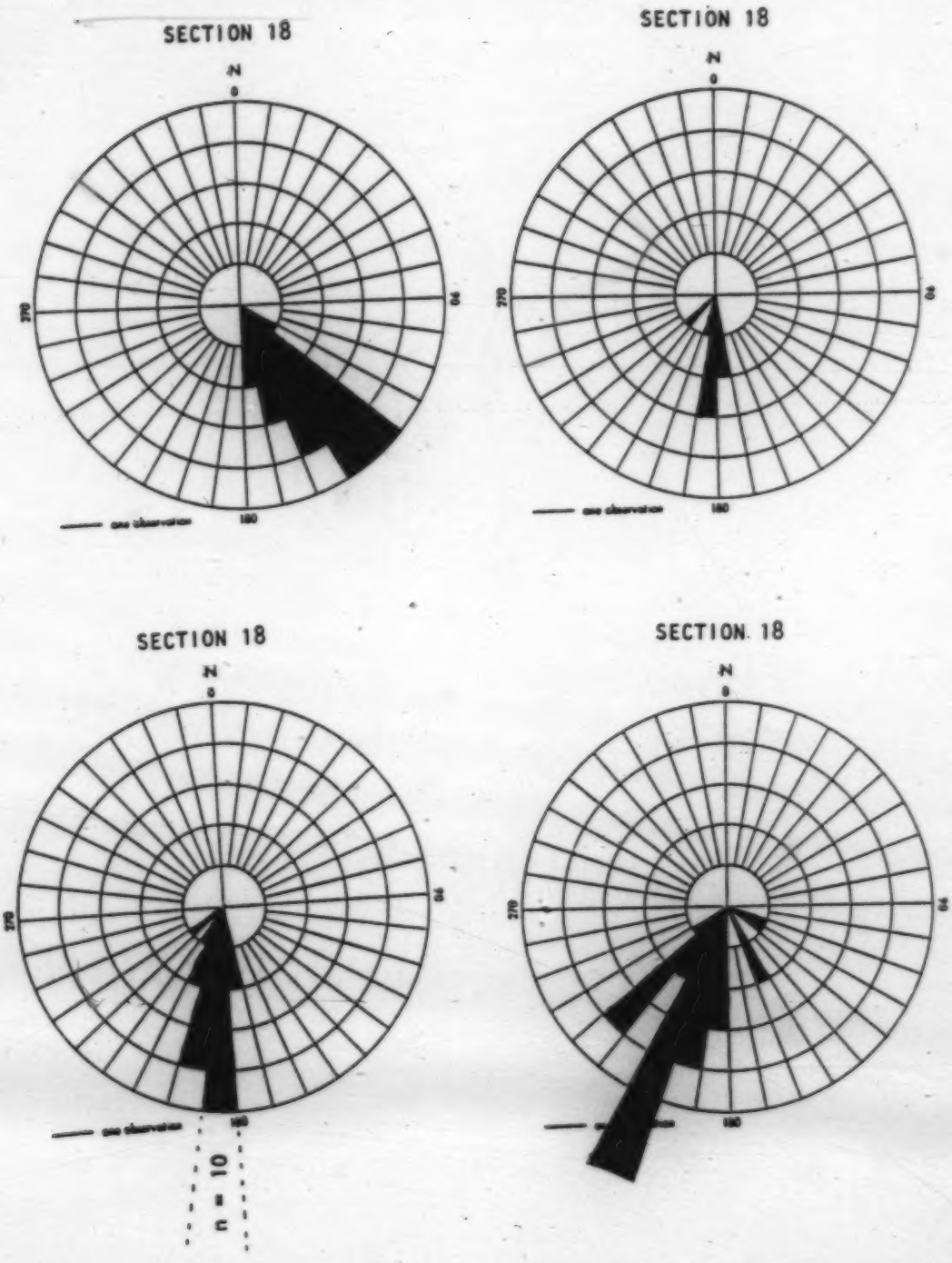

Figure II.24. Paleocurrents measured from LA IV in section 18A.

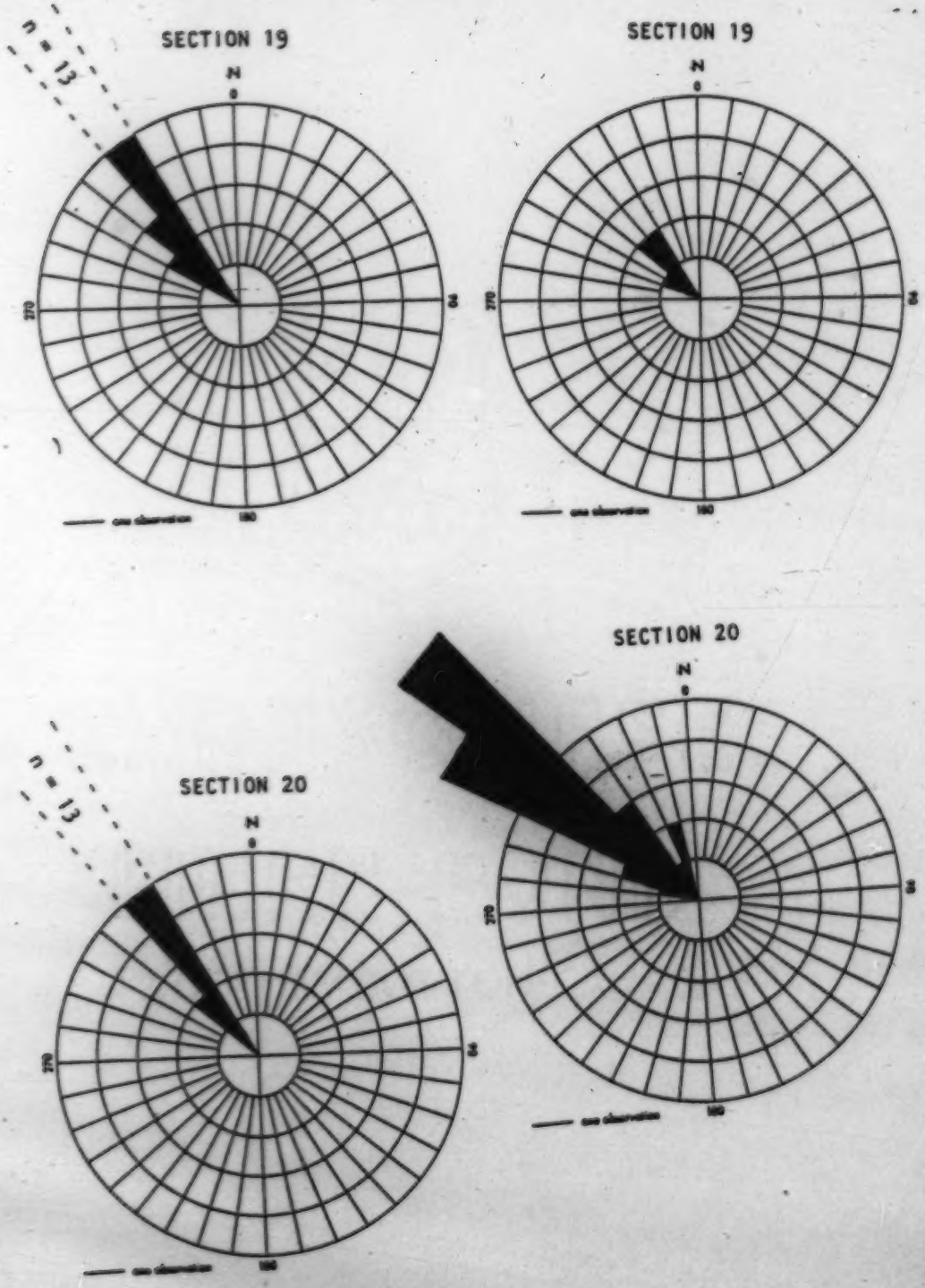

Figure II.25. Paleocurrents measured from LA IV in sections 19 and 20.

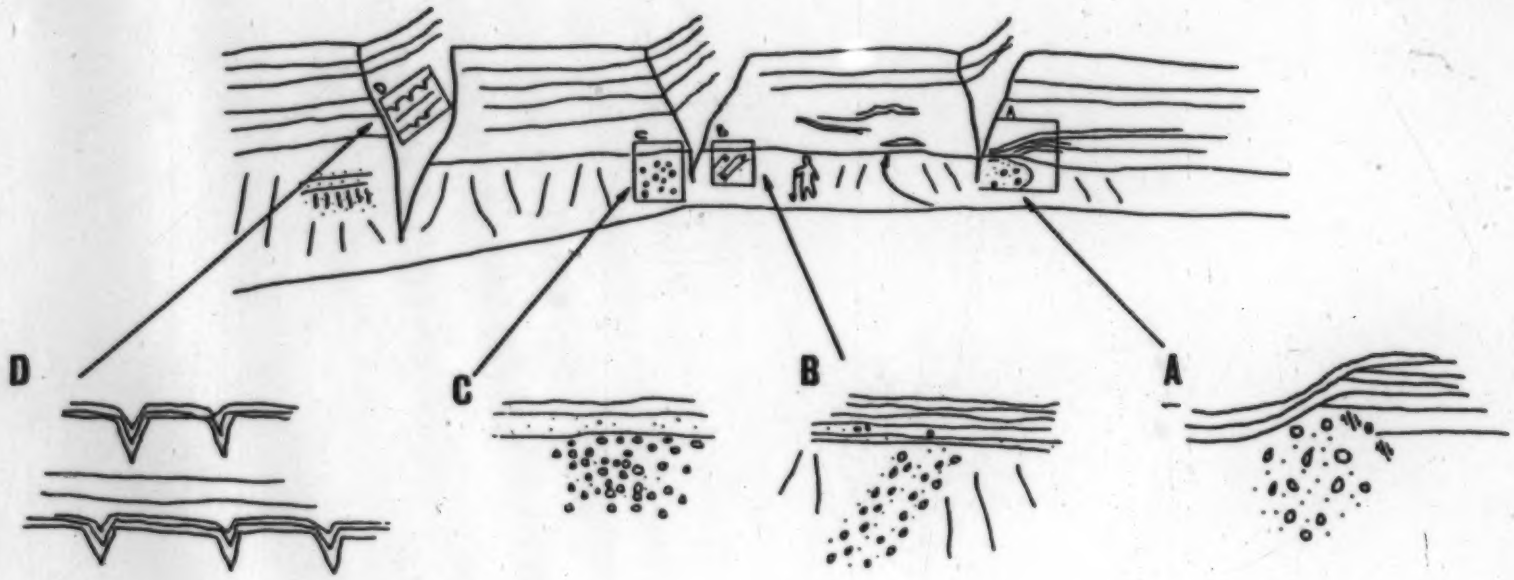

Figure II.26. Sketch of section 21. a)Diamicton draped by fine-grained turbid plume deposits. Normal faults in the diamicton with displacements of ca. 3 to 5 cm suggest the burial and subsequent melting of ice. See also Figure 27b. b)Sorted and cross-bedded gravels overlain by turbid plume deposits. c)Sorted gravels overlain by turbid plume deposits. d)Burrow structures. Arrow indicates position of pod structure shown in Figure II.27a.

Figure II.27a, b. a)Pod-shaped roll structure near center of section 21. b)Channel edge or leading edge of slumped mass above the faulted diamicton. Note that individual beds at the right can be traced to the left where they truncate against the adjacent beds which can be traced to where they conformably drape the truncated beds.

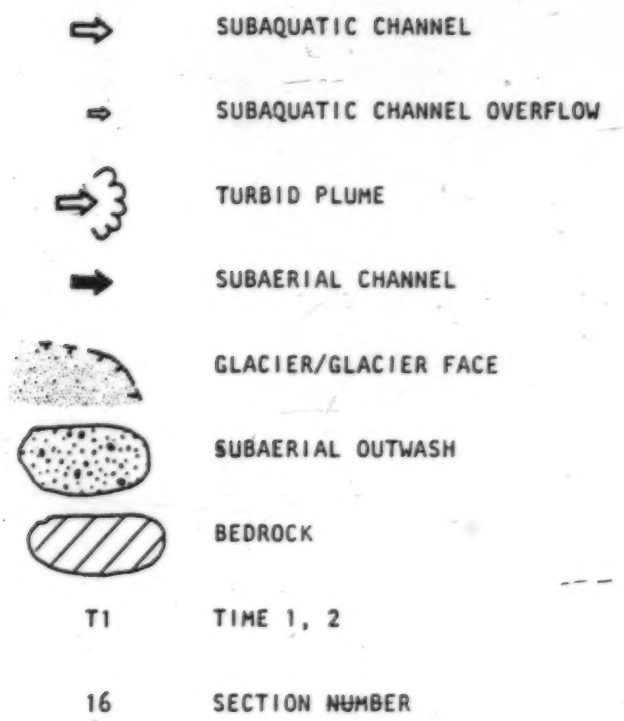

Figure II.28. Pattern of ice retreat and position of subaquatic and subaerial channels for Piper Pass.

a) T_1 represents the position of the ice face after the initial phase of rapid ice retreat (diamictons and cyclopels). At T_1 ice occupies all of Lush Acres and the mouth of Piper Pass depositing subaquatic outwash.

b) At T2 ice has stagnated within Lush Acres and is being covered by subaerial outwash. Exit of subaquatic streams has shifted and subaquatic outwash is deposited in a northerly direction.

c) At T3 ice has completely separated from Lush Acres abandoning the kame and subaerial outwash. Subaquatic streams deposit turbid plume sediments at the mouth of Piper Pass.

A
ca. 8500 BP
rsl ca. 115m

0 1 Km

N

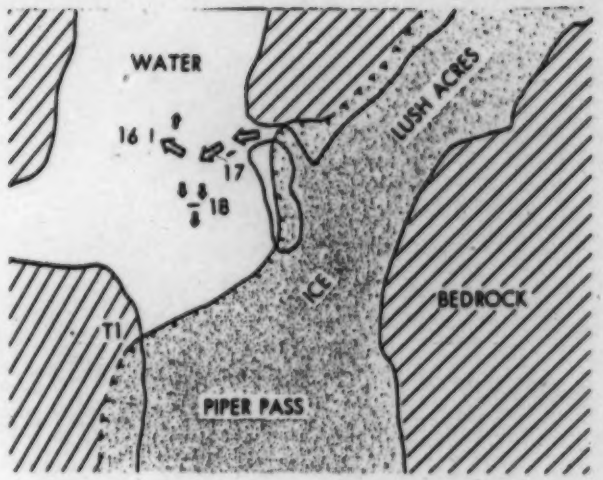

B
ca. 7800 BP
rsl ca. 103m

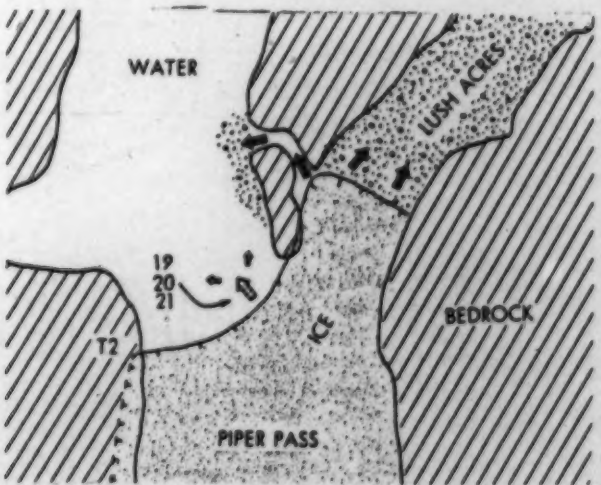

C
≤ 7800 BP
rsl ca. 100m

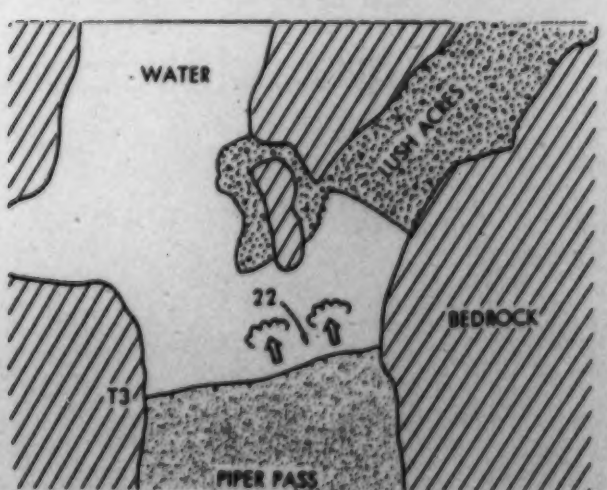

BIBLIOGRAPHY

Allen, J.R.L. 1982. Late Pleistocene (Devensian) glaciofluvial outwash at Banc-y-Warren (West Wales). Geological Journal 17, 31-47.

Andrews, J.T. 1970. A geomorphological study of postglacial uplift with particular reference to arctic Canada. Institute of British Geographers Special Publication No. 2, 156p.

Armstrong, J.E. 1981. Post-Vashon Wisconsin glaciation, Fraser Lowland, British Columbia. Geological Survey of Canada, Bulletin 322, 34p.

Bednarski, J. 1984. Glacier fluctuations and sea level history of Clements Markham Inlet, northern Ellesmere Island. Unpub. Ph.D. thesis, University of Alberta, 232p.

Bednarski, J. 1986. Late Quaternary glacial and sea level events, Clements Markham Inlet, northern Ellesmere Island, Arctic Canada. Canadian Journal of Earth Sciences 23, 1343-1355.

Bednarski, J. in press. The geomorphology of glaciomarine sediments in a high arctic fiord. Geographie physique et Quaternaire.

Bloom, A.L. 1963. Late Pleistocene changes of sealevel and postglacial crustal rebound in coastal Maine. American Journal of Science 261, 862-879.

Bovis, M.J. and Barry, R.G. 1974. A climatological analysis of north polar desert areas. In, T.L. Smiley and J.H. Zumberge, eds., Polar deserts and modern man, 23-31.

Bradley, R.S. and England, J. 1978. Recent climatic fluctuations of the Canadian High Arctic and their significance for glaciology. Arctic and Alpine Research 10, 715-731.

Cheel, R.J. and Rust, B.R. 1982. Coarse grained facies of glaciomarine deposits near Ottawa, Canada. in R. Davidson-Arnott, W. Nickling and B.D. Fahey, eds. Research in glacial, glacio-fluvial, and glacio-lacustrine systems, 279-295.

Christie, R.L. 1964. Geological reconnaissance of northeastern Ellesmere Island, District of Franklin. Geological Survey of Canada, Memior 331, 79p.

Christie, R.L. 1967. Reconnaissance of the surficial geology of northeastern Ellesmere Island, Arctic Archipelago. Geological Survey of Canada, Bulletin 138, 50p.

Clague, J.J. 1984. Quaternary geology and geomorphology, Smithers-Terrace-Prince Rupert area, British Columbia. Geological Survey of Canada, Memior 413, 71p.

Coniglio, M. 1986. Synsedimentary submarine slope failure and tectonic deformation in deep-water carbonates, Cow Head Group, western Newfoundland. Canadian Journal of Earth Sciences 23, 476-490.

Cook, H.E. 1979. Ancient continental slope sequences and their value in understanding modern slope development. in O.H. Pilkey and L.S. Doyle, eds. Geology of continental slopes. S.E.P.M. Special Publication No. 27, 287-305.

Cook, H.E., Field, M.E. and Gardner, J.V. 1982. Characteristics of sediments on modern and ancient continental slopes. in P.A. Scholle and D. Spearing, eds. Sandstone depositional environments, 329-364.

Cowan, E.A., Powell, R.D. and Smith, N.D. 1986. Effects of meltwater stream discharges and fjord water masses on sedimentary deposits at temperate tidewater glaciers. 12th International Sedimentological Congress, 24-30 August, Canberra, Australia, 70.

Dale, J.E., Aitken, A.E., Gilbert, R, and Risk, M.J. 1987. Macrofauna of Canadian arctic fiords. International Union for Quaternary Research, Abstracts, 152.

Domack, E.W. 1983. Facies of late Pleistocene glacial-marine sediments on Whidbey Island, Washington: an isostatic glacial marine sequence. in B.F. Molnia, ed. Glacial-marine sedimentation, 535-570.

Dyke, A.S. 1979. Glacial and sea-level history of southwestern Cumberland Peninsula, Baffin Island, N.W.T., Canada. Arctic and Alpine Research 11, 179-202.

Elverhoi, A., Liestol, O. and Nagy, J. 1980. Glacial erosion, sedimentation and microfauna in the inner part of Kongsfjorden, Spitsbergen. Norsk Polarinstitutt Skrifter No. 172, 33-58.

England, 1978. The glacial geology of northeastern Ellesmere Island, Northwest Territories, Canada. Canadian Journal of Earth Sciences 15, 603-615.

England, J. 1983. Isostatic adjustments in a full glacial sea. Canadian Journal of Earth Sciences, 20, 895-917.

England, J. 1985. The late Quaternary history of Hall Land, N.W. Greenland. Canadian Journal of Earth Sciences, 22, 1394-1408.

England, J. 1986. A paleoglaciation level for north-central Ellesmere Island, N.W.T.. Arctic and Alpine Research 18, 217-222.

England, J. 1987. Glaciation and the evolution of the Canadian high arctic landscape. Geology 15, 419-424.

England, J., Bradley, R.S. and Miller, G.H. 1978. Former ice shelves in the Canadian High Arctic. Journal of Glaciology 20, 393-404.

Eriksson, K.A. 1982. Geometry and internal characteristics of Archean submarine channel deposits, Pilbara Block, western Australia. Journal of Sedimentary Petrology, 52, 383-393.

Eyles, N., Clark, B.M. and Clague, J. 1987. Coarse-grained sediment gravity flows in a large supraglacial lake. Sedimentology 34, 193-216.

Eyles, C.H., Eyles, N. and Miall, A.D. 1985. Models of glaciomarine sedimentation and their application to the interpretation of ancient glacial sequences. Palaeogeography, Palaeoclimatology, Palaeoecology, 51, 15-84.

Eyles, N., Eyles, C.H. Miall, A.D. 1983. Lithofacies types and vertical profile models; an alternative approach to the description and environmental interpretation of glacial diamict and diamictite sequences. Sedimentology, 30, 393-410.

Gawthorpe, R.L. and Clemmey, H. 1985. Geometry of submarine slides in the Bowland Basin (Dinantian) and their relation to debris flows. Journal of the Geological Society of London, 142, 555-565.

Gilbert, R. 1983. Sedimentary processes of Canadian Arctic fjords. Sedimentary Geology, 36, 147-175.

Gravenor, C.P., Von Brunn, V. and Dreimanis, A. 1984. Nature and classification of waterlain glacigenic sediments, exemplified by Pleistocene, late Paleozoic and Precambrian deposits. Earth-Science Reviews 20, 105-166.

Gustavson, T.C., Ashley, G.M. and Boothroyd, J.C. 1975. Depositional sequences in glaciolacustrine deltas. in A.V. Jopling and B.C. McDonald, eds., Glaciofluvial and glaciolacustrine sedimentation. SEPM Special Publication No. 23, 264-280.

Hattersley-Smith, G. 1960. Some remarks on glaciers and climate in northern Ellesmere Island. Geografiska Annaler 42, 45-48.

Hattersley-Smith, G., Fuzesy, A. and Evans, J. 1969. Glacial depths in northern Ellesmere Island: airborne radio echo sounding in 1966. Defense Research Board, Canada, DREO Technical Note 69-6, 23p.

Hein, F.J. 1982. Depositional mechanisms of deep-sea coarse clastic sediments, Cap Enrage Formation, Quebec. Canadian Journal of Earth Sciences, 19, 267-287.

Hicock, S.R., Dreimanis, A. and Broster, B.E. 1981. Submarine flow tills at Victoria, British Columbia. Canadian Journal of Earth Sciences 18, 71-80.

Hodgson, D.A. 1985. The last glaciation of west-central Ellesmere Island, Arctic Archipelago, Canada. Canadian Journal of Earth Sciences, 22, 347-368.

Hodgson, D.A. and Vincent, J.-S. 1984. A 10,000 yr B.P. extensive ice shelf over Viscount Melville Sound, arctic Canada. Quaternary Research 22, 18-30.

Howell, D.G. and Normark, W.R. 1982. Sedimentology of submarine fans. in P.A. Scholle and D. Spearing, eds. Sandstone depositional environments, 365-404.

Iken, A. 1977. Variations of surface velocities of some alpine glaciers measured at intervals of a few hours. Comparison with arctic glaciers. Zeitschrift fur Gletscherkunde und Glazialgeologie 13, 23-35.

Ingram, R.L. 1954. Terminology for the thickness of stratification and parting units in sedimentary rocks. Bulletin of the Geological Society of America 65, 937-938.

Jorgensen, N.B. 1982. Turbidites and associated resedimented deposits from a tilted glacio-deltaic sequence, Denmark. Geological Survey of Denmark, Yearbook 1981, 47-72.

Lowe, D.R. 1982. Sediment gravity flows: II. Depositional models with special reference to the deposits of high-density turbidity currents. Journal of Sedimentary Petrology 52, 279-297.

Mackiewicz, N.E., Powell, R.D., Carlson, P.R., and Molnia, B.F. 1984. Interlaminated ice-proximal glacimarine sediments in Muir Inlet, Alaska. Marine Geology, 57, 113-147.

Macpherson, B.A. 1978. Sedimentation and trapping mechanism in upper Miocene and older turbidite fans of southeastern San Joaquin valley, California. Bulletin of the American Association of Petroleum Geologists 62, 2243-2274.

McCabe, A.M. 1986. Glaciomarine facies deposited by retreating tidewater glaciers: an example from the late Pleistocene of Northern Ireland. Journal of Sedimentary Petrology 56, 880-894.

McCabe, A.M., Dardis, G.F. and Hanvey, P.M. 1984. Sedimentology of a late Pleistocene submarine-moraine complex, County Down, Northern Ireland. Journal of Sedimentary Petrology 54, 716-730.

Miall, A.D. 1977. A review of the braided river depositional environment. Earth-Science Reviews 13, 1-62.

Mode, W.N., Nelson, A.R. and Brigham, J.R. 1983. A facies model of Quaternary glacial-marine cyclic sedimentation along eastern Baffin Island, Canada. in, B.F. Molnia, ed., Glacial-marine sedimentation, 495-533.

Muller, F. 1976. On the thermal regime of a high-arctic valley glacier. Journal of Glaciology 16, 119-133.

Muller, F. and Iken, A. 1973. Velocity fluctuations and water regime of arctic valley glaciers. Symposium on the hydrology of glaciers, International Association of Scientific Hydrology Publication no. 95, 165-182.

kMutti, E. 1977. Distinctive thin-bedded turbidite facies and related depositional environments in the Eocene Hecho Group (south-central Pyrenees, Spain). Sedimentology, 24, 107-131.

Nelson, A. R. 1981. Quaternary glacial and marine stratigraphy of the Qivitu Peninsula, northern Cumberland Peninsula, Baffin Island, N.W.T., Canada. Geological Society of America Bulletin 92, Part II, 1143-1261.

Nemec, W. and Steel, R.J. 1984. Alluvial and coastal conglomerates: their significant features and some comments on gravelly mass-flow deposits. in E.H. Koster and R.J. Steel, eds., Sedimentology of gravels and conglomerates, 1-31.

Normark, W.R. and Dickson, F.H. 1976. Sublacustrine fan morphology in Lake Superior. American Association of Petroleum Geologists Bulletin, 60, 1021-1036.

Pickering, K.T. 1983. Transitional submarine fan deposits from the late Precambrian Kongsfjord Formation submarine fan, NE Finnmark, N. Norway. Sedimentology, 30, 181-199.

Powell, R.D. 1980. Holocene glacimarine sediment deposition by tidewater glaciers in Glacier Bay, Alaska. Unpub. Ph.D. thesis, Ohio State University, 420p.

Powell, R.D. 1981. A model for sedimentation by tidewater glaciers. Annals of Glaciology, 2, 129-134.

Powell, R.D. 1983. Glacial-marine sedimentation processes and lithofacies of temperate tidewater glaciers, Glacier Bay, Alaska. in B.F. Molnia, ed. Glacial-marine sedimentation, 185-232.

Powell, R.D. 1984. Glacimarine processes and inductive lithofacies modelling of ice shelf and tidewater glacier sediments based on Quaternary examples. Marine Geology, 57, 1-52.

Powell, R.D. and Cowan, E.A. 1986. Depositional processes at McBride Inlet and Riggs Glacier. in P.J. Anderson, R.P. Goldthwait, G.D. McKenzie, eds., Observed Processes of Glacial Deposition in Glacier Bay, Alaska. Ohio State University, Institute of Polar Studies Miscellaneous Publication No. 236, 140-156.

Prest, V.K. 1970. Quaternary geology of Canada. In, Geology and economic minerals of Canada. Geological Survey of Canada, Economic Geology Report No. 1, 675-764.

Prior, D.B., Bornhold, B.D., Coleman, J.M. and Bryant, W.R. 1982. Morphology of a submarine slide, Kitimat Arm, British Columbia. Geology 10, 588-592.

Retelle, M.J. 1986. Glacial geology and Quaternary marine stratigraphy of the Robeson Channel area, northeastern Ellesemere Island, Northwest Territories. Canadian Journal of Earth Sciences 23, 1001-1012.

Rust, B.R. 1977. Mass flow deposits in a Quaternary succession near Ottawa, Canada: diagnostic criteria for subaqueous outwash. Canadian Journal of Earth Sciences, 14, 175-184.

Rust, B.R. and Romanelli, R. 1975. Late Quaternary subaqueous outwash deposits near Ottawa, Canada. in A.V. Jopling and B.C. McDonald, eds. Glaciofluvial and glaciolacustrine sedimentation, S.E.P.M. Special Publication No. 23, 177-192.

Saunders, I.R., Clague, J.J. and Roberts, M.C. 1987. Deglaciation of Chilliwack River valley, British Columbia. Canadian Journal of Earth Sciences 24, 915-924.

Seramur, K.C. and Powell, R.D. 1987. Temperate glacimarine lithofacies interpreted from seismic facies. International Quaternary Association, Abstracts, July 31 to August 9.

Shearer, D.L. 1974. Modern and early Holocene arctic deltas, Melville Island, Northwest Territories, Canada. unpublished M.Sc. thesis, University of South Carolina, Columbia, 143p.

Solheim, A. and Pfirman, S.L. 1985. Sea-floor morphology outside a grounded, surging glacier; Brasvellbreen, Svalbard. Marine Geology 65, 127-143.

Sollid, J.-L. and Reite, A.J. 1983. The last glaciation and deglaciation of central Norway. in J. Ehlers, ed., Glacial deposits of northwest Europe, 41-59.

Steel, R.J. and Thompson, D.B. 1983. Structures and textures in Triassic braided stream conglomerates (Bunter Pebble Beds) in the Sherwood Sandstone Group, North Staffordshire, England. Sedimentology 30, 341-367.

Stewart, T.G. 1981. The Holocene paleoenvironment of Clements s Markham Inlet, northern Ellesmere Island, N.W.T., Canada. unpub. M.Sc. thesis, University of Alberta, Edmonton, 135p.

Stewart, T.G. and England, J. 1983. Holocene sea-ice variations and paleoenvironmental change, northernmost Ellesmere Island, N.W.T., Canada. Arctic and Alpine Research, 15, 1-17.

Stewart, T.G. and Bednarski, J. 1986 (abs.). Basal crevasses and folded foliation along the margin of a subpolar glacier. American Quaternary Association, Program and Abstracts, 9th Biennial Meeting, 2-4 June, Champaign-Urbana, Illinois, 105.

Stewart, T.G. and England, J. 1986. An early Holocene caribou antler from northern Ellesmere Island, Canadian Arctic Archipelago. Boreas, 15, 25-31.

Sugden, D.L. and Clapperton, C.M. 1981. An ice shelf moraine, George VI Sound, Antarctica. Annals of Glaciology 2, 135-141.

Thomas, G.S.P. 1984a. Sedimentation of a sub-aqueous esker-delta at Strabathie, Aberdeenshire. Scottish Journal of Geology, 20, 9-20.

Thomas, G.S.P. 1984b. A Late Devensian glaciolacustrine fan-delta at Rhosemar, Clwyd, North Wales. Geological Journal, 19, 125-141.

Thomas, G.S.P., Connaughton, M. and Dackombe, R.V. 1985. Facies variation in a Late Pleistocene supraglacial outwash sandur from the Isle of Man. Geological Journal, 20, 193-213.

Trettin, H.P. 1972. Geology of lower Paleozoic formations, Hazen Plateau and southern Grant Land Mountains, Ellesmere Island, Arctic Archipelago. Geological Survey of Canada, Bulletin 203, 134p.

Wagner, F.J.E. 1970. Faunas of the Pleistocene Champlain Sea. Geological Survey of Canada, Bulletin 181, 104p.

Walcott, R.I. 1970. Flextural rigidity, thickness and viscosity of the lithosphere. Journal of Geophysical Research 75, 3941-3954.

Walcott, R.I. 1972. Past sea levels, eustasy and deformation of the earth. Quaternary Research 2, 1-14.

Walker, R.G. 1977. Deposition of upper Mesozoic resedimented conglomerates and associated turbidites in southwestern Oregon. Geological Society of America Bulletin 88, 273-285.

Walker, R.G. 1978. Deep-water sandstone facies and ancient submarine fans: models for exploration of stratigraphic traps. American Association of Petroleum Geologists Bulletin 62, 932-966.

Walker, R.G. 1985. Mudstones and thin-bedded turbidites associated with the Upper Cretaceous Wheeler Gorge Conglomerates, California: a possible channel-levee complex. Journal of Sedimentary Petrology, 55, 279-290.

Weidick, A. 1975. A review of Quaternary investigations in Greenland. Ohio State University, Institute of Polar Studies Report No. 55, 161p.

Wightman, D,M. 1980. Late Pleistocene glaciofluvial and glaciomarine sediments on the north side of the Minas Basin, Nova Scotia. unpublished Ph.D. thesis, Dalhousie University, Halifax, Nova Scotia.

Winn, R.D. Jr. and Dott, R.H. Jr. 1977. Large-scale traction-produced structures in deep-water fan-channel conglomerates in southern Chile. Geology 5, 410-414.

III. SUBPOLAR GLACIOMARINE SEDIMENTS FROM CLEMENTS MARKHAM INLET, N.W.T., CANADA

Introduction

Most of the surficial deposits surrounding inner Clements Markham Inlet, northern Ellesmere Island consist of raised marine sediments deposited between 11,000 and 8000 BP as glaciers retreated in contact with the sea (Figs. III.1, III.2; Bednarski 1984, 1986, in press; Chapter 2). Subsequent postglacial emergence has exposed these sediments, including sandurs and deltas, to extensive subaerial erosion. This provides an excellent opportunity for studying the composition of this former nearshore environment. In this study the deposits exposed in two emergent glaciomarine deltas from the inner south shore of the inlet were selected for investigation. Fieldwork demonstrates that these raised marine sediments are predominantly subaquatic-glacial deposits related to tidewater glaciers (chapter 2). These sediments record the nature of glaciomarine sedimentation in a high arctic fiord presently occupied by permanent landfast sea ice and surrounded by subpolar glaciers. Such investigations provide the first detailed sedimentological treatment of high arctic fiords and this environment may be representative of other circumpolar areas during the last glaciation.

This study is divided into two parts. The first part examined the geomorphology, chronology and stratigraphy of the two glaciomarine deltas (Chapter 2). This chapter describes the sediments in greater detail. The raised marine sediments were subdivided into six lithofacies associations attributed to three

major depositional environments (LA I to VI, Tables II-1, II-2, II-3; Chapter 2). Stratigraphically these are arranged in a fining-upward sequence related to ice retreat (Chapter 2). The deposits related to subaerial delta progradation are assigned to LA VI and are discussed only in chapter 2. The present chapter describes and interprets the glaciomarine lithofacies utilized in the lithofacies associations.

Study Area

Clements Markham Inlet is 50 km long, 8 km wide, and trends NE-SW, extending from the Arctic Ocean-Lincoln Sea into the Grantland Mountains (Figs. III.1, III.2). Summits rise to 2000 m above sea level (asl) at the inlet head and decline to 600 m asl along the outermost coast. Despite this high relief, the adjoining valleys such as the Clements Markham and Piper Pass rivers occur at low elevations and have low gradients for many kilometers before reaching the inlet. The lower parts of these valleys are now dominated by active sandurs emanating from the numerous outlet glaciers that occur ca. 8 to 30 km inland. High postglacial seas (> 100 m asl) previously transgressed these valleys and strongly influenced the nature of sedimentation and the rate of glacial retreat (chapter 2; Bednarski 1984, 1986, in press). All the rivers and smaller gullies incise extensive postglacial sediments that emerged after the deglaciation of the inlet head (Fig. III.2).

Mean annual temperatures range from -18 °C at the coastal station of Alert to -23 °C in the continental interior surrounding Lake Hazen (Fig. III.1). The region has a polar desert climate

with a water balance close to zero (Bovis and Barry 1974). Despite this aridity and short ablation seasons (ca. 50 to 80 days, Bradley and England 1979) large volumes of meltwater are produced as indicated by the large, active floodplains of the major valleys. Today, the outlet glaciers surrounding the inlet are subpolar (Fig. III.1). This is shown by their low englacial temperatures (-24 °C at 1805 m a.s.l., Hattersley-Smith 1960); minor penetration of meltwater during the ablation season (Muller and Aiken 1973; Muller 1976; Aiken 1977); and sediment-rich basal ice (Stewart and Bednarski 1986).

DEPOSITS

Lithofacies and Lithofacies Associations

The glaciomarine sediments examined in Clements Markham Inlet are presented utilizing a lithofacies classification (Table III-2). These lithofacies are grouped on the basis of their sedimentology and stratigraphic relationships into six associations (Chapter 2; Table III-1, III-3). Bed thickness terminology is presented in Table III-4. These lithofacies associations are described below in the fining-upward sequence produced by ice retreat within the sea. Most of these sediments were deposited within tens of meters to a few kilometers of a tidewater glacier.

Facies Association I. Interbedded diamictons, sand, and silt; Dmm(r), Sm, Fl, Fm

Description

This facies association consists of thick- to thin-bedded,

matrix-supported diamictons with interbedded sands and silts and ranges in total thickness from 1.0 m to 4.0 m. The diamicton matrix (< 2 phi) is very poorly to extremely poorly sorted and plots as a straight line on logarithmic paper (see Grain Size of Lithofacies below). Clast content is estimated to range from 15 to 50%. The sand and silt interbeds are medium- to thin-bedded. Horizontal lamination was the only sedimentary structure observed in these interbeds although a deformed raft of massive sand (ca. 0.5 m diameter) occurred at one locality. The diamictons and finer-grained interbeds are horizontally-, and generally, evenly-bedded. However, several diamicton beds overlie silt beds with angular unconformity (Fig. III.3a) and they also contain silt intraclasts. In addition, excavation into apparently single diamicton beds commonly revealed intact silt intrabeds demonstrating that the diamicton actually consisted of two beds.

In most exposures the thick- and medium-bedded diamictons appeared massive. However, in those diamictons not obscured by slope wash, and which were also well desiccated, prominent parting planes were apparent that defined beds ranging from a few to tens of centimeters in thickness (Fig. III.3b). At several places isolated clasts within finer beds both deformed, and were draped by, the finer-grained sediments. Eleven fabrics, consisting of 25 to 50 measurements each, were measured from the diamictons at three sites. S1 eigenvalues range from 0.38 to 0.64 and principal azimuths from individual sites are variable (Table III-5; Figs. III.4, III.5). These data are discussed below under Fabrics.

Interpretation

The isolated pebbles and cobbles which deform underlying silts are interpreted as dropstones from iceberg-rafting. Their presence within fine-grained beds indicates that they settled through a water column in a background of suspended sediments. In comparison to the sediments penetrated by dropstones, however, the majority of diamictons are interpreted as fluid debris flow deposits because of: 1)horizontal bedding; 2)single, rather than multimodal matrix grain size distribution; 3)amalgamation of diamicton beds; 4)erosive contacts with silt beds and the presence of silt intraclasts; 5)weak fabric strength as indicated by low eigenvalues; and 6)variable mean azimuth of clast axis. Each of these considerations is discussed below.

The regularity of bedding would be difficult to explain if the diamictons originated primarily from ice-rafting. For example, Thomas and Connell (1985) illustrate a variety of gravel lenses isolated within fine grained sediment. They interpret these as the product of iceberg-rafting or dumping and none of these are horizontally bedded. Small gravel lenses were observed at some sites (sections 4 and 21, Chapter 2) but these are not prominent in the diamicton-dominated sections. Horizontally-bedded diamictons interpreted as ice-rafted deposits are reported from Puget Sound by Domack (1983) and Domack and Lawson (1985). The matrix in those beds, however, is multimodal representing influx of both coarser, poorly sorted ice-rafted material and finer, well sorted current-derived sediment. Kurtz and Anderson (1979) report similar curves for ice-rafted diamictons from

Antarctic cores. In contrast, the Clements Markham Inlet diamicton matrices plot as straight lines indicating they are composed of a single rather than multimodal population, a property not associated with ice-rafted diamictons (Fig. III.18a). Single population plots are also reported by Hill et al. (1982) for subaquatic debris flows with a non-glacial source.

The amalgamated contacts in the diamicton are indicative of an erosive contact and are similar to those described from proximal mass flow sands (see LA III below). Similarly, the silt intraclasts indicate erosion of underlying beds by a mobile diamicton. The only mechanism which consistently explains these features is a debris flow. Nemec and Steel (1984) suggest that debris flows exhibit only limited or insignificant basal erosion. In the present example the underlying fine-grained materials would probably have been poorly consolidated and this likely aided their subsequent erosion. Gravenor (1980) presented a similar interpretation for diamictons with silt intraclasts that closely resemble the units described here. The ungraded nature of the coarse clasts in the Clements Markham Inlet diamictons indicates that fluid turbulence was not developed, suggesting that they were high-strength flows (Nemec and Steel 1984). On the other hand these flows are commonly horizontal and evenly-bedded over tens of meters and do not exhibit flow noses or complex folds. These characteristics suggest very mobile or fluid debris flows. The thin bedding of much of Dmm (r) suggests that many of the debris flows were thin and this may partially account for their weak fabric (see below).

Diamicton Fabric

Fabric analysis by the eigenvalue method is commonly used for interpreting diamicton genesis in glacial deposits (Lawson 1979; Dowdeswell et al. 1986; Dowdeswell and Sharp 1986). It has also been applied to terrestrial debris flows (Mills 1984; Major and Voight 1986). The principal eigenvector V1 indicates the direction of maximum clustering and indicates the mean axis of orientation. V3 represents the minimum clustering direction and is orthogonal to the best plane through the data whereas V2 lies normal to V1 and V3. Normalized eigenvalues (significance values), $S1 \geq S2 \geq S3$, show the degree of clustering of the vector axes. Table III-5 lists the Clements Markham Inlet data (including four unpublished analyses by J. Bednarski). S1 values are low, ranging from a 0.38 to 0.64. The bivariate scatter diagram of S1 vs. S3 values plots as a wide envelope (Fig. III.4). These orientations are also plotted on Schmidt equal-area nets which also show a poorly defined orientation and variable azimuth directions between beds from the same sections (Fig. III.5).

Dowdeswell et al. (1985) and Dowdeswell and Sharp (1986) compiled data from available fabric studies. They plotted S1 vs. S3 values documenting progressively lower values of the principal eigenvector S1, and a concomitant increase in S3, for samples from debris-rich basal ice; melt-out till; and lodgement till, respectively. Although there is some overlap in the scatter plots, these sub-environments are fairly well differentiated. The decline in S1 strength reflects the progressively greater

readjustment of the highly aligned pebbles in glacier ice caused by the different processes of deposition. The data from glacigenic debris flows and waterlain glacigenic sediment (Domack and Lawson 1985) have the lowest S1 and highest S3 values and also exhibit the greatest scatter and overlap in fabric strength. The Clements Markham Inlet fabrics (Fig. III.4) show a similar scatter and plot within the same range as both the glacigenic debris flow and waterlain glacigenic sediments summarized in Dowdeswell et al. (1985) and Dowdeswell and Sharp (1986). Because of this overlap, the eigenvalue strength is not presently useful for differentiating between these two sediment types and therefore the sedimentological criteria discussed above must take precedence. The eigenvalue strengths and sedimentological criteria, however, demonstrate conclusively that these diamictons are secondary, and not primary tills (Dreimanis, in press).

Another characteristic of the ice-rafted fabrics reported by Domack and Lawson (1985) was the high number of stones with long axes dips exceeding 45°. They interpret this to result from clast settling through a water column with an upright long axis, which penetrates soft sediments thereby retaining its orientation. They also note that near-vertical stones do occur in some subaerial debris flows. The stones measured in Clements Markham Inlet have a high percentage of steep dips (note azimuth plunge in Table III-5). However, direct comparison with Domack and Lawson's (1985) data is not possible. This is because Domack (1980, from which the data of Domack and Lawson 1985 were obtained) did not measure near-vertical stones because of the difficulty of

determining a vector orientation for them. I felt, however, that if the diamictons had an ice-rafting origin the dips of such stones warranted measurement. Further difficulties are presented by the fact that many of these stones have a blade or disc shape which poorly manifest their orientation at the time of emplacement (P. Moller, per. comm. 1986). Consequently, such shapes are avoided in many fabric studies. Johnson et al. (1985, p. 33) note a similar propensity for high dip angles in blades and discs from terrestrially deposited melt-out tills. Although clast-angle interpretation is problematic its continued consideration in debris flow deposits seems warranted.

Facies Association II. Gravels; Gp, Gm, Sm, Fm, Fl

Description

Gravels occur near the base of several sections but are poorly exposed (Chapter 2). Medium-bedding is most common but both thin- and thick-bedding also occur. Individual beds are often overlain by medium- to thin-bedded silty sand or mud. Some beds are reverse graded, from a basal layer of matrix-supported, coarse sandy gravel to clast-supported gravel. More commonly beds are normally graded with matrix- to clast-supported sandy gravel overlain by gravelly coarse sand. Evenly-bedded, clast supported gravels also occur. Examples of other gravels are a 1.5 m thick bed of massive- to faintly-bedded, clast-supported gravel and a 0.8 m thick planar cross-stratified gravel; and 4 m of dipping, thin-bedded clast-supported gravels with a prominent up-slope imbrication (sections 21 and 17, respectively, Chapter 2).

Interpretation

Stratigraphic relationships indicate that these gravels are proximal deposits of subaquatic outwash fans derived from glaciers occupying paleowater depths between 35 and 100 m (Chapter 2). Their coarse size indicates transport by high velocity flows. The combinations of reverse and normal grading in individual sequences indicates variations in transporting flow. These variations result from normal climatically-induced changes in discharge as well as from flow expansion when streams exit the glacier into the marine water (see Depositional Model). Matrix-supported gravels indicate a highly concentrated slurry or debris flow with sufficient density to prevent coarse particles from sinking or sufficient clast-to-clast collisions to maintain these particles in suspension. This slurry would then experience abrupt velocity reduction preventing gravels from sinking to the bottom. On the other hand, normal grading occurs in turbulent fluid flow where individual gravel clasts are free to migrate to the bottom (Walker 1978). The reverse graded units represent deposition from flows with increasing velocities or perhaps true debris flows. The cross-bedded units indicate the presence of migrating bedforms or localized scour fills. Finally, continued flow reduction allows deposition of the overlying sands and silts. In conclusion, the gravels are interpreted as deposits of high density turbidity current or mass flows in an ice proximal, channelized setting.

The gravels located on high-angle slopes likely represent avalanche sedimentation directly onto a proglacial slope from an

englacial stream. Though these resemble foreset beds of a Gilbert delta the stratigraphy indicates that these are not related to subaerial delta progradation. Rather, they are ice-proximal subaquatic outwash. These deposits are similar to those found in sections from Norway where they are called "Tronder moraines" (Sollid and Reite 1983, Figure 55).

Facies Association III. Massive, graded, amalgamated sands, medium- to thin-bedded; Sm, SB

Description

These are medium- to fine-grained and medium- to thin-bedded sands (Fig. III.6a, b, c). In sections they were only sometimes associated with gravels of LA II but are always found below LA IV (see Chapter 2). Small amounts of coarse sand and gravel may be present. Beds are ungraded, normal or reverse graded. The sand is well to moderately sorted (see Lithofacies Associations Grain Size). Bed tops are sometimes defined by horizontal sand laminae or thin- (sometimes medium-) bedded mud. Individual sand beds were observed that terminated abruptly in ripple-forms. These do not have foreset laminae but the ripple-form is apparent because of draping by darker, poorly sorted, sandy silt. In that bed (section 4, Fig. II.10b, Chapter 2) the ripple crests are pierced by water escape pillars and post depositional settling caused by fluid loss is evident. These finer laminae are often eroded by overlying beds. Erosion into underlying sand beds is also indicated by the presence of floating sand intraclasts (Fig. III.6c) and truncation of deformation structures. The most common deformation features are: water escape structures such as type B

pillars and dishes (Lowe and Lopicollo 1974), flame and load structures, convoluted bedding, and ball and pillow.

Interpretation

The transport mechanism for LA III is interpreted to be high density turbidity currents and mass flows in a relatively proximal position (Lowe 1982). This proximity provides currents with sufficient power to erode underlying beds, producing amalgamation. The remaining normal turbidity current travels beyond the site of deposition (see LA IV). If described by the common Bouma terminology these beds are repetitive Ta, Ta... (Walker 1978). This feature is commonly reported from sandy deposits in the channelized parts of deep-sea fans (Howell and Normark 1982). The deposits from Clements Markham Inlet have many similar properties and given their relationship to the retreating ice front and the paleowater depths they are therefore interpreted as channel deposits of a subaquatic outwash fan (see Channel Form section below). They are also equivalent to the glaciomarine subaquatic outwash fan channel sands reported by Rust (1977), Rust and Romanelli (1975) and Cheel and Rust (1982).

In addition to bedding characteristics, Middleton (1967) proposed that deposits from high and low density turbidity currents (sediment concentrations ca. 40% and 20% by volume, respectively) could sometimes be differentiated by the presence of coarse-tail grading vs. distribution grading, respectively. His data were based on flume experiments using sediments concentrations of ca. 40% and 20% for high and low density flows, respectively. In coarse-tail grading only the coarsest fraction

(e.g. the coarsest few grains) show a vertical variation and the finer fractions remain the same. In distribution grading all grain sizes progressively fine-upwards. However, Middleton (1967) also reports that in a single high-density deposit the grading changed from coarse-tail to distribution type in a distance of a few meters. Analysis of samples from the bottom and top of normally graded sand beds in this study (Fig. III.18c) shows a distribution type grading initially suggesting deposition by low density turbidity currents. Lowe (1982) also indicates that high density deposits can have both types of grading and suggests that distribution grading results when the late-stages of the sediment cloud settle as a non-turbulent suspension producing the Ta horizon. The Ta horizons produced by this direct sedimentation commonly exhibit secondary water-escape structures (type B pillars and dishes) because these deposits have high water contents, are very loosely packed, and subsequently undergo consolidation (Lowe 1982). Distribution grading from Ta graded sands is also recorded by Saunderson (1977) and Leckie and McCann (1982) from glaciolacustrine density current deposits and by Komar (1985) from a deep sea fan turbidity current deposit. Thus the presence of repetitive Ta beds with amalgamation are most important for indicating deposition by high density and powerful turbidity currents in a proximal environment.

Most of facies association III is composed of graded and amalgamated Sm deposited from suspension. However, the presence of Bouma sequence Tb and Tc laminae (e.g. the pierced ripples described above) indicate deposition from traction. Below, it

will be argued that many of the turbidity current and mass flows were generated from slumps near the head of the subaquatic outwash fan. Lowe (1982) describes how such retrogressive slumping can generate several surges of deposition which can override the previously deposited material. The bottom-flowing current can also set the overlying ambient water into motion by friction along the interface (Maxworthy 1983). These overlying currents may continue after the initial suspension deposition and by reworking the sediment, form caps of traction structures. Various complex interactions are common in the turbidity current deposits in Clements Markham Inlet (see LA IV and Depositional Model).

Lithofacies Association IV. Graded, laminated and current bedded sand.

This lithofacies association consists of four members that are usually repetitively interbedded. Laminated parts of LA IVa and IVd are quite similar and the interbedding makes it difficult to distinguish between them (see below). LA IV is interpreted as turbidity current deposits in a levee/overbank to pro-channel position rather than in the channelized setting as proposed for LA III (see Depositional Model). LA IV is generally found overlying LA III.

IVa. Bouma sequence; SB

Description

This lithofacies may consist of medium to fine sand that grade continuously upwards to silt and mud. These graded units

may occur individually and usually display sharp contacts with underlying beds. Commonly, however, the facies has more complex, repetitive sequences of very thinly-bedded, graded to ungraded sand overlain by thinly-laminated alternations of very fine sand to coarse silt (Fig. III.7; also II.10c, II.24b, Chapter 2). Interspersed with these are starved ripples of sand or coarse silt (LA IVc, Ssr). Microlaminae vary in number from ca. 10 to >20 (Fig. III.10a). These laminae are horizontal where they overlie the graded sands but, when overlying ripples, they conform to these features with no variation in laminae thickness. Though the microlaminae are predominantly horizontal, micro-ripples (< 5 mm in height) can sometimes be found when laminae are traced over a distance of several meters. The graded beds sometimes have regular wavy or sharply rippled tops.

Interpretation

These sediments are interpreted as turbidity current deposits. The basal sand records deposition from suspension and is equivalent to the Ta division of the classic Bouma sequence. Their thinness suggests that these beds were deposited either by smaller-scale flows (compared to the medium-bedded sands of LA III) or from the distal parts of the same turbidity currents. This latter relationship is supported by the continuity of grain size parameters (mean and sorting) for LA III and IVa (see Lithofacies Associations Grain Size). Alternatively, some layers may result from individual underflows initiated by englacial stream discharge into the marine environment (see Depositional Model below). These simple graded units are similar to what

Ashley (1975) and Banerjee (1977) call multiple graded units in glaciolacustrine deposits. These are also interpreted as turbidity current deposits.

The regular wavy bedding at the top of Ta beds (Fig. III.10a) resembles those illustrated by Lowe (1982, Fig. III.9). He interprets these as final-stage reworking by Helmholtz waves produced at the interface between the turbidity current and the overlying ambient fluid. Maxwell (1983) produced similar wave forms along this interface involving gravity currents of variable inflow. The sharply rippled tops of individual, thin-bedded Ta in this lithofacies association are also interpreted as deposition by rapidly decelerating turbidity currents (Banerjee 1977) or by late stage reworking.

The sediments of LA IV are interpreted as levee/overbank deposits. The alternation of individual components of the Bouma sequence suggests a pulsating flow within channelized turbidity currents that repeatedly overtopped the channel spilling sediment onto the levee (see Depositional Model). Rapid deceleration likely resulted from both interaction with the overlying ambient water and by settling of the main flow back below the channel, thereby cutting off the overbank flow.

The uniform laminae that overlie graded sands, ripples and Helmholtz waves are more difficult to interpret because their position varies within individual depositional sequences. The horizontal laminations resemble several published examples and all of these examples relate to deposition from turbidity currents. These examples include the horizontally laminated Tb

and Td intervals of the Bouma sequence (e.g. Howell and Normark 1982). The Td intervals are commonly associated with turbidity current body-spill on channel levees from the contemporary deep-ocean Laurentian fan (Chough and Hesse 1980; Hesse and Chough 1980; Hesse et al. 1987) and on levees associated with channels formed by direct, deep-water discharge of mine sludge into a fiord (Hay 1983). These also closely resemble parts of Larue and Speed's (1983) oscillatory sequence (their facies types 23 and 24). Where it drapes ripples (Ssr, Scr) it also resembles the sinusoidal lamination of Jopling and Walker (1968) and the draped lamination of Gustavson et al. (1975). Based only on its general appearance this facies cannot be differentiated from the above examples.

Interpretation of this horizontal lamination must rely on its association within observed sequences. When overlying undulatory bedforms without a variation in thickness, they must represent deposition from suspension in order to mimic the underlying surface. In these cases draped lamination (Gustavson et al. 1975; Ashley et al. 1982) is the appropriate interpretation which is designated by Sl within LA IVd (Table III-2).

At one site (section 1, Chapter 2) there is a 2 m sequence with an alternation of Ta, horizontal lamination and starved ripples (Fig. III.7). Horizontal lamination overlying a graded (Ta) bed suggests that it is a Tb interval within the normal Bouma sequence. However, within a few cm (vertically), identical laminae occur which drape starved ripples with no erosional

discontinuity or variation in thickness which suggests deposition from suspension. T_b intervals originate from the upper flow regime and would not be expected to mimic underlying bedforms with such regularity. In Gustavson et al.'s (1975) original description of draped lamination they also present photographs of it conformably overlying horizontal units. In addition, Ashley et al.'s (1982) flume data demonstrate that draped laminations can form at velocities of up to 15 cm/sec. In coarse silt such velocities are sufficient to produce ripples indicative of bedload transport (McBride et al. 1975; Carey and Roy 1985). These hydrodynamic observations account for the interbedding of ripples and lamination. Thus the laminae are interpreted to be draped lamination.

IVb. Climbing ripples; Scr

Description

Climbing ripples occur primarily with stoss and lee preservation (Fig. III.8) although stoss preservation has also been observed (types B and A, respectively, Jopling and Walker 1968). Sinusoidal lamination (type S) is considered with the previous lithofacies. Units are composed of very fine sand to very fine sandy coarse silt and are thin- to medium-bedded. Ripple heights are 1 to 3 cm, wavelengths are 10 to 15 cm and angles of climb vary from 15 to 50°.

Interpretation

Climbing ripples originate when transporting currents are operating in a range where both traction sedimentation and

suspension fallout are occurring (Jopling and Walker 1968). Sediment moves along the bed as ripple trains but the large amount of suspension settling preserves individual ripples. Subsequent ripple trains migrate over the former and are themselves preserved. The prevalence of type B ripples demonstrates a general dominance of suspension settling over bedload transport (Jopling and Walker 1968). Based on its position relative to the observed channels this facies was probably deposited on levees and interchannel areas adjacent to turbidity current channels, or where turbidity currents spread out onto the basin plain (e.g. Mutti 1977; Eriksson 1982; Pickering 1982, 1983).

IVc. Starved ripples; Ssr

Description

This lithofacies consists of fine sand to coarse silt laminae from ca. 0.1 to 2.0 cm thick that form prominent ripples. The ripples are not isolated features but rather dominate the laminae for the entire length of their exposure (3 to 10 m). They form a gradational series from repetitively alternating rippleforms (Fig. III.7) to isolated ripples overlain by draped lamination (Fig. III.9) to isolated starved ripples in a background of sandy silt (Fig. III.10a, b).

Interpretation

The ripples result from traction transport on the sea floor. The presence of sandy ripples within finer-grained suspended sediment (Fcpl, Fm; Fig. III.10a,b) indicates that coarser sediment was only intermittently present. When isolated, the

ripples indicate that the tractive current's sand supply was progressively diminished by deposition. Thus it is likely that the current was competent to move larger grains but these were unavailable (Eriksson 1982). This facies is interpreted as channel overspill from turbidity currents which injected sand and coarse silt onto levee/overbank positions of a subaquatic outwash fan. The alternation of draped lamination with starved and climbing ripples records both head and body overspill of a turbidity current that experienced intermittent accelerations (see Depositional Model).

IVd. Draped lamination, Sl

Description

This lithofacies consists of alternating laminae of very fine sand and very fine sandy silt (Figs. III.7, III.9, III.10a). The laminae mimic underlying beds or laminae. For example, they are undulating over starved or climbing ripples and Helmholtz bedding. When undulatory these laminae are uniform in thickness.

Interpretation

Like the previous discussion of draped lamination these result from sediment settling through the water column with minimal horizontal velocity. Thus underlying bedforms are mimicked without erosional modification.

Lithofacies Association V; Interbedded and interlaminated sand and silt

Facies V is divided into two end members: one sand-dominated (Va) and the other mud-dominated (Vb). They may grade upwards

from Va to Vb; be interbedded with each other; or with other mass flows or turbidity current deposits.

Va. Cyclopsams, Sand:Mud > 0.1; Scps

Description

This lithofacies is horizontally- and very thinly-bedded to thickly-laminated. These units occur in repetitiously alternating graded sequences of very fine sand to very fine sandy silt (Fig. III.11; Chapter 2, Fig. II.11). They uniformly drape underlying surfaces and individual beds may possess some water escape or deformation structures. Current bedding was not observed. Interlaminae of silt or mud occur but these generally comprise a minor part of an individual sequence (< 10%).

Interpretation

The draping of underlying forms indicates that these deposits originate from suspension settling. They can usually be differentiated from draped lamination because they are coarser grained and have thicker laminae. These sediments are similar to those collected from sediment traps and cores adjacent to meltwater streams entering Glacier Bay, Alaska (Cowan et al. 1986; Powell and Cowan 1986; E. Cowan, pers. comm. 1986). These workers call these sediments cyclopsams, referring to the cyclic repetition of sand. They are deposited by direct suspension sedimentation from turbid plumes generally less than 0.5 km from the ice front where subglacial streams exit into the marine water. In these proximal positions the flow velocity is still sufficient to transport sand in suspension. The laminae originate

from discrete settling layers produced by hydrodynamic isolation of sands by: large-scale variations in the streamflow; turbulent eddies in the resultant plume; and hydraulic interactions between the plume and the marine water which produce progressive plume decay (Powell and Cowan 1986). These isolated layers settle through the water column reaching the fiord floor and producing the observed laminations.

At one site the following sequence was observed. It begins with sand, deformed by water escape structures, that is directly overlain by horizontal sand laminae (Fig. III.11). This is interpreted as a mass flow or turbidity current overlain by cyclopsams. The lack of fine-grained sediments or other deposits between the mass flow and the cyclopsams indicates that the sequence must be the result of an individual event. In this case, it is likely that streamflow first deposited sediment on the fiord floor that failed in a liquified flow. Concomitantly, the overflowing turbid plume dropped sand through the water column depositing the cyclopsams directly on top of the mass flow deposit. Domack (1984) recognized similar deposits of mass flow origin overlain by fine-grained turbid plume deposits (i.e. cyclopels, see below). Though such flows may relate to an annual ablation cycle (Domack 1984) the numerous variations in englacial streamflow during a year (e.g. channel path changes, glacier flow closing conduits, synoptic activity controlling ablation and periodic rain) suggest that these repetitive deposits are the result of hydrologic conditions of unknown duration.

Vb1 Muds with interlaminated sand, S:M < 0.1, Cyclopels,

Fcpl

Description

These are horizontally- and very thinly- to thinly-bedded silty clay and clayey silt with interlaminated and interbedded sand (Figs. III.12a, b; also Chapter 2, Figs. II.10d, II.11, II.13). The sand ranges from one or two grains in thickness to very thinly-bedded. Current structures in these sands are very rare. The finer portion can be very fine grained (see Chapter 2, Fig. II.11b) or they can contain minor to significant components of sand (Fig. III.12a, b; Chapter 2, Fig. II.13a; see also Grain Size of Lithofacies below).

Interpretation

These are interpreted as suspension sediments transported by and deposited from turbid overflow plumes. The interlaminae of sand and coarse silt are the finer-grained and thinner-bedded distal equivalents of the sands composing the more proximal cyclopsams. These sediments display a striking similarity to those collected from turbid plumes in the modern glaciomarine environment of Glacier Bay, Alaska (Mackiewicz et al. 1984; Powell and Cowan 1986). These workers use the term cyclopel and this is applied here. The cyclopels also resemble true distal silt turbidites deposited in deep ocean basins (Piper 1978; Stow and Shanmugam 1980; Stow and Piper 1984; Carey and Roy 1985). Within Clements Markham Inlet the stratigraphy and lack of fossils indicate that these are proximal glaciomarine deposits from turbid plumes (Chapter 2). Additionally, the thick sequences of cyclopels in Clements Markham Inlet indicate that turbid

plumes were the dominant depositional process during deglaciation (Chapter 2). Since turbidites do occur in this environment, it is likely that individual beds of cyclopels result from them.

Vb2. Silts, non-laminated; Fm

Description

In several sections, 5-15 cm fine-grained units were observed without distinguishable sand partings (Figs. III.10b, III.13). These are likely more widespread than presently recognized because such deposits are difficult to recognize beneath the silty slopewash that commonly coats exposures.

Interpretation

The non-laminated silts represent suspension deposits from turbid plumes which had already lost their coarser component. These sediments are equivalent to what Powell and Cowan (1986) call homogeneous mud. They may also relate to low density turbidity currents that had similarly lost all coarser sediment. Pickering et al. (1986) suggest that similar deep-sea sediments (their facies D1.2) are deposited by rapid deposition of silt grains and mud flocs from a highly-concentrated, mud-dominated turbidity current. This essentially describes the final concentrated stages of a turbid plume as it settles towards the bottom. Plumes have not been observed to flow along the fiord floor but with appropriate slopes and densities such behavior is likely. However, at present no traction structures have been observed in the silts in Clements Markham Inlet.

Collapse of Previously Deposited Sediments

Description

There are many contorted horizons within the deposits that do not involve penecontemporaneous deformation structures (e.g., load casts) or rotational slumps related to channel margins. These were recognized only in LA IV and V. These are most often folds with amplitudes from tens of centimeters to several meters and heights of similar magnitude. One large-scale fold is truncated along its top by uncontorted beds (Fig. III.14). On a smaller-scale, the bedding may be fragmented to chaotic and also intersects overlying beds with an angular unconformity (Fig. III.15a, b).

In one exposure LA Vb1 overlies several coarser lithologies (Fig. III.16). Immediately above this contact is a curious elongated pod structure of thickly-laminated sand and silt (Fig. III.16). Above and to the right of this structure, but still within the LA Vb1 silts, individual beds drape over similar beds that pinch out against them giving the appearance of a channel margin (Fig. III.16a).

Interpretation

Contorted horizons are produced by the downslope movement of sediment which causes distortions within the moving sediment and/or within the underlying units by shear along a dislocation surface (Nardin et al. 1979; Cook 1979; Gawthorpe and Clemmey 1985; Coniglio 1986). As in the terrestrial environment a variety

of subaquatic mass movements can occur. On the one hand, slow, downslope creep produces a bedding-parallel translation. This can leave the moving sediments undeformed and their vertical succession unaffected. On the other hand, rapid movement (i.e. slides) removes sediment from one site and deposits it downslope where bed repetition can occur (Fig. III.17; Nardin et al. 1979). Removal of this sediment also undermines the area upslope so that further creep and bedding translation may occur there (Fig. III.17). Slides are subdivided into slumps and glides depending on whether truncation occurs along a curved or planar surface, respectively. However, differentiation between these in the stratigraphic record is not generally possible (Coniglio 1986). Slides occur at virtually any lateral scale and the slide package itself may be < 1 m to 100s of meters thick (Nardin et al. 1979; Coniglio 1986). Thus, proper identification of mass movement requires exceptional exposures (Coniglio 1986). The exposures in Clements Markham Inlet are predominantly in gullies and therefore contorted horizons could be traced for only short distances laterally.

The folded, chaotic layer, and the overturned fragment shown in Figure III.15 suggests significant displacement of the overlying sediment. The overturned fragment (Fig. III.15b) particularly resembles one illustrated by Coniglio (1986, Figure 5f) and interpreted as the product of shear along the truncation surface of a slide mass (Fig. III.17).

The features in both Figures III.14 and III.16 are also related to slide movement. The large size of the fold in Figure

III.14 suggests that it may be part of the forward, compressive nose of a slump. Position a in Figure III.16 represents the displaced slide mass which overrides the adjacent sediment producing a repetition of beds (Fig. III.16a; Gawthorpe and Clemmey 1985; Coniglio 1986). The pod structure along the base is interpreted as a roll structure formed by shear at the base of a slump sheet and particularly suggests movement of the overlying mass. A similar feature is illustrated by Cooke (1979, Fig. 24; Cook et al. 1982, Fig. 31) at the base of a slump sheet of continental slope deposits.

Grain Size of Lithofacies

Grain size characteristics of the lithofacies also reflect the depositional processes that occurred during the deglaciation of Clements Markham Inlet. A total of 99 grain size analyses were made using standard sieve techniques for sands, and hydrometer analyses for silts and clays (Folk 1980; ASTM 1977). Analyses were made from the following sediments: 1)diamicton matrix; 2)silt interbedded with the diamicton; 3)amalgamated sand; 4)Bouma sequences (generally Ta); 5)starved ripples; and 6)cyclopels. Results are plotted in a ternary diagram (Fig. III.18); as logarithmic cumulative frequency curves (Fig. III.19), as well as bivariate plots of sample mean vs. sample sorting and skewness (Fig. III.20). Summary statistics are presented in Table III-7. These statistical parameters were calculated using the inclusive graphic method of Folk (1980; also see Warren 1964). Complete data for all samples is in Appendix I.

The diamicton matrix (< 2 phi) is very poorly sorted (ca.

50% sand and 50% silt and clay, Fig. III.18). The diamicton matrix plots virtually as a straight line (Fig. III.19a) which represents a single grain size population. Thus, despite evidence of erosion of the silts, the diamicton shows no peak in the silt fraction indicating pronounced mixing of the interbedded, finer-grained turbid plume sediments.

The silts interbedded with the diamicton as well as the cyclopels are interpreted as turbid plume deposits from more proximal to distal positions, respectively. This related origin is reinforced by their overlapping plots of the mean vs. sorting and mean vs. skewness (Fig. III.20). Envelopes of the grain size curves for all of the interbedded silts and cyclopels (Fig. III.19b) show similar overlapping though the interbedded silts have a coarser tail (sand contents of 0.4 to 4.5%, Appendix I) reflecting their more proximal position. Cyclopels can also be deposited in proximal positions and these individual samples do possess similar sand contents (Fig. III.19b; Appendix I).

Three samples from a thinning-upward sequence of cyclopels were analyzed (Fig. III.19b). This sequence begins with thinly-bedded to thinly-laminated sands. Successive sand laminae thin and fine upwards and the intervening silts also thin upward. Samples from successive silt laminae show a progressive fining trend associated with the laminae thinning. This thinning- and fining-upward trend in both the sands and silts results from the sediment injection of a single discharge event with progressive turbulent decay within the plume. These sequences are similar to ones Domack (1984) suggests are annual deposition cycles (see LA

Vb1 above and Chapter 2).

Considered as a group the silts interbedded with the diamictons and cyclopels become better sorted as mean grain size decreases (Fig. III.20). This results from a progressive dominance of finer silts and clay as coarse silt is lost from the plumes. This relationship is also observed in equivalent glaciolacustrine sediments by Banerjee (1973b) and Ashley (1975) and is similar to that reported by Bartolini et al. (1975) and Piper (1978) for deep-sea turbidites. An opposite sorting trend is reported by Stow and Bowen (1980) for similarly-sized deep sea fan sediments. They propose a turbidity current model involving the formation of successive, dense, flocculated layers within the flow. These layers successively settle to the bottom forming discrete beds and laminae quite similar to cyclopels (Stow and Bowen 1980; Stow and Shanmugam 1980). Such sorting trends may be useful in differentiating these varying deposition mechanisms.

The grain size characteristics (mean and sorting) of the interbedded silts and cyclopels of Clements Markham Inlet overlap with those reported by Mackiewicz et al. (1984) as type 1 and 2 turbid plume suspension sediments (cyclopels) from Alaska. The curves are also similar to flocculated suspension sediments from ice-proximal positions on eastern Baffin Island (Gilbert 1982, 1983). However, muddy sediments from other depositional environments, such as mud drapes on foreset beds of the 103 m delta at the Arrowhead River, have similar grain size characteristics indicating their equivalent glacial origin or reworking of previously deposited cyclopels (Appendix I). Thus,

grain size alone is insufficient to characterize the glaciomarine lithofacies and the presence and characteristics of the sand interlaminae and interbeds are essential to their recognition.

The amalgamated sands are moderately to moderately well sorted and their mean vs. sorting values plot in a cluster similar to that reported by Bartolini et al. (1975) for proximal turbidites (Fig. III.19). The normally graded, amalgamated sands have distribution grading produced by suspension deposition from high to low density turbidity currents. The Ta divisions of the Bouma sequence generally show a similar pattern though closely spaced samples sometimes cross-over in the finer grades (Fig. III.19c).

Elsewhere it is argued that the amalgamated sand is a proximal representative of the more distal Bouma sequence. The mean vs. sorting plot of these two lithofacies shows that as mean size declines there is a concomitant change from poorer to better sorting (Fig. III.20). In the present comparison of these two lithofacies, their difference is diminished because the samples of Bouma sequence are exclusively from the Ta division which is the coarsest part of this lithofacies. This sorting trend suggests that the flow responsible for the amalgamated sands was less well differentiated and deposited a wider range of grain sizes. Conversely, then, the Bouma sequences are deposited from more fully differentiated turbidity flows that deposit sediments in a more systematic manner. This supports the argument that the Bouma sequences are the more distal or overbank equivalents of the amalgamated sands. This trend toward better sorting with

distance is also reported from a single, large turbidite (Elmore et al. 1979).

The skewness of the amalgamated sands and Bouma sequences tends to increase to a mean grain size of ca. 3.5 phi and then abruptly decline (Fig. III.20). This indicates that first more fines and subsequently less fines are incorporated within the coarser sediments. This generally parallels the increased sorting found within the progressively finer mean grain sizes of these two lithofacies. Starved ripples are an approximate end product of the amalgamated sand to Bouma sequence but the two analyzed samples become more positively skewed as their mean grain size decreases, the opposite trend to that of these related lithofacies. Starved ripples represent the termination of turbidity current head flows injected by channel overspill onto overbanks dominated by fine-grained, suspension sediments. Thus, as the traction current transporting sand across the fiord floor slows, more and more background fines can be incorporated into the starved ripple. Shaw and Archer (1978, Fig.5) examined sandy cross-laminae within the winter portion of glaciolacustrine varves which have a similar skewness trend. These cross-laminated sediments are considered to originate from distal turbidity currents generated by slumps from a delta front. Therefore, this resulting sedimentation is hydrodynamically equivalent to the starved ripples described here.

DEPOSITIONAL MODEL

For the past two decades extensive field studies have

concentrated on the late Quaternary history of Arctic Canada. Not withstanding the importance of raised marine deposits for the understanding of glacioisostatic adjustments and for providing a chronology for past glaciations, little effort has been made to provide a systematic description of their stratigraphy and sedimentology which also pertain to this history. Given the amount of field work that remains to be done in the arctic, a depositional model is considered timely. Such a depositional model for deglacial marine sediments should also prove useful to the understanding of modern fiord sediments, such as is being proposed by the Ocean Drilling Project (1987).

The depositional model for Clements Markham Inlet is divided into three parts, each based on the dominant mode of transport and deposition. First are sediment gravity and turbid plume flows that produce the interbedded diamictons, sands and silts of LA I. Second, is the generation, flow and spreading of mass flows and turbidity currents in channel, and interchannel to pro-channel positions responsible for LA II, III and IV. Included within the interchannel section are the effects of pulsating flows. Third, the relationship of LA V to the injection of sediment-charged fresh water and the evolution of the resultant turbid plumes is considered. The model is summarized in Figures III.23 to III.26.

The hydraulics, sediment dynamics and depositional processes related to the influx of proglacial meltwater into the marine environment have been described by many authors (Gilbert 1983; Domack 1984; Mackiewicz et al. 1984; Cowan and Powell 1986). Additional data come from the investigations of prodelta fiord

environments (Syvitski and Murray 1981; Syvitski et al. 1985). The behavior of a freshwater stream as it debouches from a glacier into marine waters depends on the density contrast between the two waters. If the inflowing water is more dense than the ambient marine water then it will sink and flow along the bottom as an underflow. If the densities are approximately equivalent then the flow will travel at an intermediate level, forming an interflow. If less dense the flow immediately rises to the surface as a buoyant plume where it then spreads out essentially as a two-dimensional jet called an overflow. For Clements Markham Inlet the glaciomarine lithofacies and the possible transport mechanisms responsible for them are shown in Figure III.21. Similar but more complex diagrams are found in Gilbert (1982) and Stow and Piper (1984b).

The density stratification of marine waters depends on the combined effects of temperature and salinity. Below the surface arctic marine water commonly has a salinity of 34 ppt and a temperatures of 0 °C (Lake and Walker 1976; Sadler 1976) giving a density of ca. 1.028 g/ml. Therefore, meltwater can descend below this surface layer only if it contains a sediment concentration above ca. 40 g/l (= 15.1 % by volume with a density of 2.65 g/l; see also Gilbert 1983, Table I). Most recorded glaciofluvial flows do not have suspended sediment concentrations this high, suggesting that true underflows are rare (Gilbert 1983). However, short-term concentrations well above the threshold for underflows have been recorded indicating that these events can occur intermittently (Gilbert 1983; J. Shaw, pers. com. 1987). When

velocities and coarse sediment concentrations are too low to form underflows, the gravels and much of the sand would simply be dumped near the stream exit. Eventual failure of this material by slumping can subsequently produce debris flows and turbidity currents.

Streamflows with sediment concentrations ranging from ca. 20 to 60 % by volume are hyperconcentrated (Bradley and McCutcheon 1985). These fluid flows are transitional to mud or debris flows. Their fluid character is indicated by the settling of sediment coarser than sand size to the flow bottom (Pierson 1985) where it moves as bedload if the velocity is sufficient (Wan 1985; Smith 1986, 1987). Terrestrial, hyperconcentrated flow deposits range from massive to bedded gravels to faintly stratified, coarse sand with localized, small pockets of gravel (Pierson and Scott 1985; Smith 1986, 1987).

In terrestrial environments the gravels can be transported several kilometers (Smith 1986, 1987). However, in the proglacial environment, underflows experience flow expansion, as well as mixing with the ambient water, reducing their velocity and causing gravel deposition, possibly within tens to hundreds of meters from an ice front. Gravel transport in the proglacial marine environment may also occur similarly to deep-sea situations described by Hein (1982). She suggests that overriding turbidity currents impart a dispersive pressure to the gravels producing a saltating, modified grain flow, layer. Sand, on the other hand, remains in suspension at much lower velocities and, after gravel deposition, the flow might retain sufficient

concentrations to continue on as a density underflow. Nevertheless, mixing with the ambient fluid would eventually cause such sandy underflows to dissipate. However, if these underflows descend a steep slope, and then encounter a lower slope, they may undergo a hydraulic jump. This transforms the excess energy into turbulence generating a true turbidity current.

Diamictons and Interbedded Sand and Silt

Debris flows are the primary source of diamictons in Clements Markham Inlet. The stratigraphic relationships discussed in Chapter 2 indicate that the retreating glaciers in Clements Markham Inlet were either tidewater glaciers or very small ice shelves. Although extensive debris flow deposits are commonly reported in the proglacial marine environment (e.g. Gravenor 1980; Hicock et al. 1981) their origin is somewhat problematic. Powell (1983b) points out that tidewater glaciers maintain a frontal ice cliff precluding a low-angle ramp at its snout. Therefore basal and englacial debris cannot accumulate on the surface as occurs in the subaerial environment. For ice shelves the problem of debris transport to the ice margin is similar because sediment is also concentrated at the glacier base. Therefore, sediment in an ice shelf is released primarily from icebergs or basal melt-out. Diamictons are difficult to derive from surpraglacial positions of tidewater glaciers and ice shelves unless they originate from lateral or medial moraines.

Other sources for diamictons are previously deposited materials beyond retreating tidewater glaciers and ice shelves.

The paleocurrent azimuths in Clements Markham Inlet that are oriented towards the retreating ice suggest that redeposition of debris from the valley sides was an important sediment source. Glaciers occupying tributary, hanging valleys can also stabilize at the juncture with the main valley. The high relief at these sites permits the dumping of significant quantities of debris (diamictons) into the adjacent trough (Bednarski 1986). These debris flows could be reoriented within that trough in the same manner as described above.

In all of these scenarios, the failure, flow and deposition of debris flow material is an intermittent event. The concomitant delivery of sediment by subglacial streams to the ice front results in the interbedding of sand and silt within the diamictons. The overall product of these processes is a horizontal fiord floor fill.

Eyles et al. (1985) have criticized the interpretation that all diamictons provide a reliable indication of an ice-proximal environment because they can be deposited far from an ice front. These result from the resedimentation of fine-grained sediments with a dropstone component or the resedimentation of previously deposited diamicton. Nonetheless, the documented deglaciation of Clements Markham Inlet (Bednarski 1986) shows that the interbedded diamictons here are ice proximal sediments. The stratigraphic and sea level data indicate rapid ice retreat whereby deep-water muds or cyclopels overlie the diamictons (Bednarski 1986, in press). Furthermore, at Piper Pass, the diamictons are related to a large subaquatic outwash fan

recording a proximal glaciomarine environment (Eyles et al. 1985).

Channelized to Overbank Deposition

Channel Forms and Channel Deposition

Channelized flow has been inferred from certain sediment types and sedimentary structures. The stratigraphic relationships of the LA II gravels indicate that they were deposited at water depths of 30 to 80 m in close proximity to the ice front (Chapter 2). Furthermore, LA III strongly resembles sediments described from deep sea and subaquatic outwash fans which are generally found in channelized settings (e.g. Dott and Bird 1979; Eriksson 1982; Howell and Normark 1982; Link and Welton 1982; Chan and Dott 1983). Indeed, both LA II and III occur within recognizable channels (Chapter 2). Consequently, the parts of other sections dominated by LA III are also interpreted as channel fills. Prominent channel forms were recognized in 5 of the 22 sections examined and these are illustrated in Figure III.22 a to g (sections 4, 16, 17, 18, 20, Table III-6). The characteristics of these channels include: 1)the thinning and pinching out of individual beds towards the channel margins; 2)draping of beds over the channel margins; 3)the erosional undercutting and slumping of channel margins (either overbank/levee or channel fill sediments); 4)change from LA III to LA IVa and IVc when traced along an exposure from a channel to an overbank position; 5) draped infill of finer-grained suspension deposits (Fcpl, Fm) mimicking the channel form; and 6)the overall fining-upward trend

of channel fills which was a function of glacier retreat and the concomitant reduction in the sediment source (Table III-6).

In the marine environment, mass or turbidity current flows are produced by direct, high-concentration inflow (see above) or by the dumping of sediment from supra-, en- or subglacial streams onto the sea floor. Subsequent slumping of this sediment can generate liquified or turbidity current flows. In proximal channel positions these flows deposit beds of graded to massive gravel and sand whose surfaces are commonly reworked by later stages of the same flow or eroded (amalgamated) by subsequent ones. When streamflow ceases or is significantly reduced, the more coarse deposits may be draped by muds. These turbidity currents also overtop their confining channels as indicated by the common occurrence of LA IV overlying LA III.

Channel to Overbank Transition

The stratigraphic sequences in Clements Markham Inlet commonly display an upward transition from gravels and sands of turbidity current channels (LA II and III) to laminated and current bedded sand (LA IV; sections 2, 3, 4, 19, 20, see Chapter 2). This transition from gravel to sand in the proglacial marine environment, where water depths were 30 to 80 m, must indicate the presence of subaquatic outwash. LA IV is composed of thin-bedded turbidites similar to those previously called distal turbidites and interpreted as deposits on basin plain environments (Walker 1967). However, these have been reinterpreted as proximal channel overspill deposits of levees

and overbank areas on the mid-portion of submarine fans (e.g., Howell and Normark 1982; Walker 1985). A similar model is illustrated for Clements Markham Inlet in Figures III.23 and III.24. Comparison of LA IV with examples from the literature on deep-sea fans supports this origin for LA IV (Mutti 1977; Dott and Bird 1979; Eriksson 1982; Howell and Normark 1982; Pickering 1982; Stow and Piper 1984b; Walker 1985). Specifically, these thin-bedded turbidites are characterized by Ta divisions; starved ripples (Eriksson 1982); climbing ripples (Eriksson 1982; Walker 1985); and parallel lamination (Sturm and Matter 1978; Chough and Hesse 1980; Hay 1983). They are sometimes found in association with channel margins and commonly are located stratigraphically above channel sands (Pickering 1982; Walker 1985).

An alternative, but closely related, explanation is that LA IV also represents deposition from a decelerating turbidity current as it exits a channel to be deposited as a fan lobe on the adjacent suprafan (Figs. III.23, III.24). Certain characteristics of LA IV resemble Larue and Speed's (1983) oscillatory sequence which they interpret as deposition on a fan lobe. Fan lobes correspond to a zone of decelerating flow similar to a levee and thus they should have similar depositional characteristics. Indeed Bouma's (1962) original model showed a progressive base-cut-out sequence on the suprafan (see Howell and Normark 1982, Fig. 7; also Fig. III.24) and this relationship was one basis for Walker's (1967) definition of proximal versus distal turbidity current deposits. These fan lobes are generally quite sandy and are incised by shallow channels which may become

progressively more braided as they lose their sediment load (Hiscott 1980; Pickering 1981). Certain aspects of the channels in the LA III to IV transition may relate to similar conditions. However, there is an important difference between the sequences reported here and those from turbidite basins. In turbidite basins, the depositional lobes coarsen-upwards both in grain size and bed thickness, whereas in Clements Markham Inlet both the general stratigraphic sequence and that within LA IV fines-upwards. LA IV also displays a hydrodynamically complex interbedding (e.g. Fig. III.7) and it is difficult to envisage dozens of successive turbidity currents reaching the same pro-channel site in virtually identical hydrodynamic states to deposit such repetitive sequences. Therefore a levee/overbank area is the preferred interpretation.

Pickering (1982) suggests that the channel margin may be the most distinctive and recognizable turbidite facies association because of its rotational slumps and the thinning and fining of beds (see also Mutti 1977). This juxtaposition of channel and levee-overbank deposits is well recorded in Clements Markham Inlet (Table III-6; also section 20, Chapter 2). For example, the cross-cutting of Sm-filled channels through LA IV sediments (Fig. III.22f) indicates a genetic relationship between the two lithofacies associations. Additionally, when channels and LA IV occur in the same section, paleocurrent directions determined from climbing or starved ripples are oblique or perpendicular to the channels supporting the channel overspill interpretation (Fig. III.22a, e).

Turbidity current overspill occurs from both the head and body of a flow (Komar 1972). Hesse and Chough (1980) point out that on many deep-sea fan levees that Bouma Tc and Td laminae are the only primary sedimentary structures present. They argue that the Td silty to clayey laminations do not result from large-scale velocity fluctuations but rather from burst and sweep processes in the viscous sublayer of turbulent flows. The LA IV deposits examined in Clements Markham Inlet, however, are coarser-grained than those examined by Hesse and Chough (1980) and have more primary sedimentary structures. Repetitive alternations commonly occur in Clements Markham Inlet between Ta, Tb, Ssc (Tc), Sd, Ssr and Fm (Figs. III.7 to III.10) and, as discussed above, this is produced by fluctuating energy levels in the transporting flow. The interbedding observed in LA IV is considered to originate by fluctuations in turbidity current flow similar to those previously described for LA III, and these are discussed in more detail below.

Once initiated, flow variations in turbidity currents are produced by changing slope angles, progressive loss of sediment by deposition, and incorporation of ambient fluid (Akiyama and Stefan 1985, 1986). Additionally, such pulsations may be produced by an extension of the retrogressive slumping mechanism that produces surge-type turbidity currents (e.g., Rupke 1976; Shaw and Archer 1978; Pickering 1979). In this case, initial slumping generates a turbidity current that overtops the channel during the initial surge, predominantly from passage of the turbidity current head. This deposits Ta, Tb and Tc laminae while

subsequent body spill produces Td and Te laminae. Retrogressive slumps which occur in rapid succession produce surges that can lag behind, overtake or outrun preceding flows. This produces both a series of mixing events and flow pulses. New surge heads may overtop the channel and insert themselves beneath the ongoing body spill. Channels in Clements Markham Inlet commonly have rotational slumps along their margins which would similarly influence the turbidity currents (Fig. III.21a). Mixing of these causes the turbidity current surface to rise and lower so that intermittent channel overtopping occurs. These flow additions cause the turbidity current to overtop the channel with alternating head flow (Ta, Tb, Tc or Scr, Ssr) and body flow (Td, Te or Fm) as each new surge passes a given site.

Basal Bouma sequences and starved ripples are common in these sequences and must originate from the head of the turbidity current. This suggests that injections over the channel tops are commonly individual turbidity current flows, i.e. individual heads. The common presence of draped lamination derived from suspension-settling at a lower velocity than that which produces climbing ripples (Ashley et al. 1982) may be produced by velocity reduction in a single flow or by the subsequent overtopping by body flow. Thus the Clements Markham Inlet deposits represent deposition from a turbidity current which is a hybrid form between that of a simple surge and continuous turbidity current. Larue and Speed (1983) interpret their similar oscillatory sequence as related to cyclic variations in the concentration of organics in the transported sediment. Such an explanation in the

glaciomarine environment of Clements Markham Inlet is highly unlikely as organic contents are essentially non-existent.

Turbid Plumes

Turbid plumes are freshwater inter- or overflows with varying sediment concentrations (Fig. III.25). During initial entry these plumes are highly turbulent. This is especially apparent in buoyant plumes which rise to the surface creating fountains or boils in the water surface (Gilbert 1983; Cowan and Powell 1986). The turbulence within these surface plumes is sufficient to transport coarse sand in suspension. Cyclopsams from these proximal plumes are reported up to 0.5 km from the ice front in Alaska (Cowan and Powell 1986). As turbulence subsides and the sand supply is depleted, minor amounts of finer sands are deposited in a dominant matrix of silt producing finer cyclopels. These fine laminae are found up to 2.6 km from the glaciers in Alaska (Cowan and Powell 1986). Bedding and laminae thickness will also thin upward in sequences deposited from these progressively decaying turbid plumes.

Plumes which have lost all coarse sediment, and whose fine-grained sediment has undergone flocculation, may produce discrete settling layers recorded by massive silt beds (Hoskins et al. 1978; Gilbert 1983) or what Cowan and Powell (1986) call homogeneous mud. In certain areas within Clements Markham Inlet there are sections where sedimentation occurred only from suspension (e.g. Figs. III.13, III.14; sections 6, 15 and 22, Chapter 2). This is indicated by the complete lack of channel to overbank transitions and the absence of Bouma or climbing ripple

sequences.

Summary

In Clements Markham Inlet deposition beyond the retreating ice margin of the last glaciation produced a fining-upward sequence of subaquatic deposits. The basal unit is a diamicton-dominated horizon originating predominantly from debris flow with subsidiary deposits from ice-rafted debris, turbidity current and turbid plume materials. Subaquatic streams were prominent as indicated by the subsequent deposition of subaquatic outwash fans over the diamicton horizons. These outwash fans record channel deposition of gravels and sands by high density mass flows and turbidity currents. Related levee-overbank sediments were deposited by overspill from these channels. Meltwater streams also generated turbid plumes which produced a final draping of cyclopsams and cyclopels by suspension through the entire water column.

Glaciomarine Sedimentation, Glacial Limits and Paleoclimatic Change

The stratigraphy and sedimentology of raised marine sediments in Arctic Canada have much to contribute to our understanding of past ice limits and paleoclimatic conditions during deglaciation. It is apparent that conditions at the glacier bed exert an important control on the mechanisms of sediment influx to the glaciomarine environment (Eyles et al. 1983, 1985; Powell 1984). For example, modern, northern hemisphere subpolar glaciers, although not as extreme in

character as Antarctic polar glaciers, nonetheless have frozen beds which restrict their meltwater-sediment contribution to the stratigraphic record. Presently, these subpolar glaciers commonly have thick (up to 3m +) debris-rich basal ice (Boulton and Spring 1986; Gemmel et al. 1986; Stewart and Bednarski 1986; Sugden et al. 1987). During the last glaciation it is likely that even colder and more arid conditions prevailed (England and Bradley 1978; England 1986; Koerner et al. 1987). Despite this, the predominance of subaquatic outwash, cyclopsams, and cyclopels bear a striking similarity to sediments deposited adjacent to modern temperate tidewater glaciers (Powell 1983a; Mackiewizc et al. 1984; Cowan and Powell 1986) and to late Pleistocene glaciomarine lithofacies attributed to a temperate environment (Domack 1983, 1984). Furthermore, the deposits in Clements Markham Inlet are analogous to those described by Rust and Romanelli (1975), Rust (1977), Cheel and Rust (1982) from the southern margin of the Laurentide Ice Sheet.

The abundance of these lithofacies in Clements Markham Inlet demonstrates that during deglaciation significant amounts of meltwater reached the sediment-rich basal ice. This penetration of meltwater to the glacier base contrasts sharply with present conditions where meltwater is generally restricted to the surface of subpolar glaciers. Therefore, although subpolar glaciers may produce a distinctive terrestrial lithofacies sequence (Eyles et al. 1983) the evidence presented here does not support such uniqueness for the marine environment during the last deglacial cycle.

The information presented here necessitates warm conditions at the onset of the Holocene. Preliminary work on a core from the Mer de Glace Agassiz (Fig. III.1) suggests a significant climatic amelioration at ca. 10,000 to 8000 BP (Koerner et al. 1987; R. M. Koerner, pers. comm., 1987). Evans and Lemmen (1987) also report well-developed early Holocene sea ice-pushed ridges from NW Ellesmere Island that they interpret as indications of greater open water at that time. In contrast, several other paleoenvironmental reconstructions in this region document the mid-Holocene as the warmest interval. These latter interpretations are based on a variety of independent data (emergence, driftwood, fossil bryophytes, pollen; England 1983; Stewart and England 1983; Bourgeois 1986; LaFarge-England 1988) but, at present, the early Holocene data base is insufficient to resolve this discrepancy. Additional material from this period is necessary and an integration of the offshore marine and terrestrial biological record is especially required.

The Arctic Ocean basin is well known for its low sediment accumulation. Eyles et al. (1985, p. 38, 51) speculate that the lack of coarse-grained sediments in the Arctic Ocean basin is due to the fact that glaciers rimming its border were cold-based and produced little meltwater during deglaciation. However, the glaciers in Clements Markham Inlet produced abundant meltwaters which were able to deposit sedimentary sequences indistinguishable from those of the warm middle latitudes. If Clements Markham Inlet is representative of other localities in the Canadian Arctic Islands and northern Greenland then restricted deglacial

sediment volumes are not the reason for the limited clastic sediment in the Arctic Ocean. To the contrary, the limited deposition in the Arctic Ocean basin must be a function of sediment entrapment in the inner fiord environments where the last ice limit was located. Indeed, this circumstance was recognized by Eyles et al. (1985: 38) for other coastlines. It also follows that abundant glaciomarine sediments commonly reported from fiord heads are a good indication of the last ice limit (England 1986). Therefore, this sediment entrapment marks the generally restricted ice advance in the Canadian Arctic Islands and northern Greenland. Similar trapping of sediment could well have occurred on the broad continental shelves bordering the Siberian rivers. The lack of coarser sediments within the Arctic basin is a result of restricted ice advance and broad continental shelves rather than cold-based glaciers. One should map the distribution of submarine sediments from the last ice limit onto the continental shelves to test whether there have been more extensive, earlier ice margins in the fiords of northern Ellesmere Island. The unknown distribution of these sediments and their characteristics constitute a major gap in our understanding of paleoenvironmental change in high latitudes.

TABLE III-1

Lithofacies codes for sediments observed in Clements Markham Inlet (modified from Eyles et al. 1983)

Code	Lithofacies Type	Description
Dmm(r)	Diamicton, matrix-supported massive, evidence of resedimentation	Intraformational rip-up clasts, bed amalgamation, bedding planes evident
Dmg	Matrix-supported, graded	Variable vertical grading in matrix or clasts
Gm	Gravel, massive or crudely bedded	Horizontal bedding, graded, imbrication, planar crossbeds
Gp	Gravel, stratified	Planar crossbeds
GSt	Gravelly sand, stratified	Trough crossbeds
GSf	Gravelly sand, bedded	Large-scale deltaic foreset beds
Sm	Sand, massive to graded	Dish structures, $\bar{x}$ = 2 - 4 phi
SB	Sand, graded to laminated	Bouma sequences, Tabc, Tac, Tae
Scr	Sand, rippled	Climbing ripples, type B dominant
Ssr	Sand, rippled	Starved ripples
Sl	Fine sand to coarse silt, laminated	Draped lamination
Scps	Sand, graded, laminated	Cyclopsams
Fcpl	Mud, interlaminated	Cyclopels
Fm	Mud, massive	Clast poor
Fl	Mud, laminated	

TABLE III-2

Facies Association	Interpretation
I. Interbedded Diamicton, Sand, Silt	Subaquatic Debris Flow, Mass Flow, Turbid Plume, Ice Rafting
II. Gravels	Subaquatic Outwash Channel, Englacial Stream
III. Amalgamated/Graded Sand	High Density TCs, Mass Flow, Channelized
IV. Graded Laminated and Current Bedded Sand	Levee-Interchannel Turbidity Current (TC) Deposit
A. Bouma Sequence	Low Density TC
B. Climbing Ripples	Traction-Suspension TC
C. Starved Ripples	Traction w. Low Sediment Concentration
D. Draped Lamination	Suspension Sedimentation from TC
V. Interbedded and Interlaminated Sand	Suspension Sedimentation from Turbid Plume
A. Cyclopsams	Proximal
B1. Cyclopels	Distal
B2. Silts, non-laminated	Distal
VI. Gravels, Large-Scale Crossbeds	Sandur and Related Deltaic Sediments

TABLE III-3

Stratigraphic Differentiation of Lithofacies and Lithofacies Associations

Stratigraphic Event	Lithofacies	Lithofacies Association
3. Glacial Retreat: prograding sub-aerial deltas	Gp, Gm, GSt, GSf	VI
2. Glacial Retreat: glaciomarine sediments	Scps, Fcpl, Fm	V
	Sm, SB, Scr, Ssr	IV
	Sm, SB	III
	Gm, Gp	II
	Dmm(r), Sm, Fl, Fm	I
1. Pre-last Glaciation: prograding subaerial sandur (?)	Gp, Gm, GSt, St	VI

Note that the stratigraphic sequence of event 2 represents a fining-upwards trend related to ice retreat

TABLE III-4

Stratification types and thicknesses (after Ingram 1954)

Very thickly bedded	> 1 m
Thickly bedded	30 - 100 cm
Medium bedded	10 - 30 cm
Thinly bedded	3 - 10 cm
Very thinly bedded	1 - 3 cm
Thickly laminated	3 - 10 mm
Thinly laminated	1 - 3 mm
Very thinly laminated	< 1 mm

TABLE III-5

Diamicton fabric characteristics from Clements Markham Inlet

Section. Sample	Vector Strength R	Eigenvalues S1	S2	S3	Principal Eigenvector Azimuth A	Plunge P
5.1	27.3	0.38	0.26	0.36	348.0	33.2
5.2	16.9	0.55	0.25	0.2	194.8	41.8
5.3	24.3	0.51	0.34	0.15	151.8	16.3
13.4	39.0	0.64	0.22	0.14	23.5	21.0
13.5	29.8	0.43	0.36	0.2	139.5	23.0
14.1	17.8	0.56	0.32	0.12	7.9	22.0
14.2	32.7	0.5	0.31	0.19	0.6	2.4
14.3	31.1	0.48	0.38	0.19	19.5	23.3
14.4	37.7	0.61	0.18	0.21	9.8	28.8
14.5	15.5	0.5	0.23	0.26	137.5	8.2
14.6	34.0	0.55	0.23	0.21	157.0	5.6
1*		0.51	0.44	0.05	218.0	11.4
2*		0.6	0.32	0.08	13.5	5.8
3*		0.58	0.16	0.26	175.0	43.7
4*		0.61	0.28	0.11	333.0	4.0

* unpublished data provided by J. Bednarski

TABLE III-5 - Summary Statistics

	Mean	SD	Skew.	Kurt.	%Sand	%Silt	%Clay
Diamicton Matrix							
Mean	4.9	3.9	-0.05	0.8	38.4	36.3	25.4
SD	0.36	0.11	0.08	0.07	4.9	4.1	3.1
Min.	4.4	3.7	-0.25	0.7	27.0	29.0	21.0
Max.	5.8	4.1	0.06	1.0	45.0	45.0	34.0
N = 17							
Silts interbedded in Diamicton							
Mean	7.5	2.0	0.18	0.9	2.3	60.6	37.1
SD	0.4	0.1	0.04	0.12	1.4	4.1	4.8
Min.	6.7	1.8	0.13	0.8	0.6	55.4	29.0
Max.	7.9	2.2	0.27	1.2	4.5	66.6	44.0
N = 8							
Cyclopels							
Mean	7.7	2.0	0.19	0.8	1.7	54.6	43.8
SD	0.8	0.2	0.15	0.1	3.3	12.4	13.1
Min.	5.9	1.6	-0.19	0.7	0.01	32.0	17.0
Max.	8.8	2.7	0.62	1.4	13.0	81.0	64.0
N = 34							
Amalgamated Sand							
Mean	2.9	0.6	0.13	1.1	89.1	10.2	0.8
SD	0.5	0.1	0.10	0.1	12.8	12.8	0.6
Min.	1.9	0.5	-0.16	0.8	45.0	1.0	0.2
Max.	4.0	1.0	0.34	1.3	98.8	55.0	3.0
N = 25							
Bouma Sequence							
Mean	3.7	0.6	0.06	1.1	64.0	35.5	0.6
SD	0.3	0.1	0.19	0.3	15.6	15.9	0.4
Min.	3.0	0.4	-0.39	0.8	37.0	7.8	0.0
Max.	4.2	0.8	0.28	1.6	91.0	63.0	1.2
N = 13							
Starved Ripples							
Mean	3.9	1.4	0.43	1.7	65.0	29.6	5.4
SD	0.7	0.4	0.10	0.2	20.0	16.4	3.6
Min.	3.2	1.0	0.33	1.6	45.0	13.2	1.8
Max.	4.6	1.8	0.52	1.9	85.0	46.0	9.0
N = 2							

TABLE III-7

Classification of sorting values in phi units (after Folk 1984)

> 4.0	extremely poorly sorted
2.0 - 4.0	very poorly sorted
1.0 - 2.0	poorly sorted
.71 - 1.0	moderately sorted
.50 - .71	moderately well sorted
.35 - .50	well sorted

TABLE III-8

Characteristics of Channel forms observed in Clements Markham Inlet

Section	Figure	Dimensions (w x d) m	Recognizeable Channel to Inter-channel Facies Transition	Erosional Undercutting/ Slumping at Margin	Beds Thin Towards Margin	Draping of Channel by Fines	Fining Upward Succession
4	22b	25 x 10		X	X	X	X
20	-	2.5 x 1.5	X	X	X	X	
20	22f	2 x 1			X	X	X
16	22c	10 x 2.5	X		X	X	
17	22g	.5 x .2	X		X	X	
18A/B	22a	Channel truncated ca. 5 m depth	X		X	X	X
21 Channel or Slump	16	ca. 1 m deep			X		

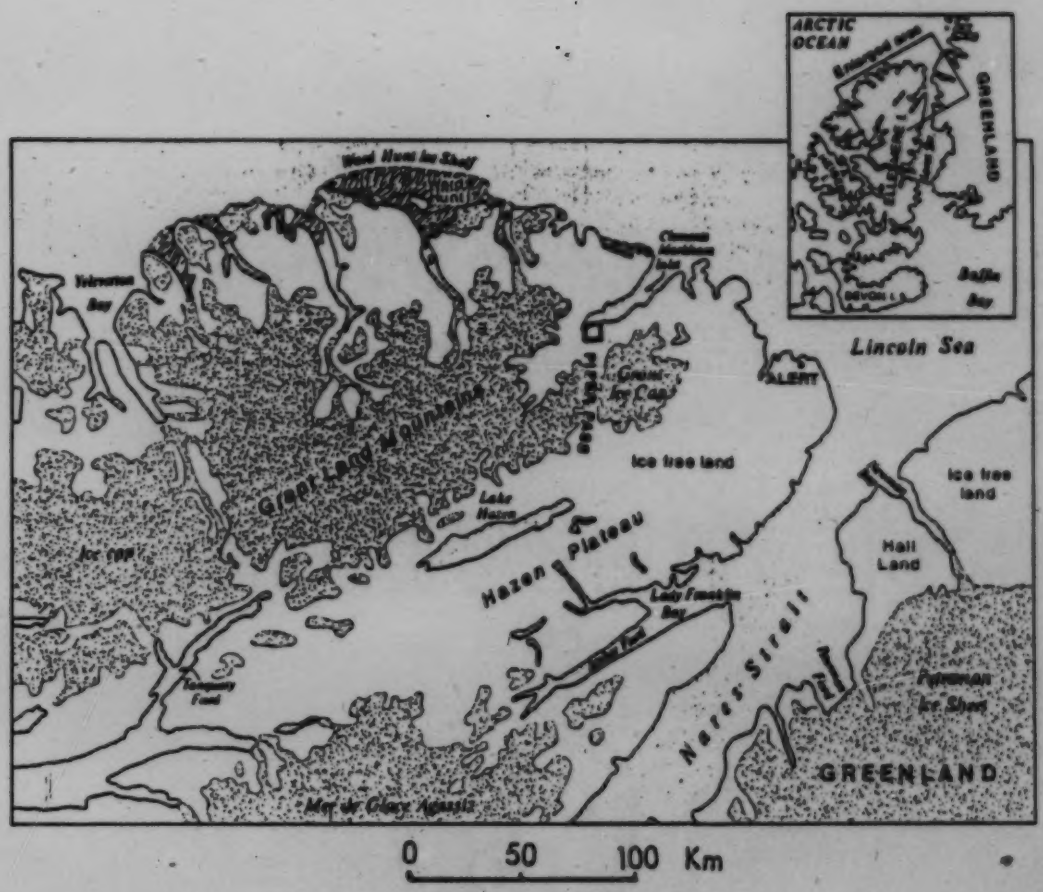

Figure III.1. Northern Ellesmere Island. Study area is located at the north end of Piper Pass where it joins Clements Markham Inlet. Note the extent of permanent icefields and outlet glaciers (stippled) which cover most of the Grant Land Mountains. Inset shows the relationship of Ellesmere Island to NW Greenland. Square at the head of the inlet corresponds to the field area shown in Figure 2.

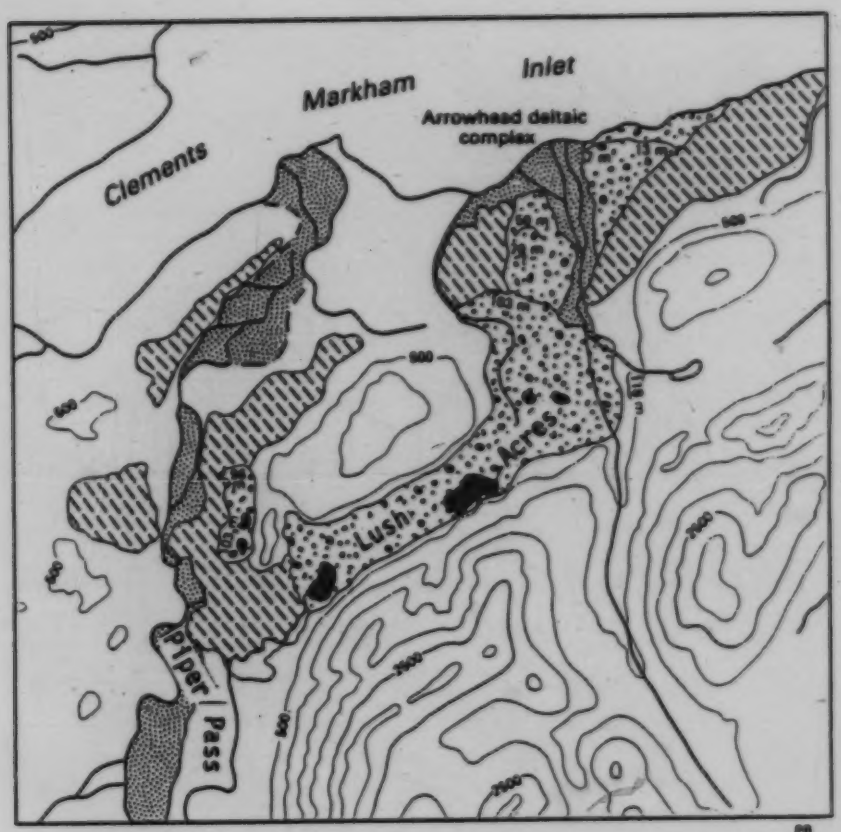

Figure III.2. Surficial geology of the Arrowhead and Piper Pass area.

a)

b)

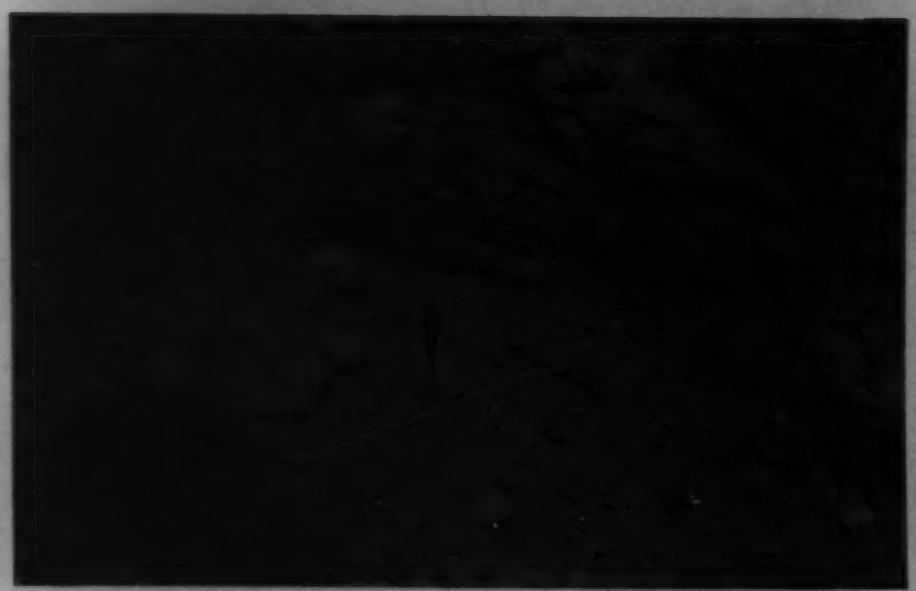

Figure III.3a, b. Diamicton units of section 14, Chapter 1. a)Note how silt interbed at rifle shell (30.06) thins to the right. This bed disappears beyond the photograph where the diamicton beds enclosing it become amalgamated. Also note silt bed below the rifle shell is eroded out. b)Diamicton with parting planes interpreted as bedding planes.

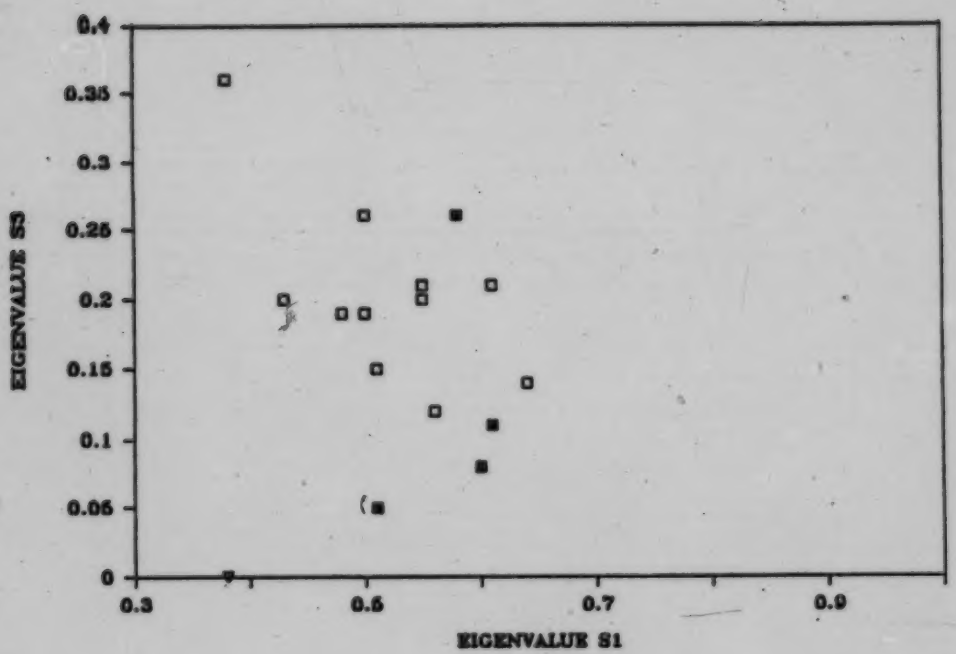

Figure III.4. Bivariate plot of S1 versus S3 eigenvalues for fabrics from Clements Markham Inlet. Open squares from this study, black squares from unpublished measurements by Jan Bednarski (personal communication, 1987).

Figure III.5. Contoured Schmidt equal-area nets for pebble orientations from diamictons interbedded with sands and silts. Arrows indicate computed mean axis direction. Black is area of maximum concentration. N = number of observations; A = computed axis azimuth; S1 = eigenvalue. Contour interval is 2 sigma. Sections are described in Chapter 2.

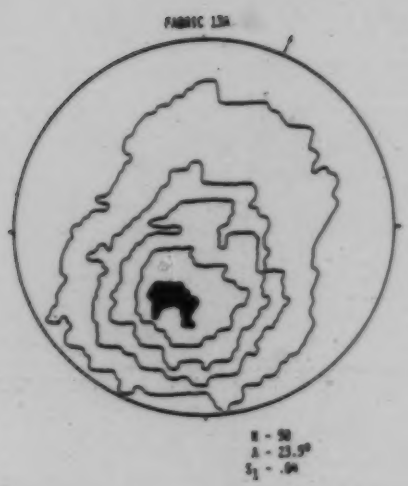
FABRIC 13A
N = 50
A = 23.5°
S1 = .64

FABRIC 13B
N = 50
A = 146°
S1 = .43

FABRIC 5A
N = 50
A = 34°
S1 = .38

FABRIC 5B
N = 25
A = 159°
S1 = .55

FABRIC 5C
N = 46
A = 152°
S1 = .53

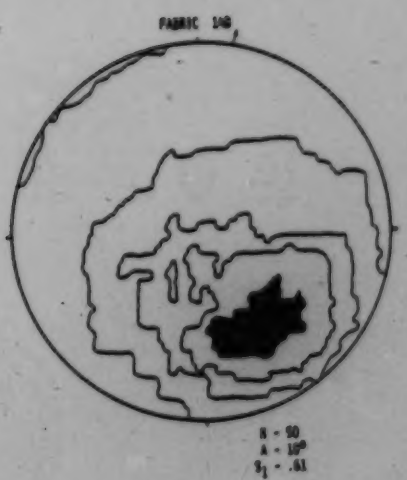

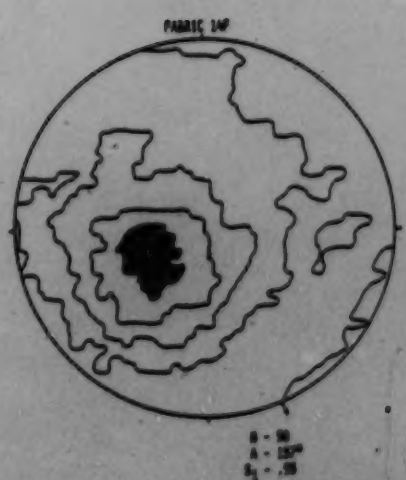

a)

Figure III.6a, b, c. Lithofacies Association III. a)Overview photograph of section 19. Section consists of Sm from base to just below the "shoulder" or break in slope at upper right. Note top of red ruler at base. b)Sm at base of section 19. Ruler is in same position as in a. c)Graded sand beds; note loading of sand into underlying sand and the floating sand clasts indicating bed amalgamation.

b)

c)

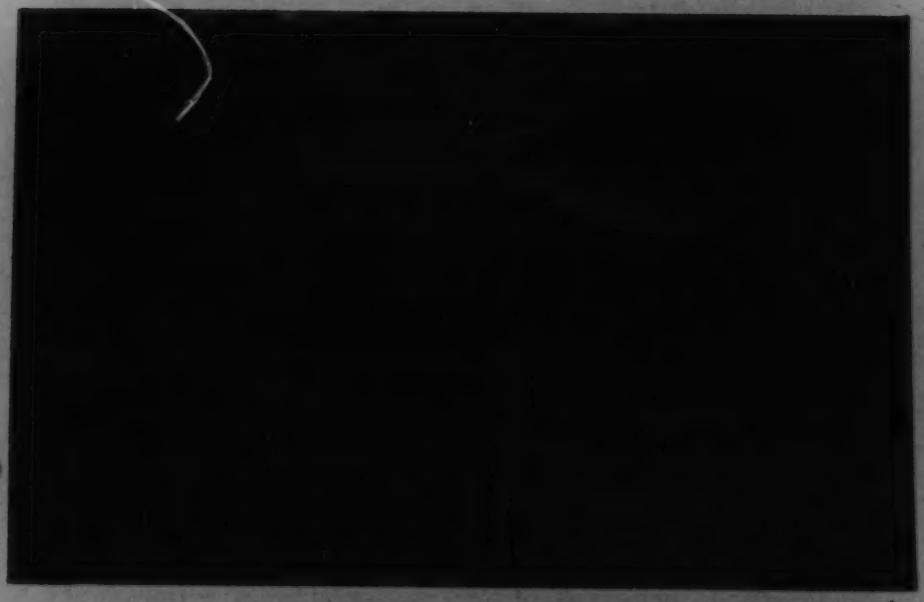

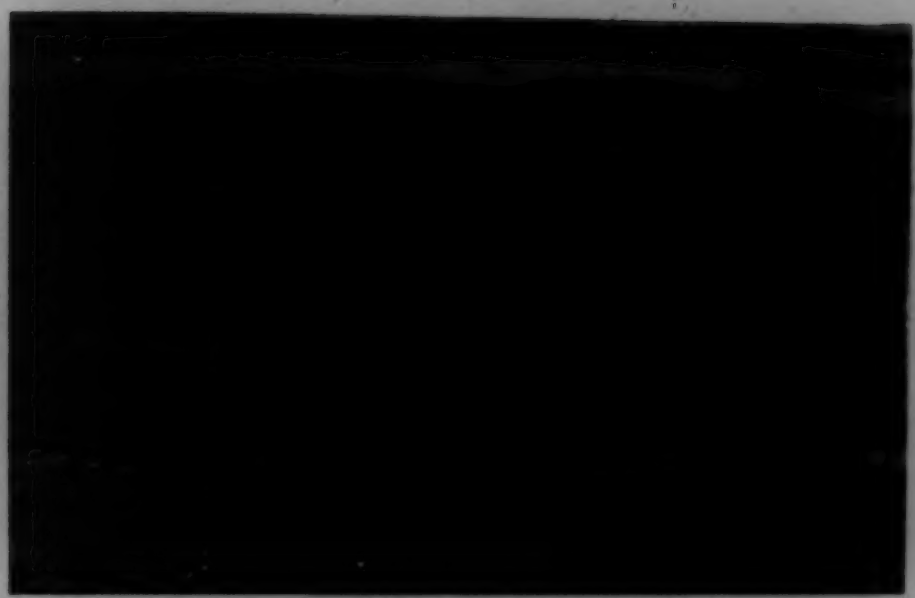

Figure III.7. Repetitive interbedding of graded sand (Ta), draped lamination and starved ripples (from section 1, Chapter 2). Note that the flame and loading structures deflected from right to left in left center of photograph. Paleocurrent direction from right to left (north).

Figure III.8. Type B climbing ripples. Paleocurrent direction from right to left (north).

Figure III.9. Central part shows starved ripples overlain by draped lamination. Note microflame structures to left of ruler 5 inches.

Figure III.10a, b. a)Photograph of a fining-upward sequence of graded sand overlain by draped and starved ripple laminations. Note undulations at the surface of the graded sand. The starved ripples are repetitively interspersed with the draped lamination near the bottom and are isolated within ungraded silt in the upper center. b)Closer view of starved ripples at top of photograph a.

a)

b)

Figure III.11. Deformed mass flow sediment overlain by cyclopsams. See text for explanation. From section 22, Chapter 2.

Figure III.12. Examples of cyclopels, Fcpl. a)Fresh exposure, white layers are sand; dark layers are silt. Note the distinctness of the sand laminae and their variation in thickness. Close inspection of the sand laminae shows microloading structures into the underlying silt. Section 6, Chapter 2. b)Dried exposure, flagginess is produced by sand laminae of similar thickness to those in photography a. Section 4, Chapter 2.

a)

b)

Figure III.13. Ungraded silt, Fm, overlain by cyclopsams, Scps. Section 15, Chapter 2.

Figure III.14. Large-scale slump folds (section 19, Chapter 2). Shovel at lower right is 1.2 m high. The prominent fold above the shovel is overlain by horizontal and apparently undisturbed beds.

a)

Figure III.15. Contorted bedding. a)Overview photograph. Note horizontal bedding of cyclopsams and disrupted horizon near top. Horizontal arrow points to large fold with fragmented beds within it. Vertical arrow points to location of photograph b. The beds capping this disrupted horizon are horizontal. Feature transecting the photograph from upper right to the center is a rill on the surface of the section. Trowell at left circled for scale. b)Close-up of part of the disrupted horizon where originally horizontal laminae are overturned and truncated by undisturbed overlying laminae.

b)

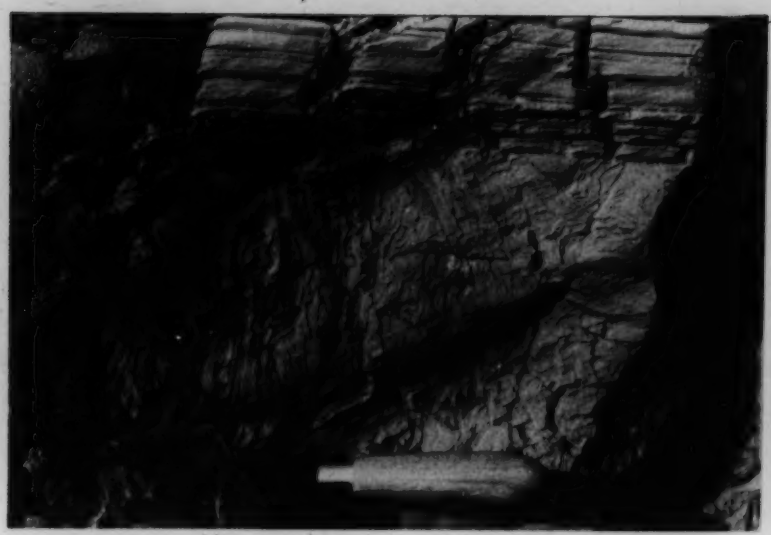

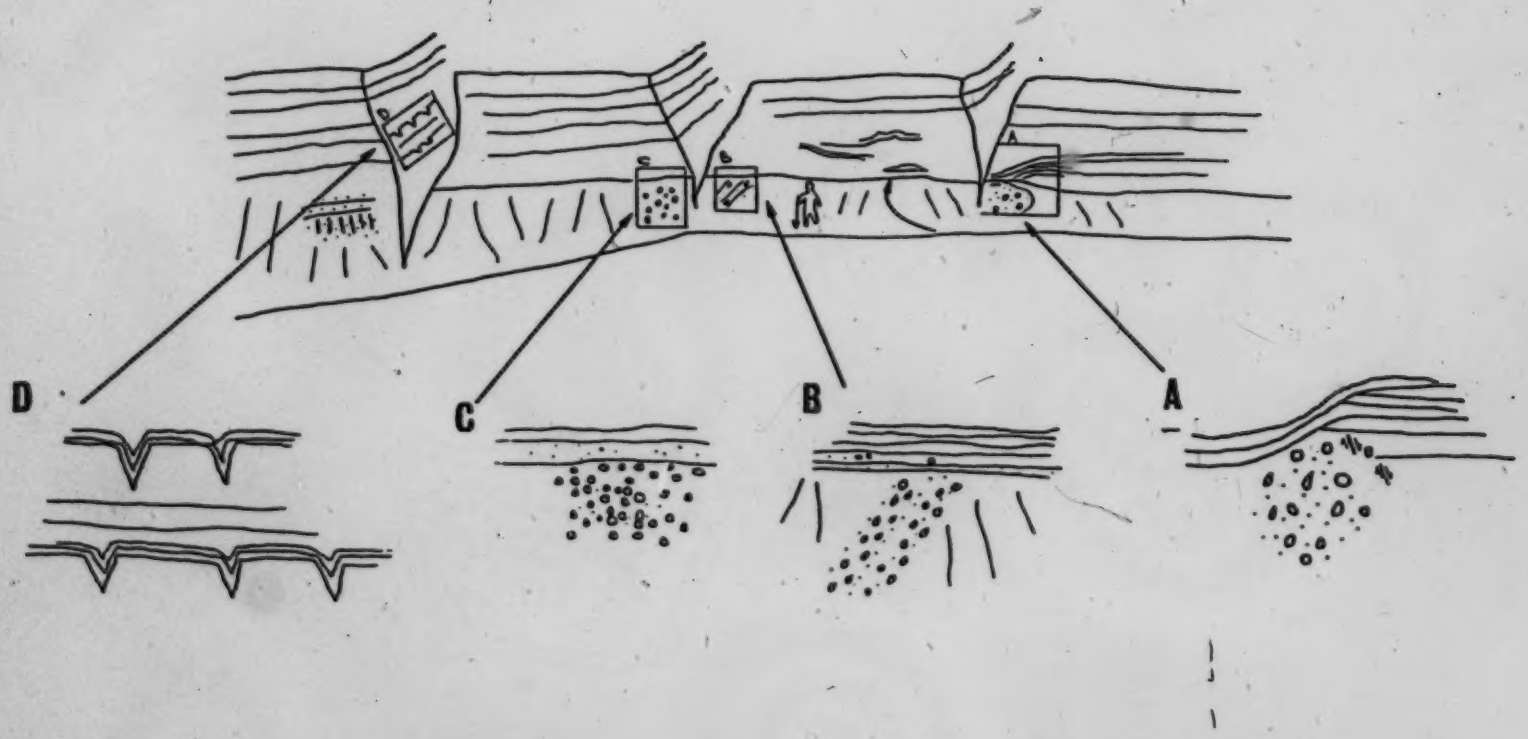

Figure III.16. Sketch of section 21. a)Diamicton draped by fine-grained turbid plume deposits. Normal faults in the diamicton with displacements of ca. 3 to 5 cm suggest the burial and subsequent melting of ice. b)Sorted and cross-bedded gravels overlain by turbid plume deposits. c)Sorted gravels overlain by turbid plume deposits. d)Burrow structures. Arrow indicates position of pod structure composed of laminated sands and silts.

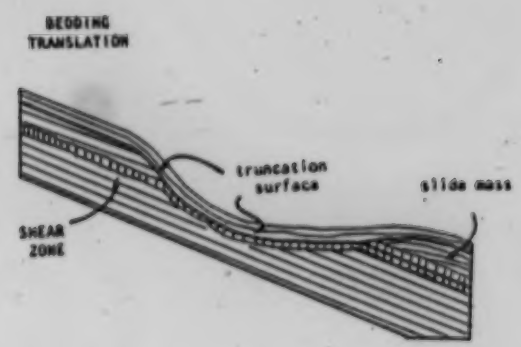

Figure III.17. Diagrammatic sketch of submarine slope failure indicating positions of synsedimentary shear zones (after Gawthorpe and Clemmeney 1985; Coniglio 1986).

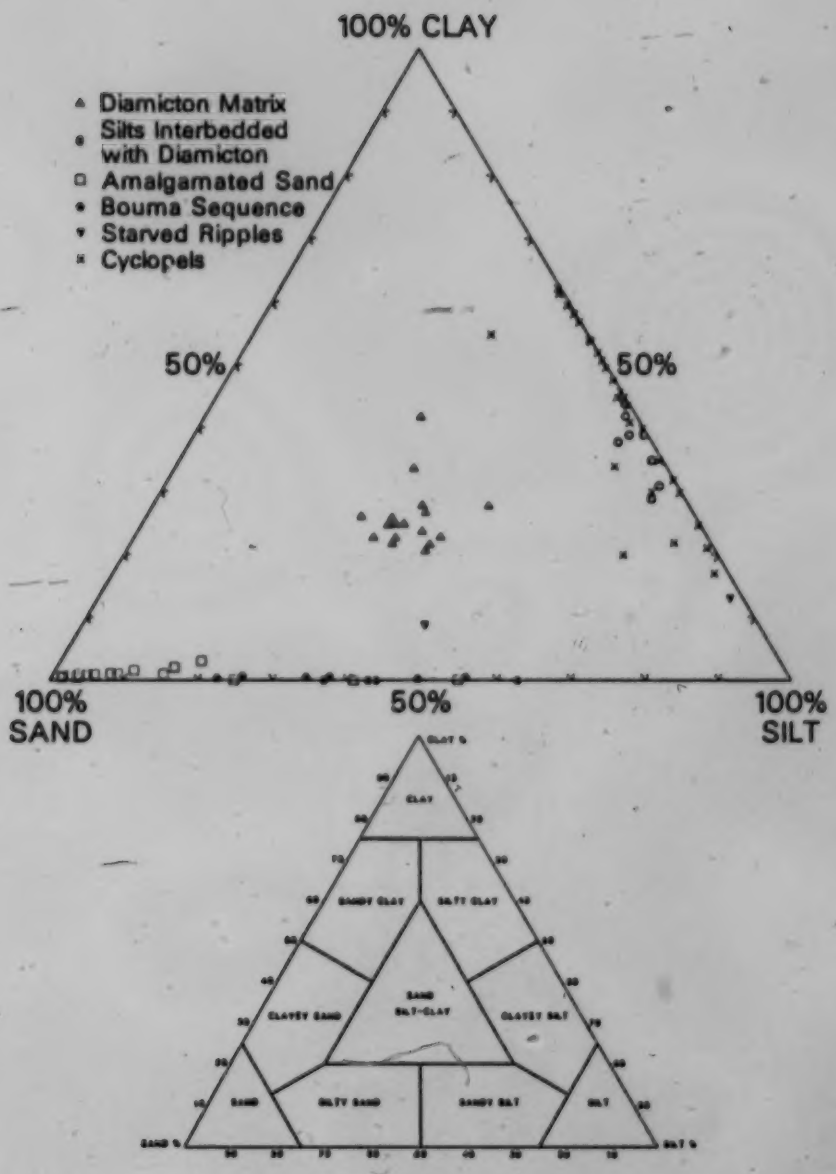

Figure III.18. Ternary plot of all grain-size samples.

Figure III.19. Grain size curves. Sample numbers refer to Appendix III-1.

a) Diamicton matrix. Envelope of all samples and two representative curves from individual samples. Note the straight line plot indicating poor sorting.

b) Silts interbedded with diamictons and cyclopels.

c) Representative grain size distribution for amalgamated and graded sand (Sm) and Bouma sequences (SB) showing both envelopes for all samples analyzed and for individual samples from the bottom and top of individual beds. These individual samples document the characteristic grading of these lithofacies.

d) Curves for the two samples of starved ripple. Note the tail in the silt and clay fraction.

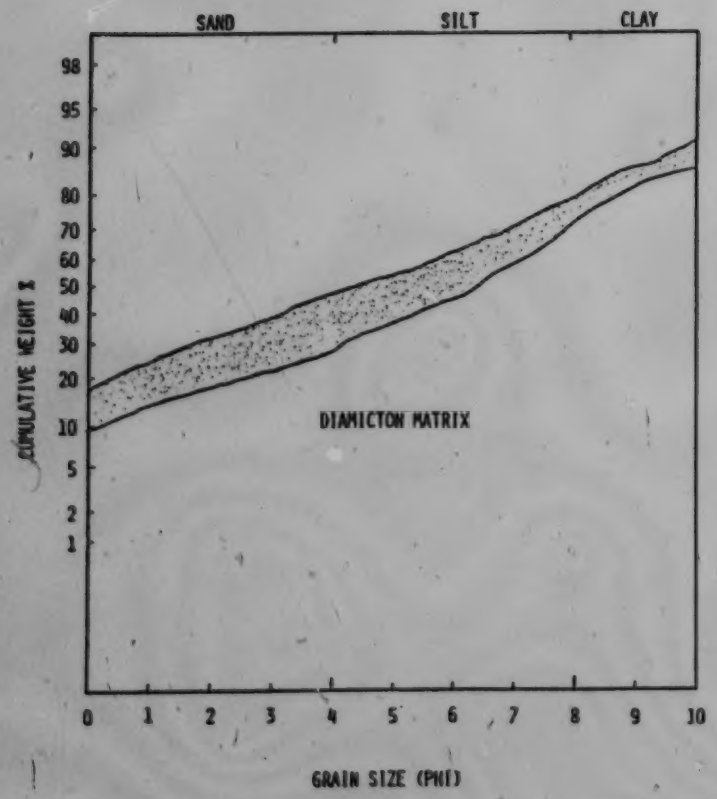
SAND
SILT
CLAY
98
95
90
80
70
60
50
40
30
20
10
5
2
1
CUMULATIVE WEIGHT %
DIAMICTON MATRIX
0 1 2 3 4 5 6 7 8 9 10
GRAIN SIZE (PHI)

a)

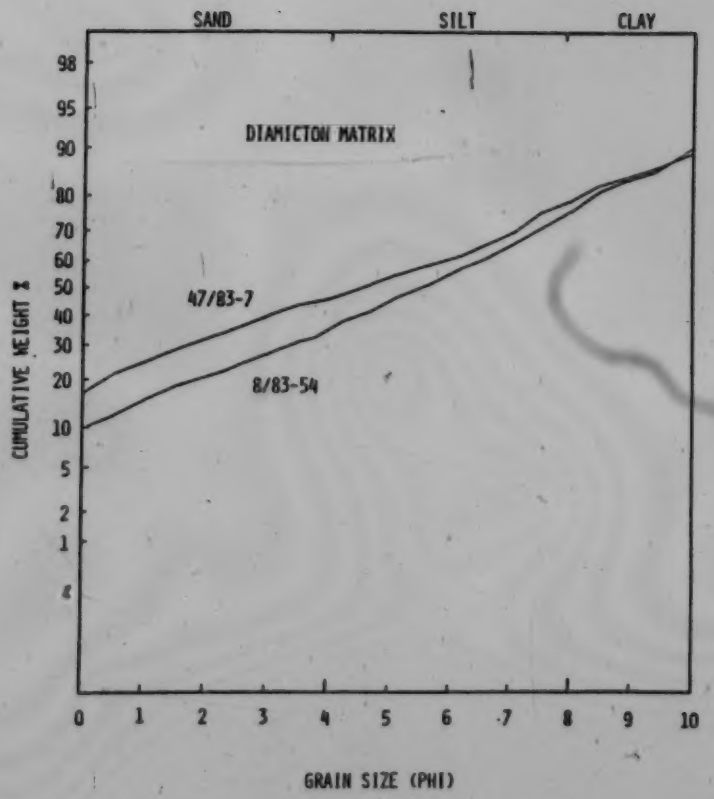
SAND
SILT
CLAY
98
95
90
80
70
60
50
40
30
20
10
5
2
1
CUMULATIVE WEIGHT %
DIAMICTON MATRIX
47/83-7
8/83-54
0 1 2 3 4 5 6 7 8 9 10
GRAIN SIZE (PHI)

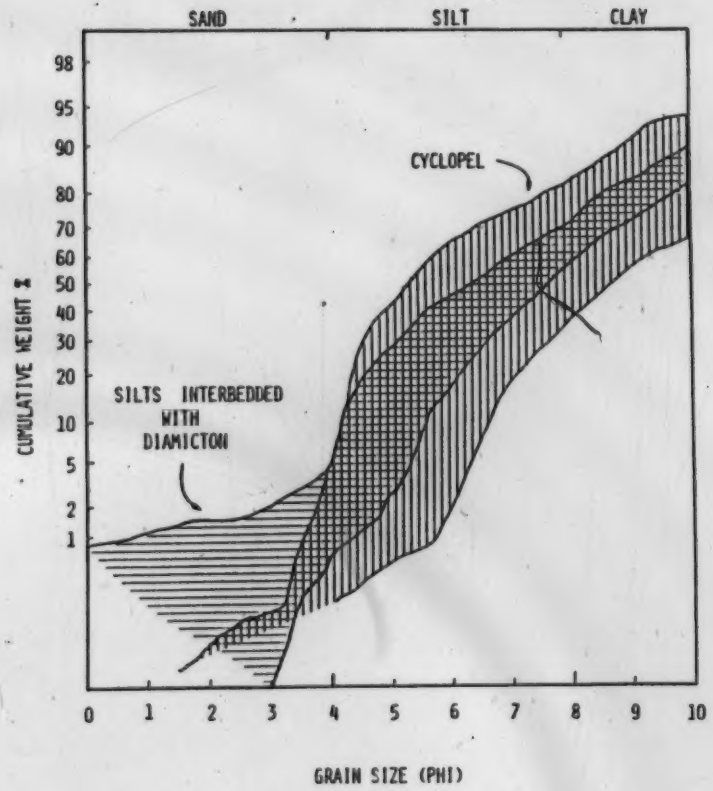
SAND
SILT
CLAY
98
95
90
80
70
60
50
40
30
20
10
5
2
1
CUMULATIVE WEIGHT %
CYCLOPEL
SILTS INTERBEDDED WITH DIAMICTON
0
1
2
3
4
5
6
7
8
9
10
GRAIN SIZE (PHI)

b)

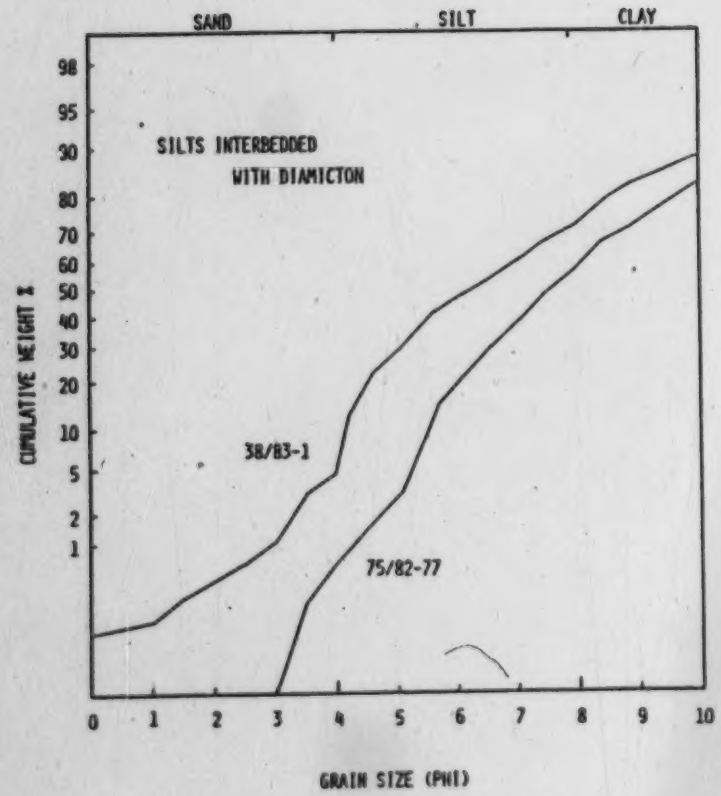
SAND
SILT
CLAY
SILTS INTERBEDDED
WITH DIAMICTON
38/83-1
75/82-77
CUMULATIVE WEIGHT %
GRAIN SIZE (PHI)

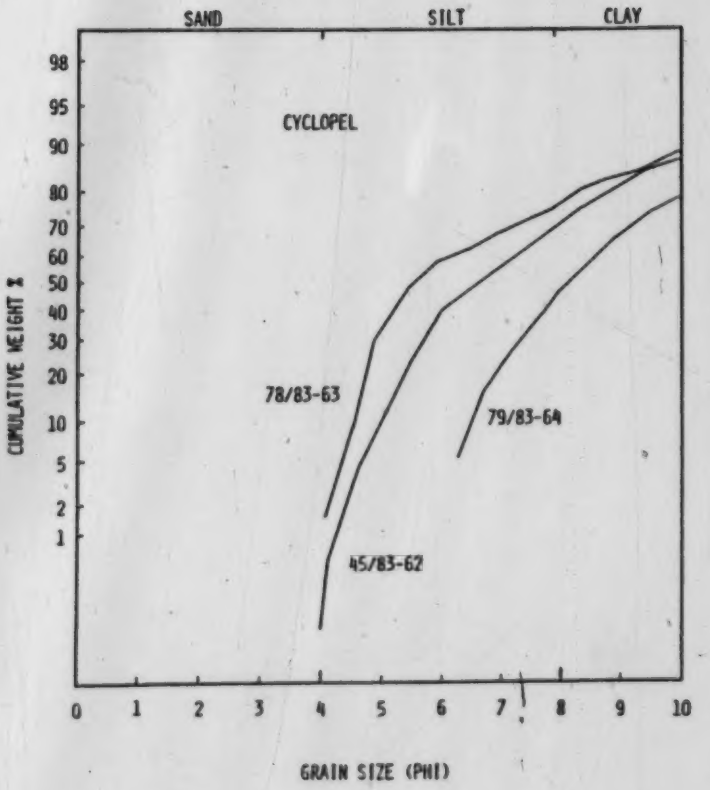
SAND
SILT
CLAY
CYCLOPEL
78/83-63
79/83-64
45/83-62
CUMULATIVE WEIGHT %
GRAIN SIZE (PHI)

b) continued

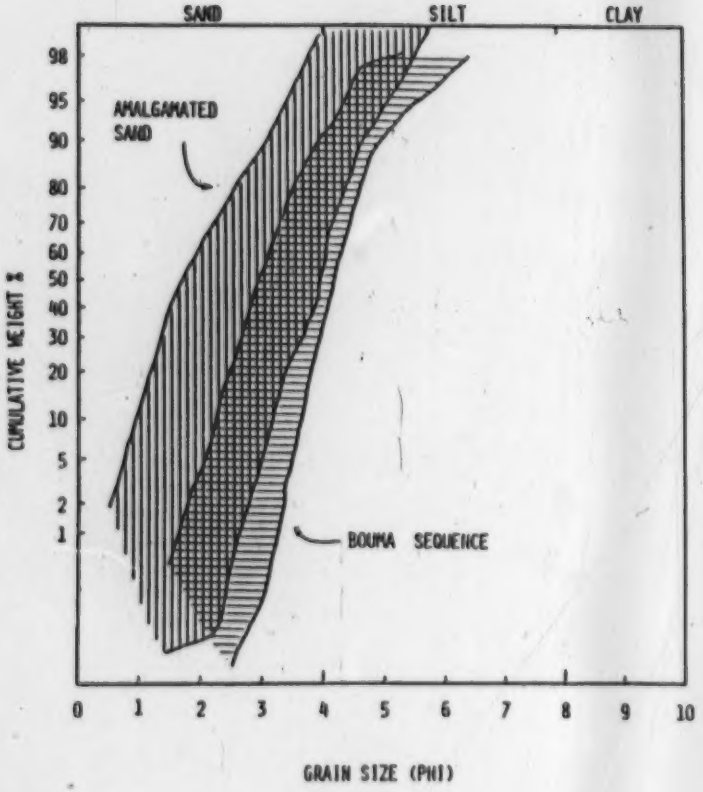
SAND
SILT
CLAY
AMALGAMATED SAND
BOUMA SEQUENCE
CUMULATIVE WEIGHT %
GRAIN SIZE (PHI)

c)

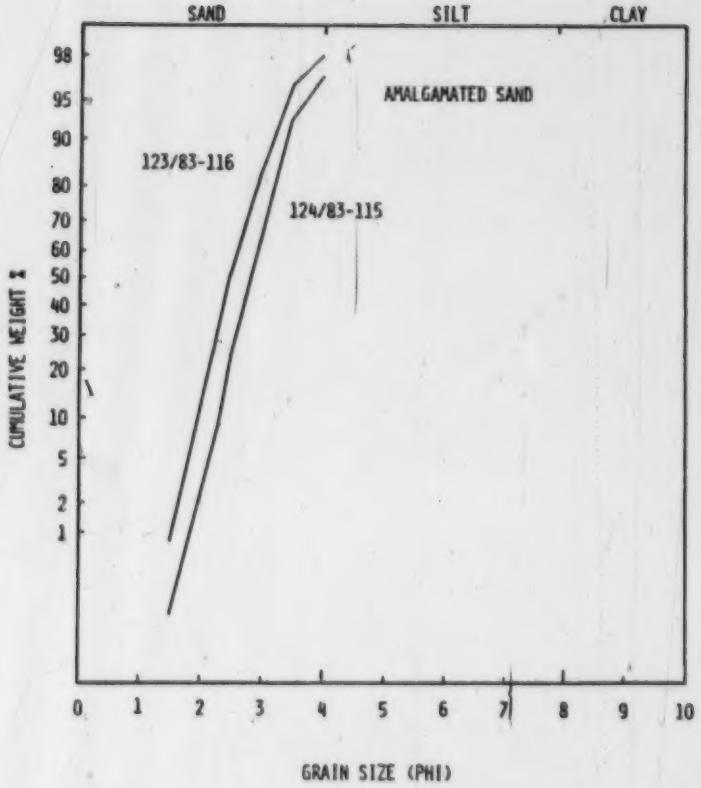
SAND
SILT
CLAY
AMALGAMATED SAND
123/83-116
124/83-115
CUMULATIVE WEIGHT %
GRAIN SIZE (PHI)

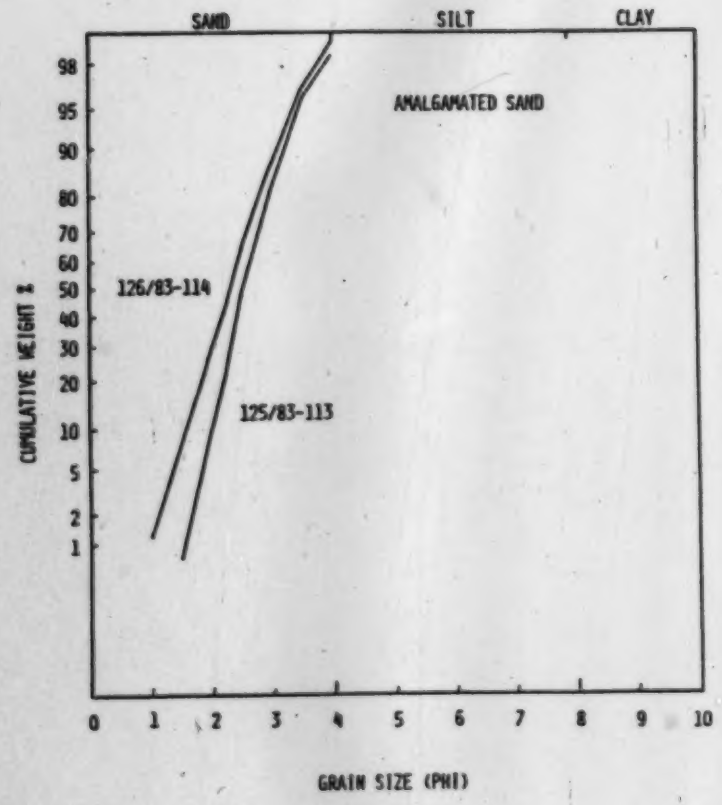
SAND
SILT
CLAY
AMALGAMATED SAND
126/83-114
125/83-113
CUMULATIVE WEIGHT %
98
95
90
80
70
60
50
40
30
20
10
5
2
1
0 1 2 3 4 5 6 7 8 9 10
GRAIN SIZE (PHI)

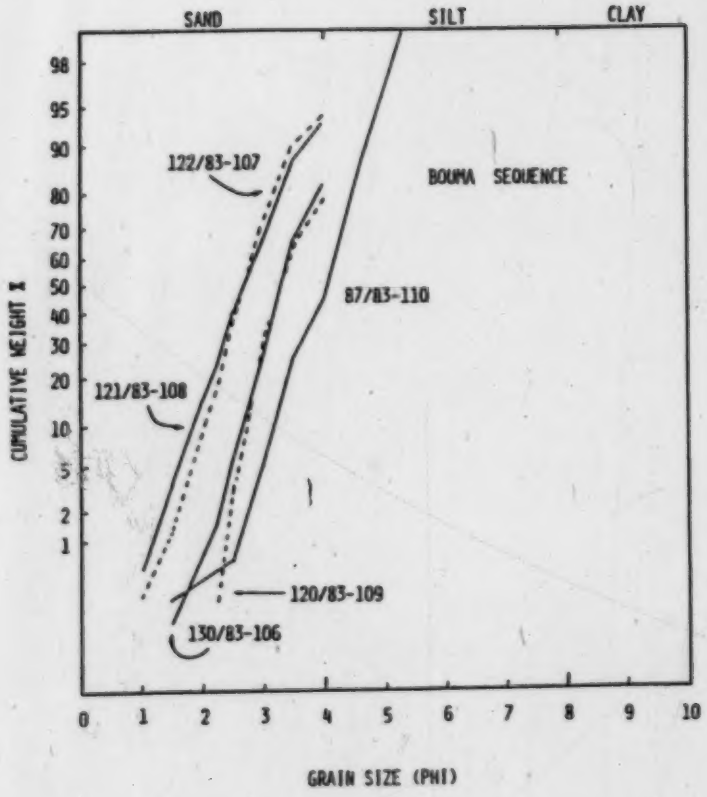
SAND
SILT
CLAY
BOUMA SEQUENCE
122/83-107
87/83-110
121/83-108
120/83-109
130/83-106
CUMULATIVE WEIGHT %
98
95
90
80
70
60
50
40
30
20
10
5
2
1
0 1 2 3 4 5 6 7 8 9 10
GRAIN SIZE (PHI)

c) continued

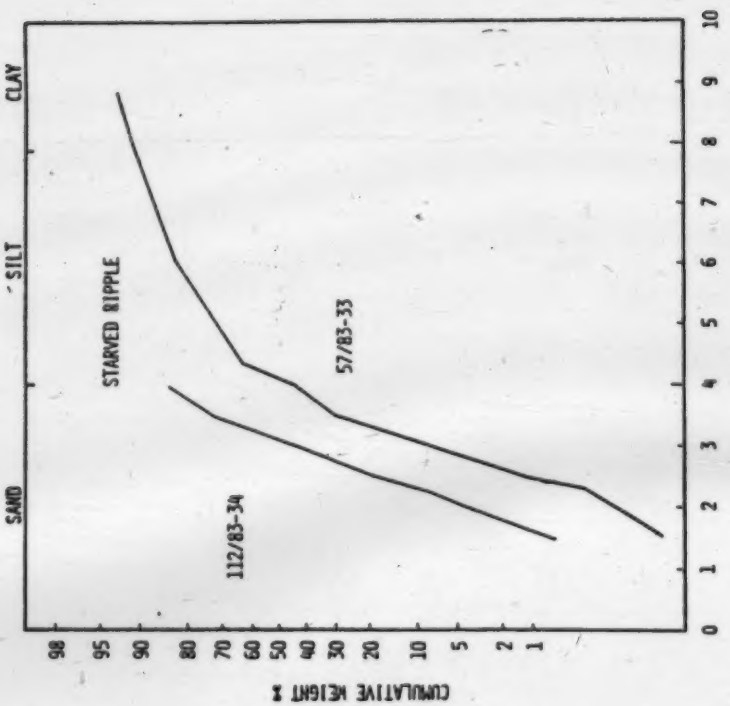
SAND
SILT
CLAY
STARVED RIPPLE
57/83-33
112/83-34
CUMULATIVE WEIGHT %
GRAIN SIZE (PHI)
98
95
90
80
70
60
50
40
30
20
10
5
2
1
0
1
2
3
4
5
6
7
8
9
10

d)

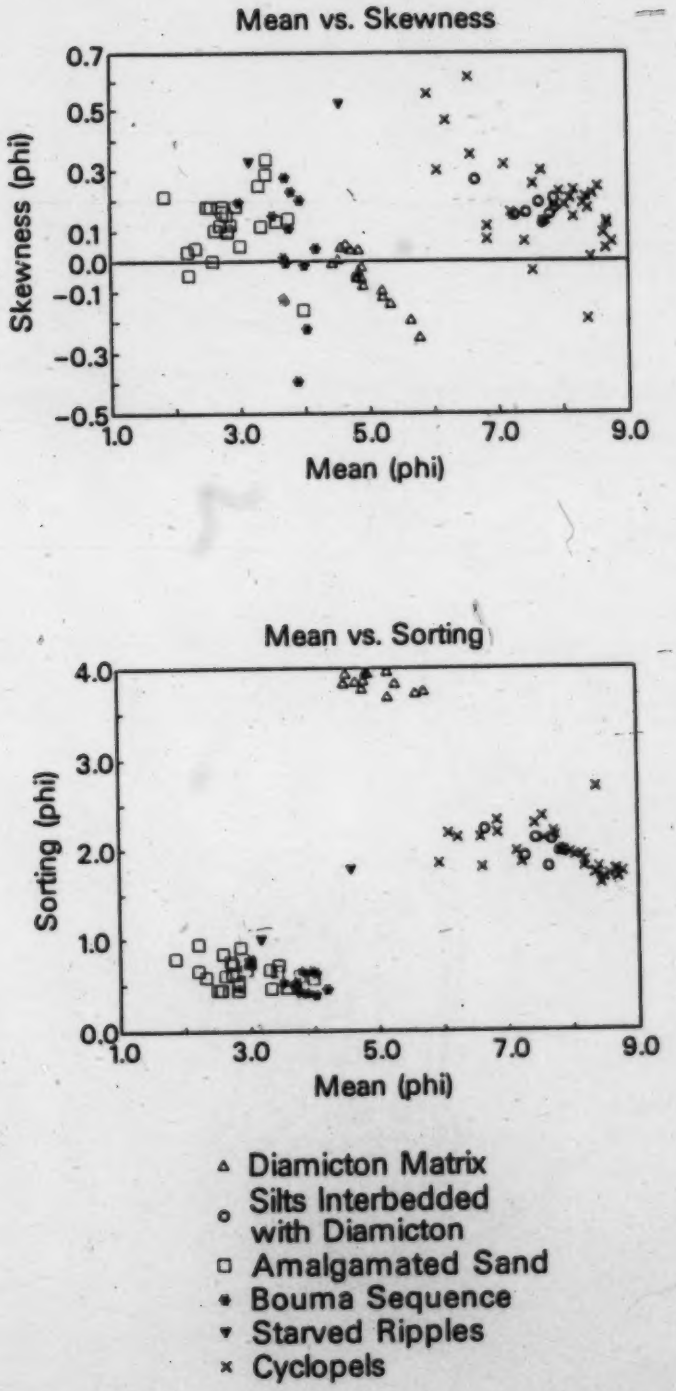

Figure III.20. Bivariate scatter plots for all grain-size samples.

INTERRELATIONSHIPS OF WATER-SEDIMENT INFLUX, TRANSPORT PATHS, AND FLOW TRANSFORMATIONS

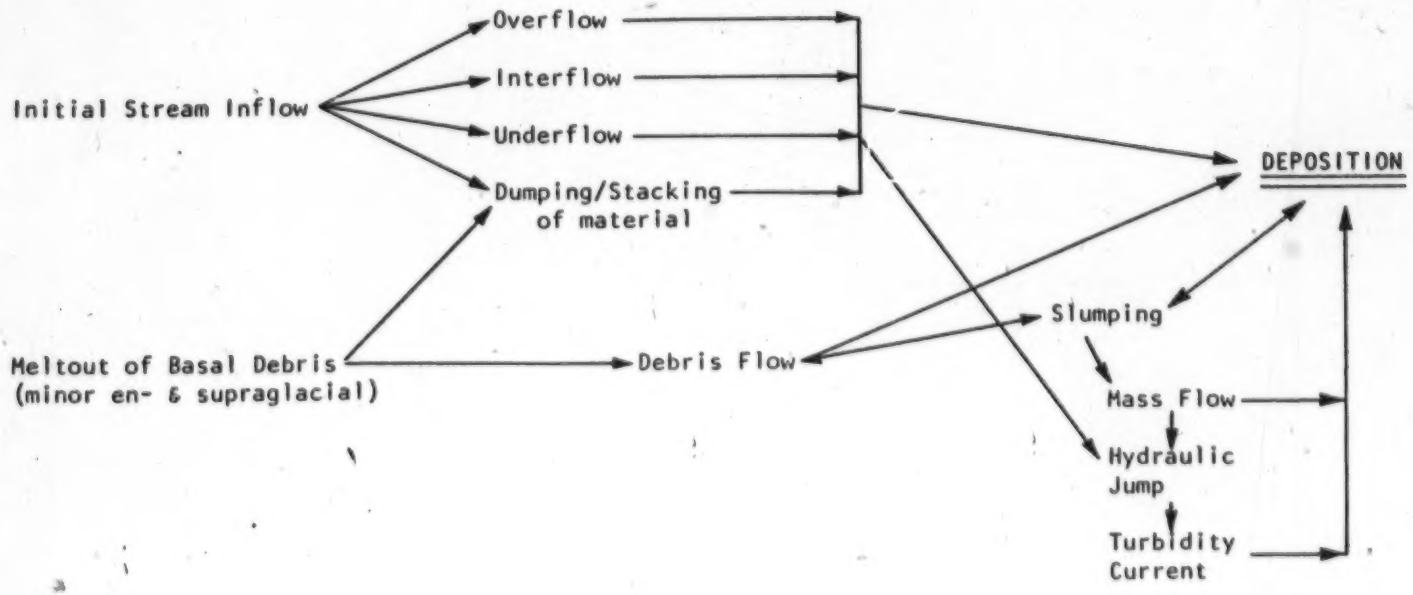

Figure III.21. Flow-sediment interrelationships.

Figure III.22. Channels observed in Clements Markham Inlet.

a) Sketch from photograph of section 18A, Chapter 2. Channels are developed within interchannel deposits of the fan flank. Also note how channel 2 crosscuts channel 1. Channel 3 is filled predominantly by cyclopels of LA V. Person and shovel for scale.

b) Large-scale channel, ca. 30 m by 5 m. LA II (gravel) and III (sand) are exposed on the right (north) and dip to the left. The channel is draped and filled by cyclopsams and then cyplopels. Left arrow points to 103 m delta lip; right arrow points to 101 m surface of cyclopel silts behind which the deltaic sediments infill (see Chapter 2).

c) Channel at section 16, Chapter 2 (outlined by arrows).

d) Channel in section 20. Note levee at upper left. Levee sediments in photograph e are to right of blue notebook (arrowed) where dark band terminates in the center of the photograph. Notebook is 20 x 26 cm.

e) LA IV levee sediments incised by a channel. This is the same channel margin as shown in photograph d. Ruler is 15 cm long.

f) Small, sandy channel incised into LA IV sediments of section 20. Note mud rip-up clasts at base and loaded horizons within channel.

g) Small channel in section 17. Note that it incises underlying laminae and that it's infill drapes it's margins. These laminae are subsequently cut by a larger channel to the right (arrowed). Shovel is 1.2 m.

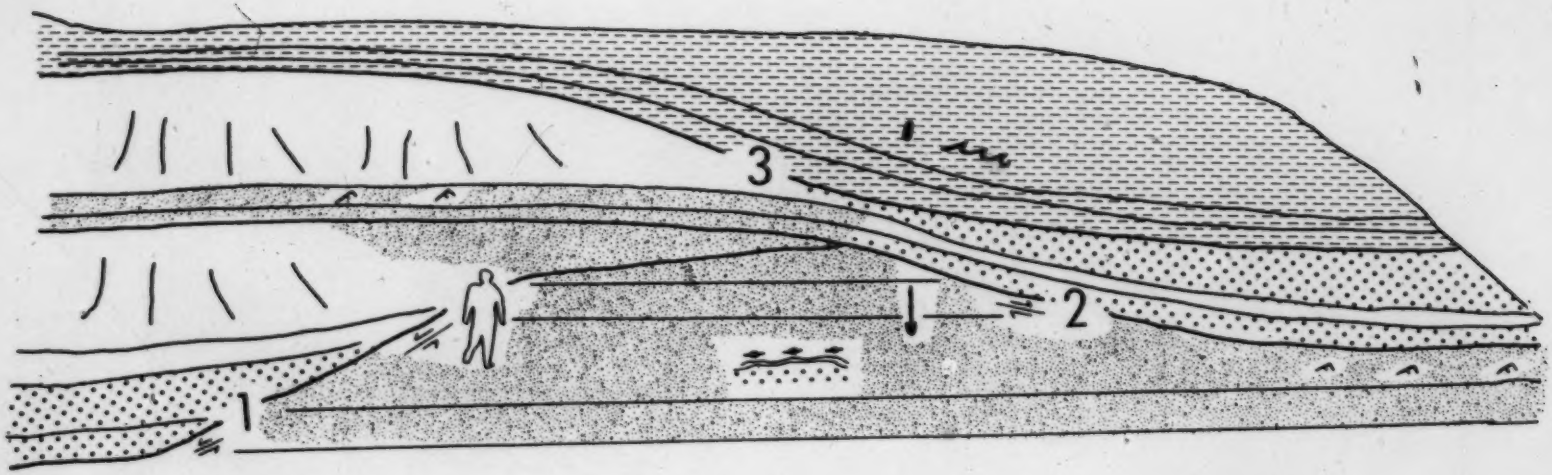

INTERCHANNEL DEPOSITS

COVERED

SILTS, LA Va,b

AMALGAMATED-GRADED SANDS, LA III

CLIMBING RIPPLES

STARVED RIPPLES

DRAPED LAMINATION

CONTORTED BEDDING

DROPSTONE

CHANNEL MARGIN ROTATIONAL SLUMP

CHANNEL MARGIN

a)

b)

c)

d)

e)

f)

g)

SUBAQUATIC OUTWASH FAN

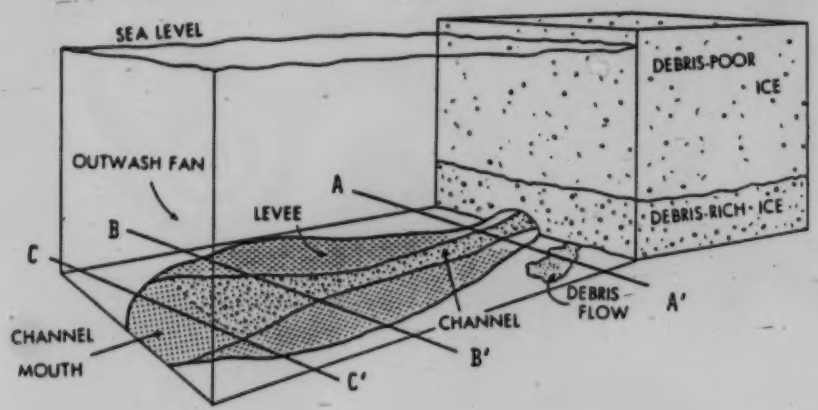

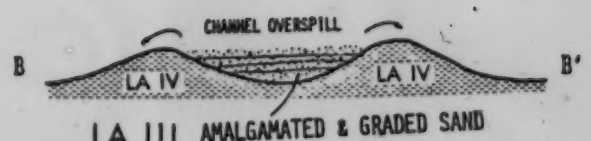

Figure III.23. Sketch of subaquatic outwash fan developed by exiting of a subglacial stream into marine water. Patterns on the fan differentiate topographic positions, not specific lithofacies associations. Cross sections A A' to C C' also show this topography with the appropriate lithofacies associations listed. Note the concentration of basal debris in the glacier that is characteristic of cold-based glaciers.

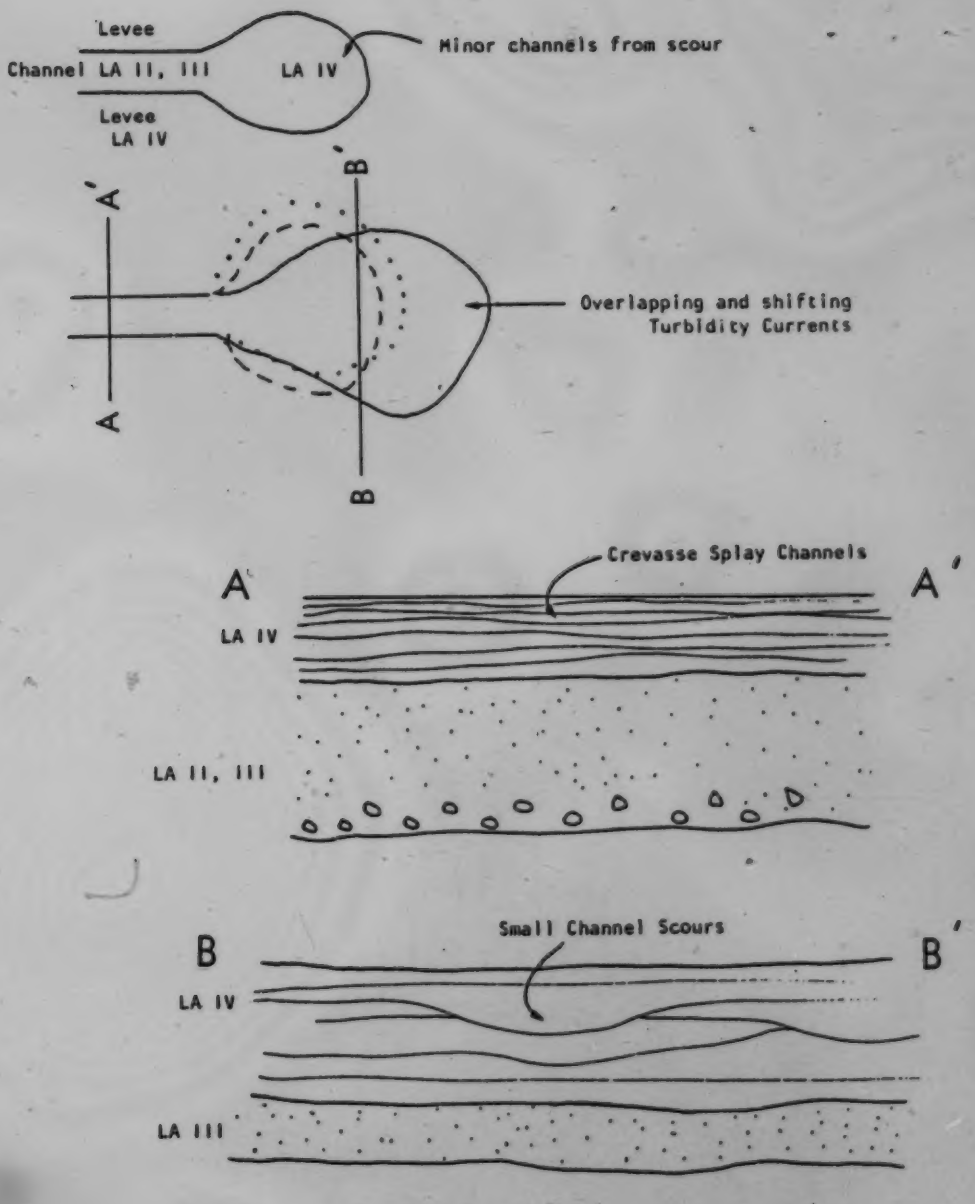

Figure III.24. Sketch showing the spreading and overlapping of turbidity currents. Positions of lithofacies associations are shown.

TURBID PLUME DEPOSITION

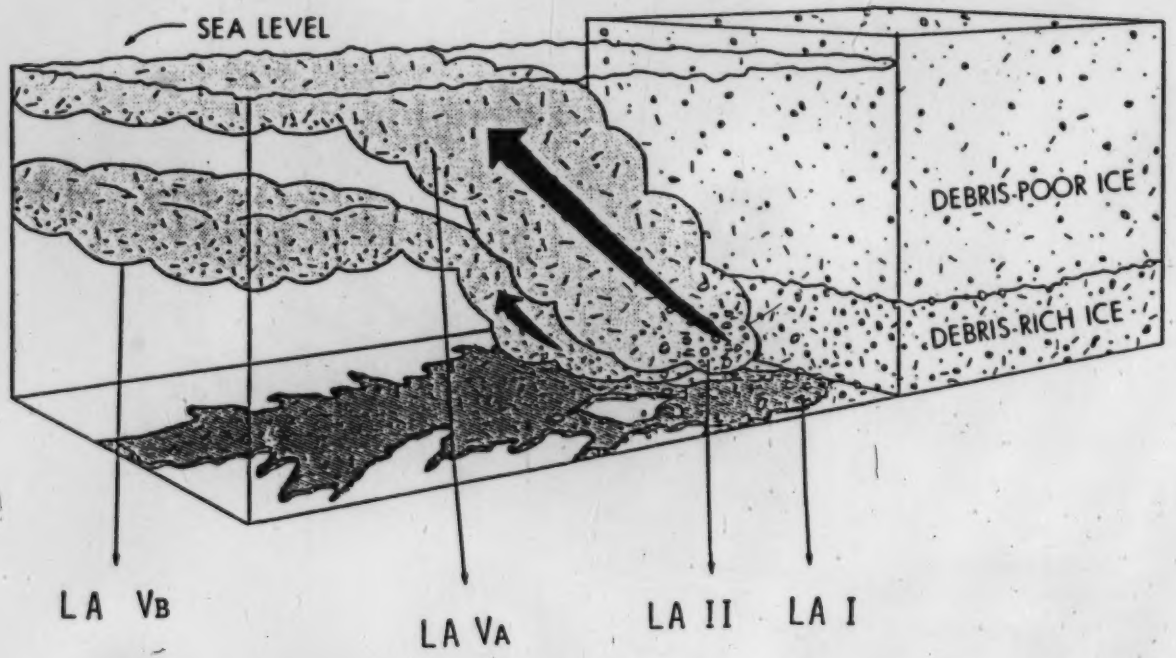

Figure III.25. Sketch of turbid overflow and interflow plumes developed by entrance of buoyant meltwater into marine water. Debris flows comprising LA I are derived predominantly from melting of the basal debris-rich ice.

BIBLIOGRAPHY

Akiyama, J. and Stefan, H. 1985. Turbidity current with erosion and deposition. Journal of Hydraulic Engineering, ASCE, 111, 1473-1496.

Akiyama, J. and Stefan, H. 1986. Prediction of turbidity currents in reservoirs and coastal regions. Third International Symposium on River Sedimentation, University of Mississippi, March 31-April 4, 1295-1305.

American Society for Testing and Materials. 1977. Standard method for particle size analysis of soils, designation D422-63. In 1977 Annual Book of ASTM standards, Philidelphia, American Society for Testing and Materials.

Ashley, G.M. 1975. Rhythmic sedimentation in glacial Lake Hitchcock, Massachusetts-Connecticut. in A.V. Jopling and B.C. McDonald, eds. Glaciofluvial and glaciolacustrine sedimentation, S.E.P.M. Special Publication No. 23, 304-320.

Ashley, G.M., Southard, J.B., and Boothroyd, J.C. 1982. Deposition of climbing-ripple beds: a flume simulation. Sedimentology, 29, 67-79.

American Society for Testing and Materials. 1977. Standard method for particle size analysis of soils, designation D422-63. In 1977 Annual book of ASTM standards. Philidelphia, American Society for Testing and Materials.

Banerjee, I. 1973a. Sedimentology of Pleistocene glacial varves in Ontario, Canada. Geological Survey of Canada Bulletin 226, Part A, 1-44.

Banerjee, I. 1973b. Nature of the grain-size distribution of some Pleistocene glacial varves of Ontario, Canada. Geological Survey of Canada Bulletin 226, Part B, 45-60.

Banerjee, I. 1977. Experimental study on the effect of deceleration on the vertical sequence of sedimentary structures in silty sediments. Journal of Sedimentary Petrology 47, 771-783.

Bartolini, C., Malesani, P.G., Manetti, P. and Wezel, F.C. 1975. Sedimentology and petrology of Quaternary sediments from the Hellenic Trench, Mediterranean ridge and Nile cone from D.S.D.P., Leg 13, cores. Sedimentology 22, 205-236.

Bednarski, J. 1984. Glacier fluctuations and sea level history of Clements Markham Inlet, northern Ellesmere Island. Unpub. Ph.D. thesis, University of Alberta, 232p.

Bednarski, J. 1986. Late Quaternary glacial and sea level events, Clements Markham Inlet, northern Ellesmere Island, Arctic Canada. Canadian Journal of Earth Sciences 23, 1343-1355.

Bednarski, J. in press. The geomorphology of raised marine sediments in a high arctic fiord. Geographie physique et Quaternaire.

Boulton, G.S. and Spring, U. 1986. Isotopic fractionation at the base of polar and sub-polar glaciers. Journal of Glaciology 32, 475-485.

Bouma, A.H. 1962. Sedimentology of some flysch deposits. Amsterdam, New York, Elsevier Publishing Company, 168p.

Bourgeois, J.C. 1986. A pollen record from the Agassiz Ice Cap, northern Ellesmere Island, Canada. Boreas 15, 345-354.

Bovis, M.J. and Barry, R.G. 1974. A climatological analysis of north polar desert areas. In, T.L. Smiley and J.H. Zumberge, eds., Polar deserts and man, 23-31.

Bradley, J.B. and McCutcheon, S.C. 1985. The effects of high sediment concentration on transport processes and flow phenomena. In, International Symposium on erosion, debris flow and disaster prevention, September 3-5, Tsukuba, Japan, 219-225.

Bradley, R.S. and England, J. 1978. Recent climatic fluctuations of the Canadian High Arctic and their significance for glaciology. Arctic and Alpine Research 10, 715-731.

Carey, D.L. and Roy, D.C. 1985. Deposition of laminated shale: a field and experimental study. Geo-Marine Letters 5, 3-9.

Chan, M.A. and Dott, R.H. Jr. 1983. Shelf and deep-sea sedimentation in Eocene forearc basin, western Oregon-fan or non-fan? American Association of Petroleum Geologists Bulletin, 67, 2100-2116.

Cheel, R.J. and Rust, B.R. 1982. Coarse grained facies of glacio-marine deposits near Ottawa, Canada. in R. Davidson-Arnott, W. Nickling and B.D. Fahey, eds. Research in glacial, glacio-fluvial, and glacio-lacustrine systems, 279-295.

Chough, S.K. and Hesse, R. 1980. The northwest Atlantic mid-ocean channel of the Labrador Sea: III. Head vs. body spill from turbidity currents on natural levees. Journal of Sedimentary Petrology, 50, 227-234.

Coniglio, M. 1986. Synsedimentary submarine slope failure and tectonic deformation in deep-water carbonates, Cow Head Group, western Newfoundland. Canadian Journal of Earth Sciences 23, 476-490.

Cook, H.E. 1979. Ancient continental slope sequences and their value in understanding modern slope development. in O.H. Pilkey and L.S. Doyle, eds. Geology of continental slopes. S.E.P.M. Special Publication No. 27, 287-305.

Cook, H.E., Field, M.E. and Gardner, J.V. 1982. Characteristics of sediments on modern and ancient continental slopes. in P.A. Scholle and D. Spearing, eds. Sandstone depositional environments, 329-364.

Cowan, E.A., Powell, R.D. and Smith, N.D. 1986. Effects of meltwater stream discharges and fjord water masses on sedimentary deposits at temperate tidewater glaciers. 12th International Sedimentological Congress, 24-30 August, Canberra, Australia, 70.

Domack, E.W. 1982. Facies of late Pleistocene glacial marine sediments on Whidbey Island, Washington. unpubl. Ph.D. thesis, Rice University, 312p.

Domack, E.W. 1983. Facies of late Pleistocene glacial-marine sediments on Whidbey Island, Washington: an isostatic glacial marine sequence. in B.F. Molnia, ed. Glacial-marine sedimentation, 535-570.

Domack, E.W. 1984. Rhythmically bedded glaciomarine sediments on Whidbey Island, Washington. Journal of Sedimentary Petrology, 54, 589-602.

Domack, E.W. and Lawson, D.E. 1985. Pebble fabric in an ice-rafted diamicton. Journal of Geology, 93, 577-591.

Dott, R.H. Jr. and Bird, K.J. 1979. Sand transport through channels across an Eocene shelf and slope in southwestern Oregon, U.S.A. S.E.P.M. Special Publication No. 27, 327-342.

Dowdeswell, J.A., Hambrey, M.J. and Wu, R. 1985. A comparison of clast fabric and shape in late Precambrian and modern glacigenic sediments. Journal of Sedimentary Petrology 55, 691-704.

Dowdeswell, J.A. and Sharp, M. 1986. Characterization of pebble fabrics in modern terrestrial environments. Sedimentology 33, 699-710.

Dreimanis, A. in press. Genetic classification of tills. in R.P. Goldthwait and C.L. Matsch, eds., Genetic classication of glacigenic deposits and their landforms.

Elmore, R.D., Pilkey, O.H., Cleary, W.J. and Curran, H.A. 1979. Black Shell turbidite, Hatteras Abyssal Plain, western Atlantic Ocean. Geological Society of America Bulletin, 90, 1165-1176.

Elverhoi, A., Liestol, O. and Nagy, J. 1980. Glacial erosion, sedimentation and microfauna in the inner part of Kongsfjorden, Spitsbergen. Norsk Polarinstitutt Skrifter No. 172, 33-58.

England, J. 1983. Isostatic adjustments in a full glacial sea. Canadian Journal of Earth Sciences, 20, 895-917.

England, J. 1985. The late Quaternary history of Hall Land, N.W. Greenland. Canadian Journal of Earth Sciences, 22, 1394-1408.

England, J. 1987. Glaciation and the evolution of the Canadian high arctic landscape. Geology 15, 419-424.

Eriksson, K.A. 1982. Geometry and internal characteristics of Archean submarine channel deposits, Pilbara Block, western Australia. Journal of Sedimentary Petrology, 52, 383-393.

Evans, D.J.A. and Lemmen, D.S. 1987. Indicators of Holocene climatic change from Wootton Peninsula/Phillips Inlet and Marvin Peninsula/Disraeli Fiord, northern Ellesmere Island. International Union for Quaternary Research, XII International Congress, Abstracts, 163.

Eyles, N., Clark, B.M. and Clague, J. 1987. Coarse-grained sediment gravity flows in a large supraglacial lake. Sedimentology 34, 193-216.

Eyles, C.H., Eyles, N. and Miall, A.D. 1985. Models of glaciomarine sedimentation and their application to the interpretation of ancient glacial sequences. Palaeogeography, Palaeoclimatology, Palaeoecology, 51, 15-84.

Eyles, N., Eyles, C.H. Miall, A.D. 1983. Lithofacies types and vertical profile models; an alternative approach to the description and environmental interpretation of glacial diamict and diamictite sequences. Sedimentology, 30, 393-410.

Folk, R.L. 1980. Petrology of sedimentary rocks. Austin, Texas: Hemphill Publishing Co., 182p.

Gawthorpe, R.L. and Clemmey, H. 1985. Geometry of submarine slides in the Bowland Basin (Dinantian) and their relation to debris flows. Journal of the Geological Society of London, 142, 555-565.

Gemmel, A.M.D., Sharp, M.J. and Sugden, D.E. 1986. Debris from the basal ice of the Agassiz Ice Cap, Ellesmere Island, Arctic Canada. Earth Surface Processes and Landforms 11, 123-130.

Gilbert, R. 1982. Contemporary sedimentary environments of Baffin Island, N.W.T., Canada: glaciomarine processes in fiords of eastern Cumberland Peninsula. Arctic and Alpine Research, 14, 1-12.

Gilbert, R. 1983. Sedimentary processes of Canadian Arctic fjords. Sedimentary Geology, 36, 147-175.

Gravenor, C.P. 1980. Heavy minerals and sedimentological studies on the glaciogenic late Precambrian Gaskiers Formation of Newfoundland. Canadian Journal of Earth Sciences 17, 1331-1341.

Gravenor, C.P., Von Brunn, V. and Dreimanis, A. 1984. Nature and classification of waterlain glacigenic sediments, exemplified by Pleistocene, late Paleozoic and Precambrian deposits. Earth-Science Reviews 20, 105-166.

Gustavson, T.C., Ashley, G.M. and Boothroyd, J.C. 1975. Depositional sequences in glaciolacustrine deltas. in A.V. Jopling and B.C. McDonald, eds., Glaciofluvial and glaciolacustrine sedimentation. SEPM Special Publication No. 23, 264-280.

Hattersley-Smith, G. 1960. Some remarks on glaciers and climate in northern Ellesmere Island. Geografiska Annaler 42, 45-48.

Hay, A.E., Murray, J.W., and Burling, R.W. 1983. Submarine channels in Rupert Inlet, Bristish Columbia, II, Sediments and sedimentary structures. Sedimentary Geology 36, 317-339.

Hein, F.J. 1982. Depositional mechanisms of deep-sea coarse clastic sediments, Cap Enrage Formation, Quebec. Canadian Journal of Earth Sciences, 19, 267-287.

Hesse, R. and Chough, S.K. 1980. The northwest Atlantic mid-ocean channel of the Labrador Sea: II. Deposition of parallel laminated levee-muds from the viscous sublayer of low density turbidity currents. Sedimentology, 27,m 697-711.

Hesse, R., Chough, S.K. and Rakofsky, A. 1987. The northwest Atlantic mid-ocean channel of the Labrador Sea. V. Sedimentology of a giant deep-sea channel. Canadian Journal of Earth Sciences 24, 1595-1624.

Hicock, S.R., Dreimanis, A. and Broster, B.E. 1981. Submarine flow tills at Victoria, British Columbia. Canadian Journal of Earth Sciences 18, 71-80.

Hill, P.R., Aksu, A.E. and Piper, D.J.W. 1982. The deposition of thin bedded subaqueous debris flow deposits. in S. Saxov & J.K. Nieuwenhuis, eds., Marine slides and other mass movements, 273-287.

Hiscott, R.N. 1980. Depositional framework of sandy mid-fan complexes of the Tourelle Formation, Ordivician, Quebec. Bulletin of the American Association of Petroleum Geologists 64, 1052-1077.

Hodgson, D.A. 1985. The last glaciation of west-central Ellesmere Island, Arctic Archipelago, Canada. Canadian Journal of Earth Sciences, 22, 347-368.

Hoskin, C.M., Burrell, D.C. and Freitag, G.K. 1978. Suspended sediment dynamics in Blue Fjord, western Prince William Sound, Alaska. Estuarine and Coastal Marine Science 7, 1-16.

Howell, D.G. and Normark, W.R. 1982. Sedimentology of submarine fans. in P.A. Scholle and D. Spearing, eds. Sandstone depositional environments, 365-404.

Iken, A. 1977. Variations of surface velocities of some alpine glaciers measured at intervals of a few hours. Comparison with arctic glaciers. Zeitschrift fur Gletscherkunde und Glazialgeologie 13, 23-35.

Ingram, R.L. 1954. Terminology for the thickness of stratification and parting units in sedimentary rocks. Bulletin of the Geological Society of America 65, 937-938.

Johnson, W.H., Hansel, A.K., Socha, B.J., Follmer, L.R. and Masters, J.M. 1985. Depositional environments and correlation problems of the Wedron Formation (Wisconsinan) in northeastern Illinois. Illinois State Geological Survey Guidebook 16, 91p.

Jopling, A.V. and Walker, R.G. 1968. Morphology and origin of ripple-drift cross-lamination, with examples from the Pleistocene of Massachusetts. Journal of Sedimentary Petrology 38, 971-984.

Jorgensen, N.B. 1982. Turbidites and associated resedimented deposits from a tilted glacio-deltaic sequence, Denmark. Geological Survey of Denmark, Yearbook 1981, 47-72.

Koerner, R.M., Fisher, D.A. and Paterson, W.S.B. 1987. Wisconsinan and pre-Wisconsinan ice thicknesses on Ellesmere Island, Canada: inferences from ice cores. Canadian Journal of Earth Sciences 24, 296-301.

Komar, P.D. 1972. Relative influence of head and body spill from a channelized turbidity current. Geological Society of America Bulletin, 83, 1151-1156.

Komar, P. 1985. The hydraulic interpretation of turbidites from their grain sizes and sedimentary structures. Sedimentology, 32, 395-407.

Kuenen, P.H. and Humbert, F.L. 1969. Grain size of turbidite ripples. Sedimentology, 13, 253-261.

Kurtz, D.B. and Anderson, J.B. 1979. Recognition and sedimentologic description of recent debris flow deposits from the Ross and Weddell Seas, Antarctica. Journal of Sedimentary Petrology 49, 1159-1170.

LaFarge-England, C. 1988. The contemporary and Holocene moss assemblages of a high arctic plateau, southern Piper Pass, northern Ellesmere Island, N.W.T., Canada. Unpubl. M.Sc. thesis, University of Alberta, Edmonton.

Lake, R.A. and Walker, E.R. 1976. A Canadian arctic fjord with some comparisons to fjords of the western Americas. Journal of the Fisheries Research Board of Canada 33, 2272-2285.

Larue, D.K. and Speed, R.C. 1983. Quartzose turbidites of the accretionary complex of Barbados, I: Chalky Mount succession. Journal of Sedimentary Petrology, 53, 1337-1352.

Lawson, D.E. 1979. A comparison of the pebble orientations in ice and deposits of the Matanuska Glacier, Alaska. Journal of Geology, 87, 629-645.

Leckie, D.A. and McCann, S.B. 1982. Glacio-lacustrine sedimentation on low slope prograding delta. in R. Davidson-Arnot, W. Nickling and B.D. Fahey, eds. Research in Glacial, glacio-fluvial, and glacio-lacustrine systems, 261-278.

Link, M.H. and Welton, J.E. 1982. Sedimentology and reservior potential of Matilija Sandstone: an Eocene sand-rich deep-sea fan and shallow marine complex, California. American Association of Petroleum Geologists Bulletin, 66, 1514-1534.

Lowe, D.R. 1982. Sediment gravity flows: II. Depositional models with special reference to the deposits of high-density turbidity currents. Journal of Sedimentary Petrology 52, 279-297.

Lowe, D.R. and Lopiccolo, R.D. 1974. The characteristics and origins of dish and pillar structures. Journal of Sedimentary Petrology 44, 484-501.

Mackiewicz, N.E., Powell, R.D., Carlson, P.R., and Molnia, B.F. 1984. Interlaminated ice-proximal glacimarine sediments in Muir Inlet, Alaska. Marine Geology, 57, 113-147.

Major, J.J. and Voight, B. 1986. Sedimentology and clast orientations of the 18 May 1980 southwest-flank lahars, Mount St. Helens, Washington. Journal of Sedimentary Petrology 56, 691-705.

Maxworthy, T. 1983. Gravity currents with variable inflow. Journal of Fluid Mechanics 128, 247-257.

McBride, E.F., Shepherd, R.G. and Crawley, R.A. 1975. Origin of parallel, near horizontal laminae by migration of bed forms in a sall flume. Journal of Sedimentary Petrology 45, 132-139.

McCabe, A.M. 1986. Glaciomarine facies deposited by retreating tidewater glaciers: an example from the late Pleistocene of Northern Ireland. Journal of Sedimentary Petrology 56, 880-894.

McCabe, A.M., Dardis, G.F. and Hanvey, P.M. 1984. Sedimentology of a late Pleistocene submarine-moraine complex, County Down, Northern Ireland. Journal of Sedimentary Petrology 54, 716-730.

Middleton, G.V. 1967. Experiments on density and turbidity currents III. Deposition of sediment. Canadian Journal of Earth Sciences, 4, 475-505.

Mills, H.H. 1984. Clast orientation in Mt. St. Helens debris-flow deposits North Fork Toutle River, Washington. Journal of Sedimentary Petrology, 54, 626-634.

Mode, W.N., Nelson, A.R. and Brigham, J.R. 1983. A facies model of Quaternary glacial-marine cyclic sedimentation along eastern Baffin Island, Canada. in, B.F. Molnia, ed., Glacial-marine sedimentation, 495-533.

Muller, F. 1976. On the thermal regime of a high-arctic valley glacier. Journal of Glaciology 16, 119-133.

Muller, F. and Iken, A. 1973. Velocity fluctuations and water regime of arctic valley glaciers. Symposium on the hydrology of glaciers, International Association of Scientific Hydrology Publication no. 95, 165-182.

kMutti, E. 1977. Distinctive thin-bedded turbidite facies and related depositional environments in the Eocene Hecho Group (south-central Pyrenees, Spain). Sedimentology, 24, 107-131.

Nardin, T.R., Hein, F.J., Gorsline, D.S. and Edwards, B.D. 1979. A review of mass movement processes, sediments and acoustic characteristics and contrasts in slope and base-of-slope systems, versus canyon-fan-basin floor systems. In, L.J. Doyle and O.H. Pilkey, eds., Geology of Continental Slopes, S.E.P.M. Special Publication 27, 61-73.

Nemec, W. and Steel, R.J. 1984. Alluvial and coastal conglomerates: their significant features and some comments on gravelly mass-flow deposits. in E.H. Koster and R.J. Steel, eds., Sedimentology of gravels and conglomerates, 1-31.

Ocean Drilling Program National Workshop. 1986. Conference held in Montreal, Quebec, December.

Pickering, K.T. 1979. Possible retrogressive flow slide deposits from the Kongsfjord Formation: a Precambrian submarine fan, Finnmark, N. Norway. Sedimentology 26, 295-306.

Pickering, K.T. 1981. Two types of outer fan lobe sequence, from the late Precambrian Kongsfjord Formation submarine fan, Finnmark, north Norway. Journal of Sedimentary Petrology, 51, 1277-1286.

Pickering, K.T. 1982. Middle-fan deposits from the late Precambrian Kongsfjord Formation submarine fan, northwest Finnmark, northern Norway. Sedimentary Geology, 33, 79-110.

Pickering, K.T. 1983. Transitional submarine fan deposits from the late Precambrian Kongsfjord Formation submarine fan, NE Finnmark, N. Norway. Sedimentology, 30, 181-199.

Pickering, K., Stow, D., Watson, M. and Hiscott, R. 1986. Deep-water facies, processes and models: a review and classification scheme for modern and ancient sediments. Earth-Science Reviews 23, 75-174.

Pierson, T.C. 1985. Effects of slurry concentration on debris flow dynamics, Rudd Canyon, Utah. In, D.S. Bowles, ed., Delineation of landslide, flash flood, and debris flow hazards in Utah, Utah Water Research Laboratory General Series UWRL/G-85/03, 132-152.

Pierson, T.C. and Scott, K.M. 1985. Downstream dilution of a lahar: transition from debris flow to hyperconcentrated streamflow. Water Resources Research 21, 1511-1524.

Piper, D.J.W. 1978. Turbidite muds and silts on deep sea fans and abyssal plains. in D.J. Stanley and G. Kelling, eds. Sedimentation in submarine canyons, fans and trenches, 163-176.

Postma, G., Roep, T.B. and Ruegg, G.H.J. 1983. Sandy-gravelly mass-flow deposits in an ice-marginal lake (Saalian, Leuvenumsche Beek Valley, Veluwe, The Netherlands), with emphasis on plug-flow deposits. Sedimentary Geology, 34, 59-82.

Powell, R.D. 1980. Holocene glacimarine sediment deposition by tidewater glaciers in Glacier Bay, Alaska. Unpub. Ph.D. thesis, Ohio State University, 420p.

Powell, R.D. 1981. A model for sedimentation by tidewater glaciers. Annals of Glaciology, 2, 129-134.

Powell, R.D. 1983a. Glacial-marine sedimentation processes and lithofacies of temperate tidewater glaciers, Glacier Bay,

Alaska. in B.F. Molnia, ed. Glacial-marine sedimentation, 185-232.

Powell, R.D. 1983b. Submarine flow tills at Victoria, British Columbia: Discussion. Canadian Journal of Earth Sciences 20, 509-510.

Powell, R.D. 1984. Glacimarine processes and inductive lithofacies modelling of ice shelf and tidewater glacier sediments based on Quaternary examples. Marine Geology 57, 1-52.

Powell, R.D. and Cowan, E.A. 1986. Depositional processes at McBride Inlet and Riggs Glacier. in P.J. Anderson, R.P. Goldthwait, G.D. McKenzie, eds., Observed Processes of Glacial Deposition in Glacier Bay, Alaska. Ohio State University, Institute of Polar Studies Miscellaneous Publication No. 236, 140-156.

Rupke, N.A. 1976. Sedimentology of very thick calcarenite-marlstone beds in a flysch succession, southwestern Pyrenees. Sedimentology 23, 43-65.

Rust, B.R. 1977. Mass flow deposits in a Quaternary succession near Ottawa, Canada: diagnostic criteria for subaqueous outwash. Canadian Journal of Earth Sciences, 14, 175-184.

Rust, B.R. and Romanelli, R. 1975. Late Quaternary subaqueous outwash deposits near Ottawa, Canada. in A.V. Jopling and B.C. McDonald, eds. Glaciofluvial and glaciolacustrine sedimentation, S.E.P.M. Special Publication No. 23, 177-192.

Sadler, H.E. 1976. Water, heat and salt transports through Nares Strait, Ellesmere Island. Journal of the Fisheries Research Board of Canada 33, 2286-2295.

Saunderson, H.C. 1977. Grain size characteristics of sands from the Brampton esker. Zeitschrift fur Geomorphologie 21, 44-56.

Seramur, K.C. and Powell, R.D. 1987. Temperate glacimarine lithofacies interpreted from seismic facies. International Quaternary Association, Abstracts, July 31 to August 9.

Shanmugam, G., Damuth, J.E. and Moiola, R.J. 1985. Is the turbidite facies association scheme valid for interpreting ancient submarine fan environments? Geology, 13, 234-237.

Shaw, J. 1977. Tills deposited in arid polar environments. Canadian Journal of Earth Sciences 14, 1239-1245.

Shaw, J. 1982. Melt-out till in the Edmonton area, Alberta, Canada. Canadian Journal of Earth Sciences, 19, 1548-1569.

Shaw, J. and Archer, J. 1978. Winter turbidity current deposits in Late Pleistocene glaciolacustrine varves, Okanagan Valley, British Columbia, Canada. Boreas, 7, 123-130.

Smith, G.A. 1986. Coarse-grained non-marine volcaniclastic sediment: terminology and depositional process. Geological Society of America Bulletin 97, 1-10.

Smith, G.A. 1987. The influence of explosive volcanism on fluvial sedimentation: the Deschutes Formation (Neogene) in central Oregon. Journal of Sedimentary Petrology 57, 613-629.

Sollid, J.-L. and Reite, A.J. 1983. The last glaciation and deglaciation of central Norway. in J. Ehlers, ed., Glacial deposits of northwest Europe, 41-59.

Stewart, T.G. 1981. The Holocene paleoenvironment of Clements s Markham Inlet, northern Ellesmere Island, N.W.T., Canada. unpub. M.Sc. thesis, University of Alberta, Edmonton, 135p

Stewart, T.G. and England, J. 1983. Holocene sea-ice variations and paleoenvironmental change, northernmost Ellesmere Island, N.W.T., Canada. Arctic and Alpine Research, 15, 1-17.

Stewart, T.G. and Bednarski, J. 1986 (abs.). Basal crevasses and folded foliation along the margin of a subpolar glacier. American Quaternary Association, Program and Abstracts, 9th Biennial Meeting, 2-4 June, Champaign-Urbana, Illinois, 105.

Stewart, T.G. and England, J. 1986. An early Holocene caribou antler from northern Ellesmere Island, Canadian Arctic Archipelago. Boreas, 15, 25-31.

Stow, D.A.V. and Bowen, A.J. 1980. A physical model for the transport and sorting of fine-grained sediment by turbidity currents. Sedimentology 27, 31-46.

Stow, D.A.V. and Shanmugam, G. 1980. Sequence of structures in fine-grained turbidites: comparison of recent deep-sea and ancient flysch sediments. Sedimentary Geology, 25, 23-42.

Stow, D.A.V. and Piper, D.J.W. 1984a. Deep-water fine-grained sediments: facies models. in D.A.V. Stow and D.J.W. Piper, eds. Fine-grained sediments: deep water processes and facies, 611-546.

Stow, D.A.V. and Piper, D.J.W. 1984b. Deep-water fine-grained sediments; history, methodology and terminology. in D.A.V. Stow and D.J.W. Piper, eds. Fine-grained sediments: deep-water processes and facies, 3-14.

Sturm, M. and Matter, A. 1978. Turbidites and varves in Lake Brienz (Switzerland): deposition of clastic detritus by density currents. Special Publication International Association of Sedimentologists, 2, 147-168.

Sugden, D.L. et al. 1987. Evidence for two zones of debris entrainment beneath the Greenland ice sheet. Nature 328, 238-241.

Syvitski, J.P.M. and Murray, J.W. 1981. Particle interaction in fjord suspended sediment. Marine Geology 39, 215-242.

Syvitski, J.P.M., Asprey, K.W., Clattenburg, D.A. and Hodge, G.D. 1985. The prodelta environment of a fjord: suspended particle dynamics. Sedimentology 32, 83-107.

Taylor, R.B. and Frobel, D. 1984. Coastal surveys of Jones Sound, District of Franklin. Geological Survey of Canada, Paper 84-1B, 25-32.

Thomas, G.S.P. and Connell, R.J. 1985. Iceberg drop, dump, and grounding structures from Pleistocene glacio-lacustrine sediments. Journal of Sedimentary Petrology, 55, 243-249.

Walker, R.G. 1967. Turbidite sedimentary structures and their relationship to proximal and distal depositional environments. Journal of Sedimentary Petrology 37, 25-43.

Walker, R.G. 1975. Generalized facies models for resedimented conglomerates of turbidite association. Geological Society of America Bulletin 86, 737-748.

Walker, R.G. 1977. Deposition of upper Mesozoic resedimented conglomerates and associated turbidites in southwestern Oregon. Geological Society of America Bulletin 88, 273-285.

Walker, R.G. 1978. Deep-water sandstone facies and ancient submarine fans: models for exploration of stratigraphic traps. American Association of Petroleum Geologists Bulletin 62, 932-966.

Walker, R.G. 1985. Mudstones and thin-bedded turbidites associated with the Upper Cretaceous Wheeler Gorge Conglomerates, California: a possible channel-levee complex. Journal of Sedimentary Petrology, 55, 279-290.

Wan, Z. 1985. Bed material movement in hyperconcentrated flow. Journal of Hydraulic Engineering (ASCE) 111, 987-1002.

Warren, G. 1974. Simplified form of the Folk-Ward skewness parameter. Journal of Sedimentary Petrology, 44, 259.

Winn, R.D. Jr. and Dott, R.H. Jr. 1977. Large-scale traction-produced structures in deep-water fan-channel conglomerates in southern Chile. Geology 5, 410-414.

IV. CONCLUSIONS

Much Quaternary research in arctic Canada and Greenland uses the level and gradients of marine limits and related raised shorelines to decipher glacial history (Andrews 1970; Dyke 1979, 1983; Bednarski 1986; England 1987). Considering the scale of this region these studies are effectively reconnaissance in nature. The stratigraphy and sedimentology of the marine sediments related to these former high sea levels are now an increasing focus of attention (e.g. Andrews 1985; Retelle 1986; Bednarski in press). This study documents the stratigraphy and sedimentology of six lithofacies associations ranging from diamictons to subaquatic outwash fan deposits to turbid plume deposits. These can serve as a framework for further investigations on the extent and characteristics of past glaciations in high latitudes.

A recurring theme in reconstructing the ice limits of the high latitudes is the concept that the region's cold-based glaciers can occupy and retreat from an area without leaving any recognizeable assemblage of landforms and sediments (Sugden and Watts 1977; Denton and Hughes 1981). This concept is not supported by this study and indicates that invoking expansive glaciations without firm geologic evidence for the presence of glaciers is inappropriate. The information provided in this study emphasizes the need for understanding glaciomarine sedimentation and its relationship to past ice positions.

The former ice margins at the head of Clements Markham Inlet are amply delineated by a thick blanket of sediments. Within

these sediments there are major suites of diamictons, channels and related channel fills, and particularly large volumes of rhythmites which are all ice proximal deposits. Not only are the sediments distinctive, but the overall package is relatively contained and does not drape the fiord sides for more than a few km in the vicinity of the former margin. This relationship may not hold in large unconstrained interisland channels but it is well illustrated throughout Ellesmere Island within the fiord systems. The correspondence of large sediment volumes to the former ice margin should directly aid Quaternary mappers. For example, Hodgson (1985) maps extensive glaciomarine sediments at the heads of a variety of fiords on central Ellesmere Island. Despite these imposing sediment volumes he proposes two contrasting models. The first recongnizes that the sediment may mark the last ice limit. However, the second proposes that ice retreated some hundred kms up the major fiord systems. Considering the evidence presented in the present study, the likelihood that this ice left no depositional record of its presence is highly improbable.

The abundance of subaquatic outwash, cyclopsams and cyclopels in Clements Markham Inlet indicates a marine deglacial environment dominated by meltwater influx. Additionally, it necessitates that this glacial meltwater reached the bed of the glaciers to remove the debris that was entrained there. This is in direct contrast to present conditions where glacial meltwater is restricted to the ice surface and margins. Therefore, climatic conditions during deglaciation were dramatically warmer than at

present or those that existed during full glacial times.

BIBLIOGRAPHY

Andrews, J.T. 1970. A geomorphological study of postglacial uplift with particular reference to arctic Canada. Institute of British Geographers Special Publication No. 2, 156p.

Andrews, J.T. 1985. Grain-size characteristics of Quaternary sediments, Baffin Island region. In, J.T. Andrews, ed., Quaternary environments-eastern Canadian arctic, western Greenland and Baffin Bay, 124-153.

Bednarski, J. in press. The geomorphology of glaciomarine sediments in a high arctic fiord. Geographie physique et Quaternaire.

Denton, G.H. and Hughes, T.J., eds., 1981. The last great ice sheets. New York, John Wiley & Sons, 484p.

Dyke, A.S. 1979. Glacial and sea-level history of southwestern Cumberland Peninsula, Baffin Island, N.W.T., Canada. Arctic and Alpine Research 11, 179-202.

Dyke, A.S. 1983. Quaternary geology of Somerset Island, District of Franklin. Geological Survey of Canada, Memior 404, 32p.

England, J. 1987. Glaciation and the evolution of the Canadian high arctic landscape. Geology 15, 419-424.

Hodgson, D.A. 1985. The last glaciation of west-central Ellesmere Island, Arctic Archipelago, Canada. Canadian Journal of Earth Sciences 22, 347-368.

Retelle, M.J. 1986. Stratigraphy and sedimentology of coastal lacustrine basins, northeastern Ellesmere Island, N.W.T. Geographie physique et Quaternaire 40, 117-128.

Sugden, D.E. and Watts, S.H. 1977. Tors, felsenmeer, and glaciation in northern Cumberland Peninsula, Baffin Island, Canada. Canadian Journal of Earth Sciences 14, 2817-2823.

Appendix I

Sample #	C(phi)	microns	5phi	16phi	25phi	50phi	microns	75phi	84phi	95phi	Mean	SD	Skew.	Kurt.	%Sand	%Silt	%Clay	Description
Si/D																		
7; 83-55	4.00	62.50	4.30	5.50	6.00	7.10	7.30	8.30	9.20	11.00	7.27	1.94	0.15	1.19	2.40	66.60	31.00	Sec. 13, bk VI p. 9, 15-22cm below upper fabric
10; 83-20	3.50	88.00	4.60	5.20	5.70	7.20	6.80	8.90	9.90	10.90	7.43	2.13	0.16	0.81	1.50	63.50	35.00	Sec. 14, sta 13, bk V(96), silts drape over till
38; 83-1	3.00	125.00	4.00	4.40	4.80	6.30	12.70	8.25	9.25	10.75	6.65	2.24	0.27	0.80	4.50	66.50	29.00	Sec 14, IV 57, 20cm si, blocky subhorizon. joints, v. dam
75; 82-77	4.30	51.00	5.30	5.80	6.40	7.65	5.00	9.30	10.20	11.10	7.88	1.98	0.17	0.82	0.60	55.40	44.00	Sec 13, IV 34, 186 32-34, si overlying cobble
76; 83-6	2.20	218.00	4.20	5.65	6.20	7.40	5.90	8.90	10.00	11.00	7.68	2.12	0.13	1.03	4.50	57.50	38.00	Sec 13, V 63-64, 210 4-6, basal 5cm of si horizon (around cobble?)
77; 83-22A	0.80	570.00	4.90	5.90	6.35	7.50	5.50	9.00	10.20	11.10	7.87	2.01	0.21	0.96	2.40	58.60	39.00	Sec 14, V 82&99, sta 6.5, 211 4-6, si 1 shovel over fabrics
81; 83-23	4.00	62.50	4.90	5.80	6.30	7.55	5.30	9.00	10.05	11.00	7.80	1.99	0.15	0.93	1.50	56.50	42.00	Sec 14, V 82&99, 211 4-6?, si 30cm thick
83; 83-8	4.35	49.00	5.10	5.85	6.15	7.40	5.90	8.70	9.65	10.85	7.63	1.82	0.19	0.92	0.70	60.30	39.00	Sec 14, V 72, v 80, 30cm to left of yellow pebble, 10-20 above si
Cyclopel																		
11; 82-25	5.45	23.00	5.60	6.00	6.50	7.80	4.50	9.70	10.30	11.20	8.03	1.92	0.19	0.72	0.02	54.00	46.00	Sec 8, Arrowhead trace fossils, 16985-14, BN 142
12; 82-44	5.50	22.00	5.75	6.30	6.75	7.85	4.20	9.80	10.40	11.20	8.18	1.85	0.24	0.73	0.06	54.00	46.00	Area distal to 103m delta, BN 153,
13; 82-45	6.10	14.60	6.50	6.90	7.30	8.55	2.70	10.20	10.60	11.40	8.68	1.67	0.14	0.69	0.28	42.00	58.00	Area distal to 103m delta, 171 20-24
82; 83-74	5.00	31.00	5.20	5.80	6.10	7.60	5.20	9.40	10.20	11.10	7.87	1.99	0.18	0.73	0.35	55.00	45.00	" " VI 47, 217 26-28, v. 75&76, 3° on ruler, loaded by 83-75
17; 82-24	6.00	15.60	6.20	6.55	6.90	8.10	3.65	9.80	10.40	11.20	8.35	1.72	0.22	0.71	0.40	49.00	51.00	Sec 8, Arrowhead trace fossils, BN 142
22; 81-45	5.60	20.60	5.90	6.20	6.70	8.00	3.90	9.70	10.30	11.00	8.17	1.80	0.15	0.70	0.02	50.00	50.00	Area distal to 103m delta, Lone Thyasira, bn 107
23; 82-21	6.10	14.60	6.30	6.90	7.30	8.70	2.40	10.30	10.70	11.50	8.77	1.74	0.06	0.71	0.30	38.00	62.00	Sec 6, .5m above 168 3-36, bn 141
24; 82-20	5.50	22.00	5.70	6.10	6.50	7.85	4.30	10.00	10.40	11.30	8.12	1.92	0.21	0.66	0.30	52.00	48.00	Sec 6, 168 29, bn 140
25; 81-21	6.45	11.40	6.25	6.75	7.20	8.55	2.70	10.30	10.60	11.50	8.63	1.76	0.09	0.69	0.40	40.00	60.00	Sec 6, 146 25-26, bn 48, base of section
26; 81-20	4.90	33.50	5.00	5.50	5.80	7.20	6.80	9.70	10.40	11.30	7.70	2.18	0.30	0.66	0.10	60.00	40.00	Sec 5, immediately above till
30; 81-16	4.60	41.00	5.80	6.80	7.20	8.40	3.00	9.70	10.10	11.00	8.43	1.61	0.02	0.85	0.30	42.00	58.00	Sec 2, barren silts
31; 81-14	-0.90	1900.00	0.50	6.35	6.85	8.30	3.20	10.10	10.50	11.30	8.38	2.67	-0.19	1.36	13.00	32.00	55.00	Sec 2, bn 37, bimodal?, dispersed granules
32; 81-38	6.25	13.20	6.40	6.80	7.20	8.25	3.30	10.20	10.60	11.40	8.55	1.71	0.25	0.68	0.02	43.00	57.00	Sec 3, bn 90, 14" above last s.
33; 81-35	5.80	18.00	6.15	6.50	7.10	8.20	3.40	10.10	10.50	11.30	8.40	1.78	0.18	0.70	0.42	45.60	54.00	Sec 1, bn 90, silt, same as oriented slab
55A; 82-42	4.20	54.40	4.50	5.00	5.40	6.25	13.20	7.65	8.55	10.50	6.60	1.80	0.36	1.09	1.00	78.00	21.00	Sec 4, bn 150, 171 8&9, barren silt?
35; 82-84	3.50	88.00	4.00	4.30	4.40	5.60	20.60	7.60	8.75	10.70	6.22	2.13	0.47	0.86	5.00	73.00	22.00	Sec 22, IV 65, 188 38, 4cm above ruler, graded s/si/cl
36; 82-89	3.80	72.00	4.10	4.40	4.55	5.30	25.40	7.10	8.10	10.20	5.93	1.85	0.56	0.98	2.00	81.00	17.00	Sec 22, IV 66, 189 90, v. 82-90, upper section
37; 82-90	4.25	53.00	4.65	5.40	5.90	7.05	7.50	8.40	9.15	10.70	7.20	1.85	0.16	0.99	0.14	68.00	32.00	Sec 22, " "
65; 83-84	4.00	62.50	4.05	4.90	5.85	7.60	5.20	9.20	10.10	11.00	7.53	2.35	-0.03	0.85	1.20	53.80	45.00	old driftwood, VI 64, 218 8-10, v 83-85 to 87, top of cl at base
43; 83-87	3.85	70.00	4.35	4.90	5.45	7.35	6.10	8.70	10.00	11.00	7.42	2.28	0.07	0.84	1.50	57.50	41.00	Old BW gully, VI 64, 218 7-10, v. 83-84 to 87, cl si at base
64; 83-69	4.20	54.40	4.60	5.50	5.90	7.10	7.30	9.10	10.05	11.00	7.55	2.11	0.26	0.82	0.31	64.70	35.00	Sec 6, VI 26, si v. s partings, 0-7cm above 83-68
63; 83-66	6.00	15.60	6.10	6.55	6.90	8.10	3.65	9.70	10.30	11.20	8.32	1.71	0.19	0.75	0.02	48.00	52.00	Sec 6, " ", top of layer, 216 4 (just above photo?)
62; 83-65	6.00	15.60	6.35	6.95	7.40	8.55	2.70	10.20	10.60	11.40	8.70	1.68	0.13	0.74	0.29	37.70	62.00	Sec 6, VI 26, base at 62-84cm, si v. partings, v. 78/79
79; 83-64	6.10	14.60	6.25	6.80	7.15	8.20	3.40	9.80	10.40	11.30	8.47	1.67	0.22	0.78	0.01	46.00	54.00	Sec 6, " ", finest 5.8-7cm
45; 83-62	4.25	53.00	4.70	5.25	5.55	6.70	9.60	8.40	9.40	10.85	7.12	1.97	0.33	0.88	0.06	70.00	30.00	Sec 6, VI 26, 216 4, graded unit, 83-63/83-62/83-64
78; 83-63	4.10	58.30	4.40	4.70	4.85	5.60	20.60	8.00	9.40	10.70	6.57	2.13	0.62	0.82	0.28	75.00	25.00	Sec 6, VI 24&26, v. 62&64, 216 4, coarsest .1-1cm
18; 82-16	4.10	58.30	4.70	5.50	6.00	7.50	5.50	9.50	10.20	11.10	7.73	2.14	0.14	0.75	0.90	55.10	44.00	Sec 7, dense, massive
19; 82-14	3.40	91.00	4.70	5.40	6.00	7.50	5.50	9.60	10.20	11.20	7.70	2.18	0.13	0.74	2.50	55.50	42.00	Sec 7, mud 25EH, 167 30-31, bn 137
20; 82-12	5.60	20.60	6.00	6.80	7.30	8.60	2.60	10.20	10.60	11.40	8.67	1.77	0.04	0.76	0.20	36.00	64.00	Sec 7, 21EH, 167 18, bn 135
27B; 82-8	5.15	28.20	5.60	6.00	6.45	7.80	4.50	9.75	10.30	11.20	8.03	1.92	0.19	0.70	0.04	53.00	47.00	Sec 7, 12EH, bn 137, laminated mud (3-8mm), 20cm thick, between s.
58; 81-8	4.95	32.00	5.30	6.00	6.40	7.60	5.20	9.25	10.25	11.20	7.95	1.96	0.23	0.85	0.16	56.00	44.00	Sec 1, bn 24, 143 25 (&23), clay v. s partings
67; 83-31	3.15	114.00	3.65	4.70	5.40	6.70	9.60	8.35	9.10	10.75	6.83	2.18	0.12	0.99	5.00	66.00	29.00	Sec 18A, " ", top of (), ripple topped graded s
66; 83-32	2.90	135.00	3.35	4.10	4.40	5.70	19.00	7.60	8.45	10.50	6.08	2.17	0.30	0.92	13.00	67.00	20.00	Sec 18A, VI 116, 212 6, bottom 1/3 of (), seq v. rippled top?
84; 83-49	3.00	125.00	3.80	4.30	5.30	6.80	9.00	8.60	9.40	10.70	6.83	2.32	0.08	0.86	7.00	59.00	34.00	Sec 18B, V 138, some adjacent s, cl layer in 212 32 (p. 124)
Ripples																		
57; 83-33	2.50	177.00	2.85	3.20	3.40	4.10	58.30	5.10	6.40	9.30	4.57	1.78	0.52	1.55	45.00	46.00	9.00	Sec 18A, 212 6, 6/22-24, between 7&8 on photo, s
112; 83-34	1.60	330.00	2.10	2.45	2.60	3.10	116.00	3.50	3.95	6.30	3.17	1.01	0.33	1.91	85.00	13.20	1.80	Sec 18A, V 116, prominent rippled si below no 7?
101; 82-80	2.40	190.00	2.60	2.90	3.00	3.25	105.00	3.55	3.85	5.80	3.33	0.72	0.43	2.38	88.00	10.50	1.50	Sec 23, IV 43, 187 27-32, cc foresets of upper climbing ripples
56; 82-50	3.50	88.00	3.80	4.15	4.25	4.95	32.00	6.60	7.90	9.70	5.67	1.83	0.59	1.03	8.00	77.00	15.00	Sec 20, bn 157-162, 179 31-34, bench 3
Bouma Sequence																		
91; 81-1	2.70	155.00	2.95	3.20	3.35	3.70	77.00	4.10	4.15	4.60	3.68	0.49	0.02	0.90	65.00	34.20	0.80	Sec 1, bn 3, 2.5cm of vfs, not rippled

90;83-102	2.80	144.00	3.10	3.40	3.50	4.00	62.50	4.10	4.20	4.50	3.87	0.41	-0.39	0.96	50.00	49.50	0.50 Sec 1, VI 68, 219 23&24, A horizon, 13.5-14.5cm, v. 83-101
100;83-101	2.65	160.00	3.00	3.20	3.30	3.60	83.00	4.10	4.30	4.70	3.70	0.53	0.28	0.87	73.50	25.50	1.00 Sec 1, VI 68, A 11.5-12.5cm, 219 23&24, 101-105=TC unit, Stats??
68; 83-99	3.10	117.00	3.35	3.60	3.80	4.10	58.30	4.25	4.35	4.70	4.02	0.39	-0.22	1.23	57.00	43.00	0.01 Sec 1, VI 68, 219 19-22, elongate rect. above 83-98, 1cm s
29; 83-97	3.20	110.00	3.45	3.70	3.80	4.15	56.00	4.50	4.65	4.90	4.17	0.46	0.04	0.85	37.00	63.00	0.10 Sec 1, VI 62, part of sequence
69; 83-96	2.80	144.00	3.10	3.35	3.45	3.90	67.00	4.25	4.55	5.50	3.93	0.66	0.21	1.23	56.00	44.00	0.20 Sec 1, " ", above rect. at right top of ruler, microlam drape
27A;83-93	2.70	155.00	3.00	3.20	3.35	3.70	77.00	4.10	4.20	4.40	3.70	0.46	0.00	0.77	63.00	37.00	0.20 Sec 1, VI 67, 219 19-22, top 1cm of 4° A v. climbing ripple above
129;83-94	2.55	172.00	2.90	3.20	3.30	3.70	77.00	4.20	4.50	5.00	3.80	0.64	0.23	0.96	65.00	34.00	1.00 Sec 1, VI 67, 216 16&17?, lower 1cm v. 83-93, graded?
28; 83-95	3.00	125.00	3.15	3.35	3.40	3.75	74.00	4.10	4.20	4.60	3.77	0.43	0.12	0.85	62.00	37.30	0.70 Sec 1, VI 68, 219 23+, from base
92; 82-75	2.30	204.00	2.65	3.00	3.15	3.43	94.00	3.95	4.10	4.35	3.51	0.53	0.15	0.87	77.00	22.60	0.40 Sec 21, IV 18, 185 26&27, rippled, below lenticular layer
86; 82-76	2.50	177.00	3.05	3.40	3.60	4.05	60.50	4.30	4.55	5.30	4.00	0.63	-0.01	1.32	44.00	55.60	0.40 Sec 21, IV 26, 186 18-21, bulk sample from trace fossil
111;83-38	1.75	300.00	2.10	2.40	2.60	3.00	125.00	3.40	3.60	5.10	3.00	0.75	0.20	1.54	91.00	8.00	1.00 Sec 18A, layer 2 (v. 35-39)
109;83-29	1.65	320.00	2.00	2.40	2.55	3.00	125.00	3.40	3.60	5.30	3.00	0.80	0.20	1.59	91.00	7.80	1.20 Sec 18A, V 118, layer 1 in 212 6
Amalgamated-Graded Sands																	
124;83-115	1.85	280.00	2.15	2.40	2.50	2.80	145.00	3.10	3.25	3.70	2.82	0.45	0.11	1.06	97.00	2.55	0.45 " ", 2nd unit
123;83-116	1.50	350.00	1.80	2.10	2.20	2.45	183.00	2.80	2.95	3.40	2.50	0.45	0.18	1.09	98.00	1.65	0.35 between sec 3&4, graded s, bottom 1" of second unit
125;83-113	1.53	350.00	1.85	2.15	2.25	2.50	177.00	2.85	3.00	3.45	2.55	0.45	0.18	1.09	98.40	1.30	0.30 " ", top 1" of 1st unit, 4.5-10° on ruler
126;83-114	1.00	500.00	1.35	1.75	1.95	2.30	204.00	2.70	2.90	3.35	2.32	0.59	0.05	1.09	98.80	0.95	0.25 bottom 1" of " "
127;83-111	2.45	183.00	2.80	3.10	3.20	3.50	88.00	4.00	4.10	4.30	3.57	0.48	0.13	0.77	75.00	25.00	0.20 Sec 2, VI 71, at .25-1" on ruler, 219 29
119;83-112	2.00	250.00	2.35	2.70	2.85	3.20	109.00	3.65	4.00	4.70	3.30	0.68	0.25	1.20	84.00	15.00	1.00 Sec 1, VI 72, 219 28-29, 4.5-5.5 on ruler
87;83-110	2.60	167.00	3.00	3.35	3.50	4.05	60.50	4.30	4.50	4.90	3.97	0.58	-0.16	0.97	45.00	55.00	0.30 Sec 2, VI 72, 219 26-29, v 107-111, fine fraction (120=co)
120;83-109	2.35	198.00	2.55	2.80	2.90	3.30	100.00	3.85	4.20	5.05	3.43	0.73	0.34	1.08	78.00	19.00	3.00 Sec 2, VI 71, v. 106-109&110(87=fine), layer 2.5cm over previous
130;83-106	2.10	235.00	2.50	2.85	3.00	3.30	100.00	3.75	4.10	4.80	3.42	0.66	0.29	1.26	82.00	16.00	2.00 Sec 2, VI 71, 219 25-27, top 0-1" v. 83-107&108+
122;83-107	1.45	365.00	1.85	2.20	2.33	2.70	155.00	3.15	3.30	4.20	2.73	0.63	0.18	1.17	94.50	4.75	0.75 Sec 2, " ", 2.5-3.25° on ruler
121;83-108	1.20	436.00	1.60	2.05	2.25	2.70	155.00	3.15	3.35	4.50	2.70	0.76	0.12	1.32	93.50	5.70	0.80 Sec 2, " ", 3.5-4.5° on ruler
113;81-13	1.20	435.00	1.70	2.10	2.30	2.70	155.00	3.20	3.40	4.40	2.73	0.73	0.17	1.23	94.00	6.20	0.80 Sec 2, bn 33, 30cm massive s (1st 6cm si defines contorted ripples)
118;82-63	0.70	610.00	1.15	1.55	1.75	2.20	218.00	2.60	2.85	3.40	2.20	0.67	0.03	1.08	98.00	1.60	0.40 Sec 20, bn 161, 180 26-29, fine v. 82-62, graded s, base of sec.
116;82-61	1.35	390.00	1.7	2.05	2.25	2.6	166.00	3	3.2	3.85	2.62	0.61	0.10	1.17	96	3.4	0.6 Sec 20, bn 167, see 82-60, fine fraction
117;82-60	0.50	710.00	0.75	1.10	1.30	1.75	300.00	2.35	2.70	3.40	1.85	0.80	0.22	1.03	98.00	1.60	0.40 Sec 20, bn 167, 181 22-24, co graded s v. water esc. & rip ups
102;83-45	2.30	204.00	2.60	2.90	3.00	3.30	100.00	3.60	3.80	4.20	3.33	0.47	0.12	1.09	91.00	7.90	1.10 Sec 18B, V 126, 14.5-16cm on ruler, top of graded unit, v 103
103;83-44	1.40	380.00	1.80	2.30	2.45	3.00	125.00	3.45	3.70	4.50	3.00	0.76	0.06	1.11	89.00	9.50	1.40 Sec 18B, " ", 8-10cm on ruler
104;83-43	1.70	310.00	2.00	2.30	2.40	2.75	149.00	3.15	3.35	3.80	2.80	0.54	0.15	0.98	97.00	2.50	0.50 Sec 18B, V 134(?), v 83-42, channel side infill
105;83-42	0.90	520.00	1.30	1.70	2.00	2.60	166.00	3.20	3.45	4.00	2.58	0.85	.00	0.92	95.00	4.30	0.70 Sec 18B, V 133, horizon above 83-41, flame of 213 15
106;83-41	1.60	330.00	2.00	2.30	2.40	2.80	145.00	3.20	3.35	3.90	2.82	0.55	0.10	0.97	95.50	4.10	0.40 Sec 18B, " "
107;83-40	0.20	870.00	0.70	1.20	1.50	2.25	210.00	2.95	3.20	3.70	2.22	0.95	-0.04	0.85	97.00	2.50	0.50 Sec 18B, v 83-41, lower co s dips to left from 10-12cm on ruler
85; 81-22	2.60	167.00	2.95	3.20	3.35	3.75	74.00	4.20	4.35	5.05	3.77	0.61	0.14	1.01	59.00	41.00	0.20 Sec 6, bn 48, 146 27-29, middle s enclosed by roll structure
95; 83-68	1.60	330.00	2.00	2.35	2.50	2.90	135.00	3.35	3.60	4.40	2.95	0.68	0.19	1.16	90.00	9.00	1.00 Sec 6, VI 26, 216 4, s above loaded base of 83-69
114;82-65	1.60	330.00	2.00	2.35	2.50	2.80	145.00	3.15	3.30	3.90	2.82	0.53	0.11	1.20	96.00	3.40	0.60 Sec 21, trace fossils, bn 169, 181 39, s below mud
115;82-64	1.50	350.00	1.50	2.00	2.25	2.80	145.00	3.40	3.75	4.60	2.85	0.91	0.12	1.10	88.00	10.60	1.40 Sec 21, bn 169, copepod burrows
Diamicton																	
6; 83-56	-1.00		-0.90	0.60	2.10	5.00		7.90	8.80	10.50	4.80	3.78	-0.05	0.81	42.00	35.00	23.00 Sec. 13, bk V, p. 37, diamicton at trowell
8; 83-54	-1.00		-1.00	1.20	2.70	5.50		7.90	8.90	10.60	5.20	3.68	-0.12	0.91	34.00	32.00	34.00 Sec. 13, " ", at clinometer
9; 83-52	-1.00		-1.00	0.70	2.40	4.70		7.70	9.10	10.70	4.83	3.87	0.04	0.90	36.00	41.00	23.00 Sec. 13, " ", D, bottom fabric
39; 83-2	-1.00	0.00	-1.00	0.35	1.85	5.00	x	8.00	9.20	10.75	4.85	3.99	-0.04	0.78	40.00	35.00	25.00 Sec 14, IV 57, Dmm immed. above B38
40; 83-3	-1.00		-1.00	1.00	2.50	5.70	x	8.15	9.25	10.70	5.32	3.84	-0.14	0.83	36.00	37.00	27.00 Sec 14, IV 57, 1-6cm si v. fs & pebble, Dmm
41; 83-5	-1.00		-1.00	1.50	3.20	6.40	x	8.30	9.40	10.70	5.77	3.75	-0.25	0.94	29.00	42.00	29.00 Sec 14, IV 61, loose blocky D, 3-10cm above contact
42; 83-10	-1.00		-1.00	0.70	2.25	5.50	x	8.20	9.40	10.90	5.20	3.98	-0.10	0.82	36.00	36.00	28.00 Sec 14, IV 75, 210 27-32, fabric gully, at brunton
44;83-12	-1.00		-1.00	0.50	1.80	4.95	x	8.10	9.20	10.70	4.88	3.95	-0.02	0.76	41.00	33.00	26.00 Sec 14, IV 80, middle of fabric at sta. 6.5, v. 83 11&13
46; 83-11	-1.00		-1.00	0.30	1.50	4.50		7.70	8.90	10.80	4.57	3.94	0.05	0.78	43.00	35.00	22.00 Sec 14, V 80, D fabric at sta 6.5, v. 44&48, at bottom
47; 83-7	-1.00		-1.00	-0.20	1.00	4.60		7.50	8.90	10.70	4.43	4.05	-0.01	0.74	45.00	32.00	23.00 Sec 14
48; 83-13	-1.00		-1.00	0.20	1.50	5.00		8.00	9.20	10.70	4.80	4.02	-0.05	0.74	42.00	33.00	25.00 Sec 14, V 80, fabric at sta 6.5,top, v. 44&46
49; 83-14	-1.00		-1.00	0.40	1.90	5.10		7.85	9.10	10.80	4.87	3.96	-0.06	0.81	38.00	38.00	24.00 Sec 14, V 82, diamicton v. many si horizons
50; 83-15	-1.00		-1.00	0.60	2.10	4.60		7.80	8.90	10.70	4.70	3.85	0.04	0.84	38.00	40.00	22.00 Sec 14, V 86, sta 6.5, base diamicton
51; 83-16	-1.00		-1.00	0.35	1.80	4.60		7.50	8.60	10.70	4.52	3.84	0.01	0.84	39.00	40.00	21.00 Sec 14, " ", top of diamicton
52; 83-17	-1.00		-1.00	1.50	3.50	6.10		8.25	9.30	10.70	5.63	3.72	-0.20	1.01	27.00	45.00	28.00 Sec 14, V 88, sta 6.5, center, no other samples

53; 83-18	-1.00		-1.00	0.40	1.85	5.20		8.00	9.10	10.70	4.90	3.95	-0.08	0.78	41.00	34.00	25.00 Sec 14, V 90, 210 34, center of fabric
90; 83-9	-1.00		-1.00	0.20	1.70	4.50		8.05	9.20	10.80	4.63	4.04	0.06	0.76	45.00	29.00	26.00 Sec 14, V 72, 219 19-20, sta 6, 10cm above boulder, v. 83-8
Sec. 12																	
54; 82-4	2.55	172.00	2.90	3.30	3.50	4.40	47.40	6.00	6.90	10.00	4.87	1.98	0.48	1.16	35.00	55.00	10.00 Sec 7, bn 133, foresets
94; 81-46	1.10	470.00	1.40	1.70	1.85	2.10	230.00	2.40	2.55	3.00	2.12	0.45	0.09	1.19	99.30	0.60	0.10 Sec 7, Lagoon, foresets, bn 109, 162 24-30
Arrowhead																	
59; 81-26	2.60	167.00	3.25	4.15	4.50	5.85	17.30	7.60	8.80	10.60	6.27	2.28	0.28	0.97	13.00	65.00	22.00 Arrowhead, bn 59, fs to s, graded & reverse graded
60; 81-27	3.50	88.00	4.00	4.70	5.30	6.50	11.00	8.30	9.40	10.85	6.87	2.21	0.25	0.94	3.00	68.00	29.00 Sec 8, bn 65, repetitive fs/sivfs/si/cl
61; 81-28	3.40	95.00	4.05	4.75	5.20	6.65	9.80	8.30	9.60	10.90	7.00	2.25	0.23	0.91	2.60	68.40	29.00 Sec 8, bn 67, top s of section
88; 83-81	0.00	1000.00	0.00	0.60	1.00	1.95	260.00	2.90	3.40	4.45	1.98	1.37	0.08	0.96	89.00	10.60	0.40 Arrowhead, VI 60, 218 344, co at bottom of knife, inside gully
89; 83-79	0.00	1000.00	0.30	0.90	1.20	2.00	250.00	2.85	3.20	4.20	2.03	1.17	0.09	0.97	93.00	6.40	0.60 Arrowhead, VI 59, 218 1, 3.5-5.5°, co (see 99), rip ups
99; 83-80	0.70	615.00	1.10	1.55	1.80	2.40	190.00	3.05	3.35	4.40	2.43	0.95	0.13	1.08	92.00	7.00	1.00 Arrowhead, VI 59, 218 1, fine at 5.5°, v 88; 83-79
Clay																	
34; 81-5	4.30	51.00	5.30	6.15	6.55	7.90	4.20	9.45	10.60	11.40	8.22	2.04	0.18	0.86	0.88	50.00	49.00 Sec 1, bn 22, 142 33&35, cl draping lenticular sand
14; 82-70	-0.25	1190.00	3.20	3.90	4.25	5.20	27.20	6.65	8.20	10.70	5.77	2.21	0.43	1.28	18.00	65.00	17.00 Rock glacier silt, in Lush Acres
128;81-25	2.50	177.00	3.40	4.60	5.75	7.50	5.50	9.10	10.10	11.00	7.40	2.53	-0.07	0.93	9.00	49.00	42.00 Crescent Glacier valley, lacustrine si
15; 83-119	2.80	144.00	3.15	3.45	3.75	4.35	49.00	5.70	6.80	9.80	4.87	1.85	0.55	1.40	32.00	57.00	11.00 Sec 17, bk VI(90), microchannel
55B;83-28	3.80	72.00	4.10	4.25	4.40	5.10	29.20	6.80	8.30	10.70	5.88	2.01	0.64	1.13	2.50	80.00	17.50 Sec 15, V 104, 1° below bottom of 3 in 211 22
Sec.5																	
16; 83-70	1.20	404.00	2.60	4.00	4.50	5.90	16.80	8.30	9.70	10.90	6.53	2.68	0.27	0.90	7.00	65.00	28.00 Sec 5, bk VI(29), lower channel s.
97; 83-91	0.00	1000.00	0.80	1.25	1.45	1.95	260.00	2.40	2.60	3.25	1.93	0.71	0.01	1.06	97.30	2.10	0.40 Sec 5, IV 66, lower gr/s, v. 83-92
98; 83-92	-0.40	1320.00	0.00	0.50	0.75	1.30	405.00	1.90	2.25	3.00	1.35	0.89	0.11	1.07	98.00	1.60	0.40 Sec 5, 217 11, graded units above channel